

GEOMETRIC REALIZATIONS OF THE \mathbf{s} -WEAK ORDER AND ITS LATTICE QUOTIENTS

EVA PHILIPPE AND VINCENT PILAUD

ABSTRACT. For an n -tuple \mathbf{s} of non-negative integers, the \mathbf{s} -weak order is a lattice structure on \mathbf{s} -trees, generalizing the weak order on permutations. We first describe the join irreducible elements, the canonical join representations, and the forcing order of the \mathbf{s} -weak order in terms of combinatorial objects, generalizing the arcs, the non-crossing arc diagrams, and the subarc order for the weak order. We then extend the theory of shards and shard polytopes to construct geometric realizations of the \mathbf{s} -weak order and all its lattice quotients as polyhedral complexes, generalizing the quotient fans and quotientopes of the weak order.

CONTENTS

| | |
|---|----|
| Introduction | 2 |
| Combinatorics | 3 |
| Lattice theory | 3 |
| Polyhedral geometry | 3 |
| Plan | 4 |
| 1. Insertion algorithm in \mathbf{s}-bushes | 5 |
| 1.1. Recollections 1: Insertion algorithm in increasing binary trees | 5 |
| 1.2. \mathbf{s} -bushes, \mathbf{s} -trees, and \mathbf{s} -trunks | 6 |
| 1.3. \mathbf{s} -insertion algorithm | 7 |
| 1.4. \mathbf{s} -insertion fibers | 7 |
| 1.5. \mathbf{s} -foam | 9 |
| 1.6. \mathbf{s} -rotations | 11 |
| 2. The \mathbf{s}-weak order and facial \mathbf{s}-weak order | 12 |
| 2.1. Recollections 2: The weak order and facial weak order | 13 |
| 2.2. The \mathbf{s} -weak order | 14 |
| 2.3. The facial \mathbf{s} -weak order | 16 |
| 3. Canonical representations in the \mathbf{s}-weak order | 18 |
| 3.1. Recollections 3: Canonical representations in the weak order | 18 |
| 3.2. Join irreducibles of the \mathbf{s} -weak order, \mathbf{s} -arcs, \mathbf{s} -shards | 20 |
| 3.3. Canonical join representations in the \mathbf{s} -weak order and non-crossing \mathbf{s} -arc diagrams | 22 |
| 3.4. Canonical complex of the \mathbf{s} -weak order and semi-crossing \mathbf{s} -arc bidiagrams | 25 |
| 4. Lattice congruences of the \mathbf{s}-weak order | 26 |
| 4.1. Recollections 4: Lattice congruences of the weak order | 26 |
| 4.2. Forcing order and subarc order | 30 |
| 4.3. Some relevant congruences of the \mathbf{s} -weak order | 33 |
| 5. Quotient foams and quotientplexes | 35 |
| 5.1. Recollections 5: Quotient fans and quotientopes | 35 |
| 5.2. Quotient foams | 38 |
| 5.3. Shardoplexes | 39 |
| 5.4. Quotientoplexes | 40 |
| 6. Tropical geometry | 42 |
| 6.1. Recollection 6: Polytopal subdivisions and tropical duality | 42 |
| 6.2. Shard tropical hypersurfaces and polynomials | 45 |
| Acknowledgements | 48 |
| References | 48 |

VP was partially supported by the Spanish project PID2022-137283NB-C21 of MCIN/AEI/10.13039/501100011033 / FEDER, UE, by the Spanish–German project COMPOTE (AEI PCI2024-155081-2 & DFG 541393733), by the Severo Ochoa and María de Maeztu Program for Centers and Units of Excellence in R&D (CEX2020-001084-M), and by the Departament de Recerca i Universitats de la Generalitat de Catalunya (2021 SGR 00697). VP and EP were partially supported by the French–Austrian project PAGCAP (ANR-21-CE48-0020 & FWF I 5788).

INTRODUCTION

The structure of permutations and associations of an n -element set is a classical topic of algebraic and geometric combinatorics. In combinatorics, it is encoded by the Cayley graph of permutations under simple transpositions and the rotation graph on binary trees. In lattice theory, it materializes in the lattice morphism from the weak order on permutations to the Tamari lattice on binary trees. In polyhedral geometry, it appears in the braid arrangement and the sylvester fan, and their polar permutahedron and associahedron. See [PSZ23] for a recent survey on these connections and their influence in mathematics.

This prototype has motivated the study of all lattice congruences of the weak order, pioneered by N. Reading [Rea04]. Combinatorially, he provided an elegant combinatorial model for the lattice theory of the weak order in [Rea15]. Namely, the join irreducible permutations are encoded as certain arcs wiggling around the vertical axis, the canonical join representations of the permutations are encoded by non-crossing arc diagrams, and the forcing order on join irreducible permutations is encoded by the subarc order on these arcs. Geometrically, he showed in [Rea05] that coarsening the braid fan according to the equivalence classes of any congruence of the weak order always yields a complete polyhedral fan. These quotient fans were shown to be normal fans of so-called quotientopes by V. Pilaud and F. Santos [PS19]. Later, A. Padrol, V. Pilaud and J. Ritter [PPR23] revisited the problem using the theory of shard polytopes, a family of polytopes indexed by the arcs (or, equivalently, by the join irreducible permutations).

C. Ceballos and V. Pons introduced in [CP24a, CP24b] the \mathbf{s} -weak order on \mathbf{s} -trees for an n -tuple \mathbf{s} of non-negative integers, generalizing the classical weak order (the case $\mathbf{s} = (1, \dots, 1)$). An \mathbf{s} -tree is a rooted plane tree on $[n]$, where the node i has $s_i + 1$ children that are all either leaves or nodes $j > i$ (note that we have changed the conventions of [CP24a] to make inductive arguments more transparent). The order among these \mathbf{s} -trees is defined by inequalities between the inversion numbers in \mathbf{s} -trees, generalizing the definition of the weak order by inclusion of inversion sets of permutations. See Figure 1 (left). They proved in [CP24a, Sect. 1] that the \mathbf{s} -weak order is a lattice, described its meet and join operations, and established lattice properties of the \mathbf{s} -weak order, in particular congruence uniformity. They also introduced in [CP24a, Sect. 2] the \mathbf{s} -Tamari lattice, a sublattice of the \mathbf{s} -weak order (and also a lattice quotient of the \mathbf{s} -weak order when \mathbf{s} contains no 0), which is isomorphic to the ν -Tamari lattice of [PRV17, CPS19] (for well-chosen \mathbf{s} and ν). They conjectured in [CP24b, Conj 3.1.2] that the Hasse diagram of the \mathbf{s} -weak order can be realized as an orientation of the skeleton of a polyhedral subdivision of the permutahedron,

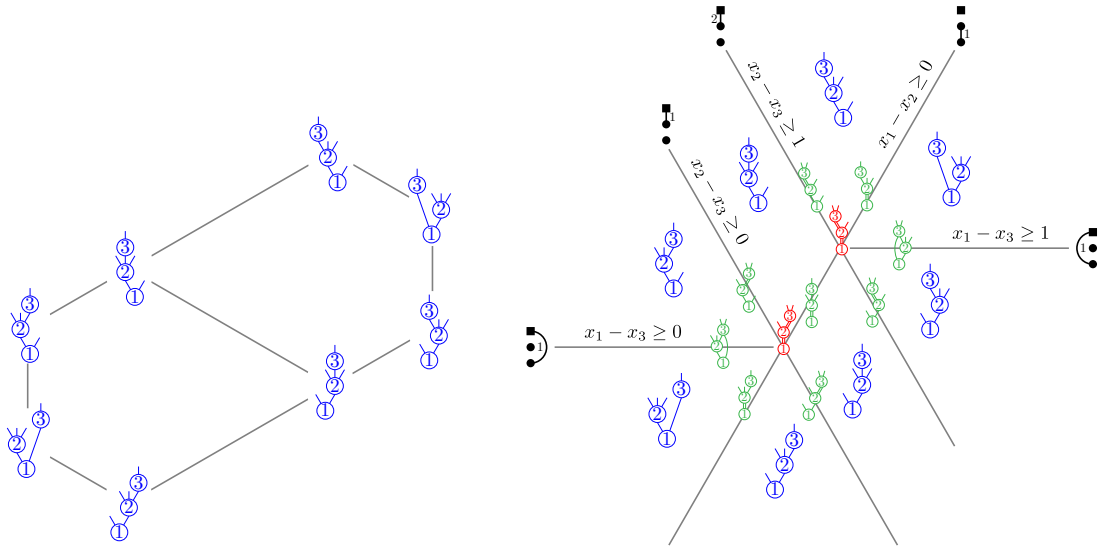


FIGURE 1. The $(1,2,0)$ -weak order (left) and the $(1,2,0)$ -foam (right).

in the same spirit C. Ceballos, A. Padrol and C. Sarmiento realized the ν -Tamari lattice as an orientation of the skeleton of a polyhedral complex in [CPS19]. In the situation when \mathbf{s} contains no 0, this conjecture was settled by R. González D’Léon, A. Morales, E. Philippe, D. Tamayo Jiménez, and M. Yip in [DMP⁺23] using the theory of flow polytopes. In this paper, we study the \mathbf{s} -weak order combining perspectives from combinatorics, lattice theory and polyhedral geometry.

Combinatorics. Our first contribution is an algorithmic perspective on the \mathbf{s} -weak order. We consider a natural *insertion algorithm* from \mathbb{R}^n to \mathbf{s} -trees, generalizing the insertion of a permutation in an increasing binary tree. The ambiguities of this algorithm on certain non-generic points of \mathbb{R}^n force us to define *\mathbf{s} -bushes* as certain degenerations of \mathbf{s} -trees, generalizing ordered set partitions. We then define the *\mathbf{s} -foam* $\mathcal{F}_{\mathbf{s}}$ as the set of fibers of our insertion algorithm in \mathbf{s} -bushes, generalizing the braid fan. See Figure 1 (right). The oriented dual graph of this polyhedral complex gives an alternative definition for the \mathbf{s} -weak order, equivalent to the original definition of [CP24a]. Exploiting the properties of this insertion algorithm enables us to prove our first battery of results.

Theorem A. *The insertion algorithm in \mathbf{s} -bushes knows the \mathbf{s} -weak order and the facial \mathbf{s} -weak order:*

- (i) *The \mathbf{s} -foam $\mathcal{F}_{\mathbf{s}}$ is a complete polyhedral complex (Proposition 19), whose oriented dual graph is isomorphic to the Hasse diagram of the \mathbf{s} -weak order (Corollary 34).*
- (ii) *Decomposing each insertion step yields a natural construction of the \mathbf{s} -weak order by interval doublings (Proposition 38), thus recovering the result of [CP24a, Thms. 1.21 & 1.40] that the \mathbf{s} -weak order is a congruence uniform lattice.*
- (iii) *Considering all faces of the \mathbf{s} -foam, there is a natural facial \mathbf{s} -weak order on \mathbf{s} -bushes (Definition 41), which is also constructible by interval doublings (Proposition 43).*

Lattice theory. Our second battery of results generalizes the combinatorial description of [Rea15] for the lattice theory of the weak order in terms of arcs, non-crossing arc diagrams, and subarcs. We define an *\mathbf{s} -arc* as an arc of [Rea15] together with an integer bounded by \mathbf{s} . We then extend to all \mathbf{s} -arcs the combinatorial notions of *crossings* and of *subarcs* to obtain the following statement.

Theorem B. *The \mathbf{s} -arcs combinatorially encode the lattice theory of the \mathbf{s} -weak order:*

- (i) *The join irreducible \mathbf{s} -trees are in bijection with the \mathbf{s} -arcs (Proposition 51).*
- (ii) *The \mathbf{s} -trees are in bijection with the non-crossing \mathbf{s} -arc diagrams (Proposition 59), and this bijection encodes the canonical join representations in the \mathbf{s} -weak order (Proposition 61).*
- (iii) *The forcing order in the \mathbf{s} -weak order is isomorphic to the subarc order on \mathbf{s} -arcs (Theorem 72), so that the congruence lattice of the \mathbf{s} -weak order is isomorphic to the distributive lattice of subsets of \mathbf{s} -arcs closed under subarcs (Corollary 74).*

We exploit Theorem B (iii) to define relevant congruences of the \mathbf{s} -weak order and their quotients, generalizing the Tamari lattice [Tam51], the Cambrian lattices [Rea06, LP18, CP17], the permutree lattices [PP18], and the simple congruences of the weak order [HM21, DIR⁺23, BNP25]. This opens appealing conjectures about the combinatorics of these congruences (Conjectures 75, 76 and 77).

Polyhedral geometry. We then construct geometric realizations of the \mathbf{s} -weak order and all its lattice quotients. Namely, we first use the \mathbf{s} -foam $\mathcal{F}_{\mathbf{s}}$ to construct polyhedral realizations of all lattice quotients of the \mathbf{s} -weak order, generalizing the quotient fans for the quotients of the weak order. See Figure 2 (middle). This gives our third battery of results.

Theorem C. *All lattice quotients of the \mathbf{s} -weak order are realized by coarsenings of the \mathbf{s} -foam:*

- (i) *For any congruence \equiv of the \mathbf{s} -weak order, gluing together the maximal cells of the \mathbf{s} -foam $\mathcal{F}_{\mathbf{s}}$ corresponding to \mathbf{s} -trees in the same congruence class of \equiv defines a complete polyhedral complex \mathcal{F}_{\equiv} (Proposition 85).*
- (ii) *The union of the walls of the quotient foam \mathcal{F}_{\equiv} coincides with the union of the \mathbf{s} -shards of the \mathbf{s} -arcs corresponding to \equiv (Proposition 84), where the *\mathbf{s} -shards* are affine cones associated to the \mathbf{s} -arcs, generalizing the shards of [Rea03].*
- (iii) *The oriented dual graph of the quotient foam \mathcal{F}_{\equiv} is isomorphic to the Hasse diagram of the quotient of the \mathbf{s} -weak order by \equiv (Proposition 86).*

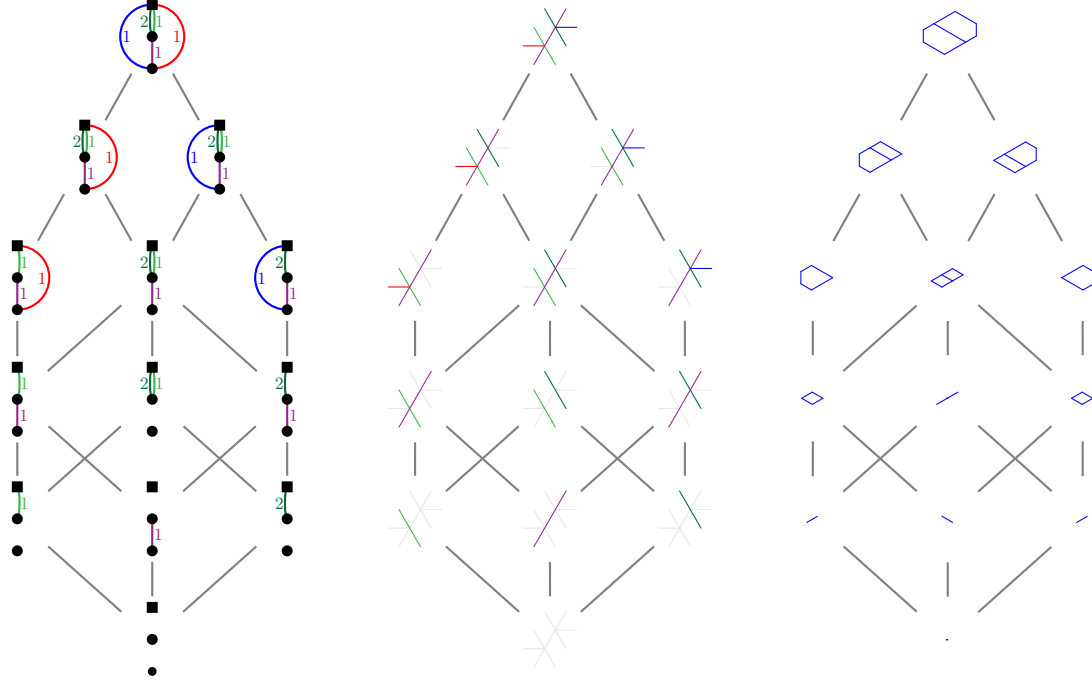


FIGURE 2. The congruence lattice of the $(1, 2, 0)$ -weak order, where each congruence \equiv is replaced by its s -arc down set (left), its quotient foam \mathcal{F}_\equiv (middle) and its quotientoplex \mathbb{Q}_\equiv (right).

We then extend the theory of shard polytopes and quotientopes [PS19, PPR23]. We define the *shardoplex* \mathbb{S}_α associated to any s -arc α , a polyhedral complex whose geometry is tuned to take care of the s -shard of α . We then use Minkowski sums of shardoplexes to construct the *quotientoplex* \mathbb{Q}_\equiv of any congruence \equiv of the s -weak order, a polyhedral complex realizing the quotient of the s -weak order by \equiv . See Figure 2 (right). This yields our fourth battery of results.

Theorem D. *All lattice quotients of the s -weak order are realized as Minkowski sums of shardoplexes:*

- (i) *For each s -arc α , the union of the walls of the dual polyhedral complex of the shardoplex \mathbb{S}_α contains the s -shard Σ_α and is contained in the s -shards of the subarcs of α (Proposition 105).*
- (ii) *For any congruence \equiv of the s -weak order, the Hasse diagram of the quotient of the s -weak order by \equiv is isomorphic to the oriented skeleton of the quotientoplex \mathbb{Q}_\equiv (Proposition 93).*
- (iii) *The quotientoplex \mathbb{Q}_\equiv is a polytopal subdivision of a quotientope \mathbb{Q}_\equiv for the congruence \equiv of the weak order obtained by projecting \equiv (Proposition 94).*

We note that the proofs of Theorem D are mainly based on tropical geometry [Jos21] (in fact, tropical geometry is convenient even to define the notion of dual polyhedral complex).

Applying Theorem D to the trivial congruence provides a definitive answer to the geometric conjecture of C. Ceballos and V. Pons [CP24b, Conj. 3.1.2] (which was already partially answered using flow polytopes and tropical geometry in [DMP⁺23], in the situation when s contains no 0).

Corollary. *For any tuple s of non-negative integers, the Hasse diagram of the s -weak order is isomorphic to the oriented skeleton of a polytopal subdivision of a graphical zonotope (Corollary 96).*

Plan. The paper is organized as follows. Section 1 describes s -bushes, the insertion algorithm, and the s -foam. Section 2 defines the s -weak order and s -facial weak order and shows that they are constructible by interval doublings. Section 3 introduces s -arcs and non-crossing s -arc diagrams, and describes canonical representations in the s -weak order. Section 4 describes the forcing order of the s -weak order in terms of subarcs, and introduces a few relevant congruences of the s -weak order. Section 5 constructs the quotient foams \mathcal{F}_\equiv , shardoplexes \mathbb{S}_α , and quotientoplexes \mathbb{Q}_\equiv . Section 6 uses tropical geometry to prove the results of Section 5. Each section starts with a recollection of definitions and results on the weak order to be extended to the s -weak order.

1. INSERTION ALGORITHM IN \mathbf{s} -BUSHES

In this section, we describe a family of insertion algorithms whose fibers define polyhedral partitions of \mathbb{R}^n . We use the notations $[n] := \{1, \dots, n\}$, $\llbracket n \rrbracket := \{0, \dots, n\}$ and $]i, j[:= \{i + 1, \dots, j - 1\}$ throughout the paper. For a property P , we denote $\mathbf{1}_P := 1$ if P and $\mathbf{1}_P := 0$ otherwise.

1.1. Recollections 1: Insertion algorithm in increasing binary trees. We first recall the classical insertion algorithm in increasing binary trees. An *increasing binary tree* is a rooted plane binary tree whose nodes are labeled by integers such that each node is strictly smaller than all its children. It is called *standard* if the nodes are bijectively labeled by $[n]$. The increasing binary trees are in bijection with words on integers with no repeated letter:

- we associate a word to any increasing binary tree by reading its node labels in inorder,
- conversely, we associate an increasing binary tree $B(w)$ to any word w inductively:
 - if $w = \emptyset$ is the empty word, then $B(\emptyset)$ is the empty binary tree, with just a root, no internal node, and a single leaf,
 - otherwise $w = urv$ where r is the minimal letter of w , and $B(w)$ is the binary tree with root r , left subtree $B(u)$ and right subtree $B(v)$.

In particular, the standard increasing binary trees are in bijection with permutations.

Consider now a point $\mathbf{x} := (x_1, \dots, x_n) \in \mathbb{R}^n$. If \mathbf{x} is generic (no repeated entry), we can consider the permutation σ of $[n]$ that sorts \mathbf{x} , that is, such that $x_{\sigma(1)} < \dots < x_{\sigma(n)}$. Then we denote by $B(\mathbf{x})$ the increasing binary tree obtained by the insertion of σ . In other words, the root of $B(\mathbf{x})$ is 1, and its left subtree contains the positions $j \in [2, n]$ such that $x_1 > x_j$ while its right subtree contains the positions $j \in [2, n]$ such that $x_1 < x_j$.

The fibers of this insertion are the (open) regions of the *braid arrangement*, defined by the hyperplanes $\{x \in \mathbb{R}^n \mid x_i = x_j\}$ for all $1 \leq i < j \leq n$. See Figure 3 for illustrations when $n = 3$ and $n = 4$. The *braid fan* is the complete simplicial fan defined by the braid arrangement. It has a cone C_μ for each ordered set partition μ of $[n]$, given by the points $\mathbf{x} \in \mathbb{R}^n$ such that $x_i \leq x_j$ if and only if the part of μ containing i appears weakly before the part of μ containing j (hence $x_i = x_j$ if i and j belong to the same part of μ). In particular, it has a region for each permutation of $[n]$, and two regions are adjacent if the corresponding permutations differ by the transposition of adjacent entries (meaning at two consecutive positions).

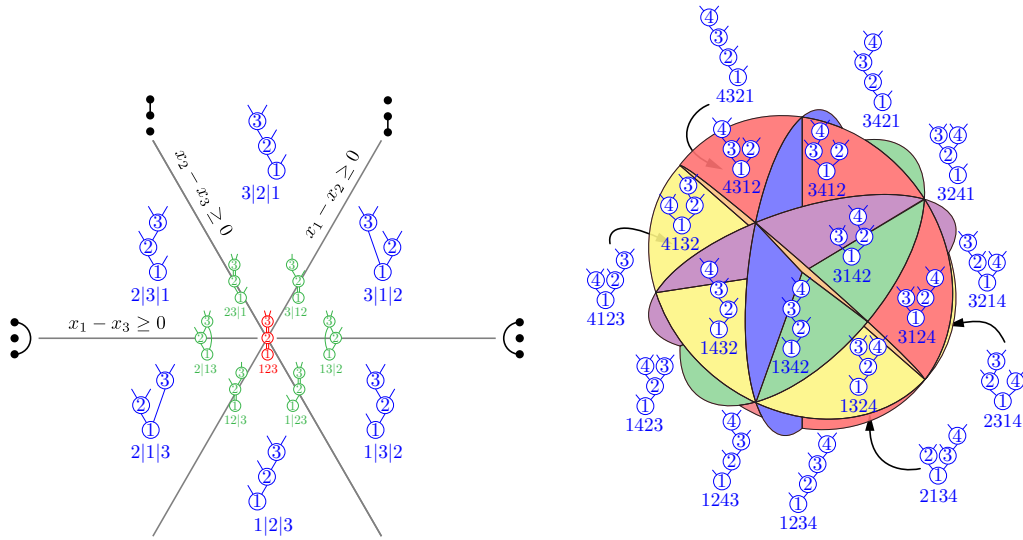


FIGURE 3. The braid fan for $n = 3$ with cones labeled by ordered set partitions and bushes (left) and for $n = 4$ with maximal cones labeled by permutations and increasing binary trees (right).

In this paper, it will be impossible to work with permutations and ordered set partitions (except if we accept to restrict the generality to strict compositions \mathbf{s}). We thus describe all the combinatorics of the braid fan with treelike structures. For this, we associate to each $\mathbf{x} \in \mathbb{R}^n$ (generic or not) a rooted plane graph $B(\mathbf{x})$ that we call a *bush*. It is constructed inductively as follows:

- start with the tree with just a root, no internal node, and a single leaf,
- at step j , attach a new node j with 2 leaves
 - either to the leaf between the two nodes u and v such that $x_u < x_j < x_v$,
 - or to the two leaves surrounding the node w with $x_j = x_w$.

This is illustrated in Figure 3(left). We naturally orient a bush increasingly, from its root to its leaves. The fiber \mathbb{F}_B of a bush B is the cone defined by the inequalities $x_u < x_j < x_v$ and the equalities $x_j = x_w$ discovered along the insertion (an alternative description will be discussed in Section 1.4). The cones of the braid fan are precisely the closures of the fibers of this insertion.

1.2. \mathbf{s} -bushes, \mathbf{s} -trees, and \mathbf{s} -trunks. Fix an n -tuple $\mathbf{s} := (s_1, \dots, s_n)$ with $s_i \in \mathbb{N}$ for any $i \in [n]$ (note that we allow $s_i = 0$). For any $j \in [n]$, we define the j -tuple $\mathbf{s}_{\leq j} := (s_1, \dots, s_j)$ and the numbers $S_j := 1 + \sum_{i \leq j} s_i$ and $T_j := 2 - \mathbf{1}_{s_1 = \dots = s_j = 0} + \sum_{i \leq j} \max(0, s_i - 1)$.

We now define a family of plane rooted labeled graphs that naturally appear in the \mathbf{s} -insertion algorithm of Section 1.3. See Figures 4 and 5 for illustrations.

Definition 1. An *\mathbf{s} -bush* is a plane graph with a root, n internal nodes bijectively labeled by $[n]$, and some leaves, defined inductively as follows:

- start with the rooted graph with just a root, no internal node, and a single leaf,
- at step j , attach either to a leaf or to two consecutive leaves, a new node j with $s_j + 1$ leaves (except that if $s_j = 0$ and j is attached to two leaves, then j gets itself two leaves).

Remark 2. A few observations on Definition 1:

- (1) For $j \in [n]$, deleting all nodes $> j$ in an \mathbf{s} -bush B gives an $\mathbf{s}_{\leq j}$ -bush $B_{\leq j}$.
- (2) An \mathbf{s} -bush is naturally oriented from its root to its leaves, so that all its edges are increasing. We draw bushes growing up, with their roots on the bottom and their leaves on top, and such that the node j is at level j . See Figures 4 and 5.
- (3) For an \mathbf{s} -bush B and $1 \leq i < j \leq n$, we say that i is an *ancestor* of j in B and that j is a *descendant* of i in B if there is an increasing path from i to j in B (we consider i to be an ancestor and a descendant of itself).
- (4) The *rank* $r(B)$ of an \mathbf{s} -bush is its number of indegree 1 nodes. An *\mathbf{s} -tree* (resp. *\mathbf{s} -trunk*) is an \mathbf{s} -bush of maximal rank n (resp. minimal rank $\min \{i \in [n] \mid s_i \neq 0\} \cup \{n\}$). Note that the \mathbf{s} -trees are precisely the rooted plane trees with internal nodes bijectively labeled by $[n]$ such that the node j has $s_j + 1$ children that are either leaves or nodes larger than j .
- (5) An \mathbf{s} -bush where $X \subseteq [n]$ is the set of indegree 2 nodes has $S_n - \#\{x \in X \mid s_x \neq 0\}$ leaves. There are $\prod_{j \in [n]} (S_{j-1} - \#\{x \in X \mid x < j \text{ and } s_x \neq 0\} - \mathbf{1}_{j \in X})$ such \mathbf{s} -bushes. Hence,
 - an \mathbf{s} -tree has S_n leaves, and there are $\prod_{j \in [n]} S_{j-1}$ \mathbf{s} -trees,
 - an \mathbf{s} -trunk has T_n leaves, and there are $\prod_{j \in [n]} \max(1, T_{j-1} - 1)$ \mathbf{s} -trunks.
- (6) In fact, denoting by

$$\Gamma_{\mathbf{s}} := \prod_{j \in [n]} [S_{j-1}] \quad \text{and} \quad \Lambda_{\mathbf{s}} := \prod_{j \in [n]} [\max(1, T_{j-1} - 1)],$$

we can associate to each $\mathbf{p} \in \Gamma_{\mathbf{s}}$ the \mathbf{s} -tree $S_{\mathbf{p}}$ obtained by attaching node j to leaf p_j , and to each $\mathbf{q} \in \Lambda_{\mathbf{s}}$ the \mathbf{s} -trunk $T_{\mathbf{q}}$ obtained by attaching node j to leaves q_j and $q_j + 1$ (or to the only leaf if there is only one).

Remark 3. Our \mathbf{s} -trees are essentially the \mathbf{s} -decreasing trees of [CP24a]. We have chosen to slightly change their conventions to simplify our presentation, in particular to allow for more natural inductive arguments. To change conventions, one just needs to reverse \mathbf{s} and relabel each node j by $n - j$. We will see that our \mathbf{s} -bushes provide alternative combinatorial models to the pure intervals of [CP24b], much more adapted to geometry. Finally, we note that our

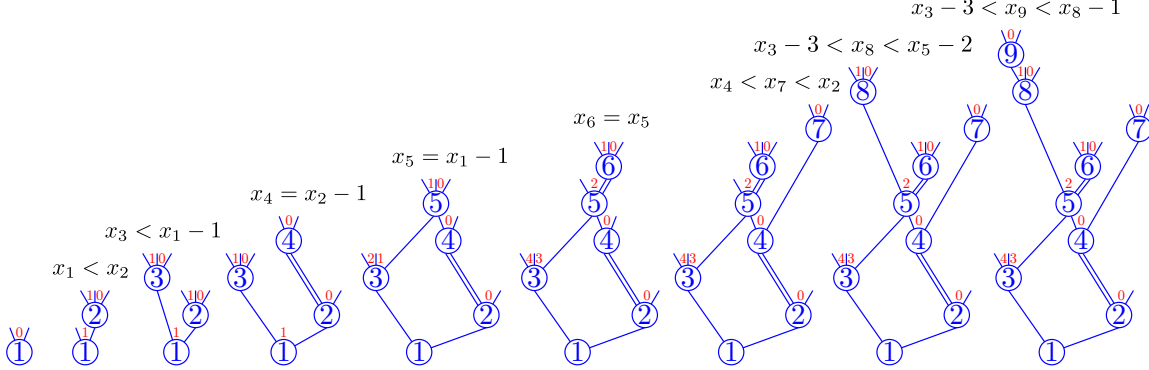


FIGURE 4. Flow of the s -insertion algorithm to compute $B(s, \mathbf{x})$ for $s = (1, 2, 2, 0, 2, 2, 1, 2, 1)$ and $\mathbf{x} = (5, 6, 3, 5, 4, 4, 5.5, 1.5, .25)$. We indicate each gap label (u, ρ) by writing ρ in red above the node u . The equalities or inequalities that led to this s -tree are indicated at each step of the algorithm.

insertion algorithm, while never made explicit in [CP24a, CP24b], is somewhat underlying in their work [Pon24].

1.3. s -insertion algorithm. We now describe an iterative insertion algorithm that sends a point \mathbf{x} in \mathbb{R}^n to an s -bush $B(s, \mathbf{x})$. See Figure 4. To run the algorithm, we actually maintain, in each gap between two consecutive leaves of our bush, a label of the form (u, ρ) , with $u \in [n]$ and $\rho \in \mathbb{N}$. We also include the label $(0, 0)$ before the first leaf and the label $(n + 1, 0)$ after the last leaf.

Definition 4. For each $\mathbf{x} \in \mathbb{R}^n$, we construct an s -bush $B(s, \mathbf{x})$ inductively as follows:

- start with the rooted graph with just a root, no internal node, and a single leaf,
- at step j ,
 - attach a new node j either to the leaf between two gap labels (u, ρ) and (v, σ) such that $x_u - \rho < x_j < x_v - \sigma$, or to the two leaves around a gap label (w, τ) such that $x_j = x_w - \tau$, (with the convention that $x_0 = -\infty$ and $x_{n+1} = +\infty$),
 - attach $s_j + 1$ leaves to the node j , with gaps labeled by $(j, s_j - 1), \dots, (j, 1), (j, 0)$ (except, if $s_j = 0$ and j has indegree 2, then we attach 2 leaves with gap label $(j, 0)$),
 - add $\max(0, s_j - 1)$ to the second entry of all gap labels on the left of j .

This algorithm is illustrated in Figure 4.

Remark 5. A few observations on Definition 4:

- (1) The crucial invariant of the algorithm is that the values $x_u - \rho$ for the gap labels (u, ρ) are always strictly increasing from left to right. This invariant is maintained by the shifts performed on gap labels at each step. It implies that the attaching step is well-defined.
- (2) The gap labels only depend on the s -bush $B(s, \mathbf{x})$, not on the exact values of \mathbf{x} .
- (3) For $j \in [n]$, deleting all nodes $> j$ in $B(s, \mathbf{x})$ gives $B(s_{\leq j}, \mathbf{x}_{\leq j})$.
- (4) If \mathbf{x} is generic enough (e.g. if $x_i - x_j \notin \mathbb{N}$ for $1 \leq i < j \leq n$), then $B(s, \mathbf{x})$ is an s -tree.
- (5) When $s = 1^n$ and \mathbf{x} is generic, this is the classical insertion in an increasing binary tree.

1.4. s -insertion fibers. We now consider the fibers of the s -insertion algorithm of Section 1.3.

Definition 6. For an s -bush B , the *fiber* of B is $\mathbb{F}_B := \{\mathbf{x} \in \mathbb{R}^n \mid B(s, \mathbf{x}) = B\}$, and the *closed fiber* of B is the closure $\bar{\mathbb{F}}_B$ of \mathbb{F}_B .

For instance, the fiber \mathbb{F}_B of the s -bush on the right of Figure 4 is the set of points $\mathbf{x} \in \mathbb{R}^9$ that satisfy the indicated equalities and inequalities, and the closed fiber $\bar{\mathbb{F}}_B$ is obtained by replacing the strict inequalities by large inequalities. We thus get the following observation.

Lemma 7. *The closed fiber $\bar{\mathbb{F}}_B$ of any s -bush B is a polyhedron.*

Proof. The fiber \mathbb{F}_B is a (relatively open) polyhedron, defined by the inequalities $x_u - \rho < x_j < x_v - \sigma$ and the equalities $x_j = x_w - \tau$ from Definition 4. Hence, the closed fiber $\bar{\mathbb{F}}_B$ is a polyhedron. \square

We now aim at an irredundant equality and inequality description of the closed fiber $\bar{\mathbb{F}}_B$ of an s -bush B . It is convenient to introduce the following definitions, illustrated in Example 13.

Definition 8. A *hole* of an s -bush B is a pair (i, j) of nodes such that j has two incoming edges whose greatest common ancestor is i .

Definition 9. The *left* (resp. *right*) *zigzag* of a node j of an s -bush B is the increasing path Z that follows the leftmost (resp. rightmost) increasing path of B starting at j until it reaches either a leaf, or a node k with two distinct parents, in which case it continues with the right (resp. left) zigzag of k . The nodes where Z exits through the leftmost (resp. rightmost) edge are the *zig* (resp. *zag*) nodes of Z .

Definition 10. An *ascent* (resp. *descent*) of an s -bush B is a pair (i, j) of nodes of B such that

- j has indegree 1,
- i is the greatest ancestor of j such that the leftmost (resp. rightmost) increasing path from i to j in B takes the leftmost (resp. rightmost) outgoing edge at each node, except at node i ,
- either $s_j = 0$ or all nodes along the left (resp. right) zigzag of j have indegree 2.

Remark 11. For s -trees, our definition of ascents and descents specializes to [CP24a, Def. 1.24]. Namely, (i, j) is an ascent (resp. descent) of an s -tree T if

- i is an ancestor of j and the increasing path from i to j in T takes the leftmost (resp. rightmost) outgoing edge at each node, except at node i ,
- either $s_j = 0$ or the leftmost (resp. rightmost) edge of j is a leaf.

Definition 12. Consider an s -bush B and $1 \leq i < j \leq n$ such that i is an ancestor of j . Let π be the leftmost (resp. rightmost) increasing path in B from i to j , and arriving through the right (resp. left) incoming edge of j if (i, j) is a hole of B . We define $\mu(B, i, j)$ (resp. $\nu(B, i, j)$) as $r - 1 + \sum_{k \in K} \max(0, s_k - 1)$ where r is the number of children of i weakly (resp. strictly) to the right of π , and K is the set of nodes $i < k < j$ and weakly (resp. strictly) to the right of π . Note that $\mu(B, i, j) \leq \nu(B, i, j)$, and $\mu(B, i, j) = \nu(B, i, j)$ if (i, j) is a hole of B .

Example 13. On the rightmost s -bush B of Figure 4,

- the holes are $(2, 4)$, $(1, 5)$, and $(5, 6)$,
- the left zigzag of 2 is $2 \rightarrow 4 \rightarrow 5 \rightarrow 6$ and the right zigzag of 3 is $3 \rightarrow 5 \rightarrow 8 \rightarrow 9$,
- the ascents are $(1, 2)$, $(4, 7)$, $(3, 9)$ and the descents are $(2, 7)$, $(5, 8)$ and $(8, 9)$,
- $\mu(B, 1, 5) = \nu(B, 1, 5) = 1$, $\mu(B, 3, 9) = 3$, $\nu(B, 2, 7) = 0$,
- the closed fiber $\bar{\mathbb{F}}_B$ is the polyhedron defined by the equalities $x_2 - x_4 = 1$, $x_1 - x_5 = 1$, $x_5 - x_6 = 0$ and the inequalities $x_1 - x_2 \leq 0$, $x_4 - x_7 \leq 0$, $x_3 - x_9 \leq 3$, $x_2 - x_7 \geq 0$, $x_5 - x_8 \geq 2$, and $x_8 - x_9 \geq 1$.

Proposition 14. The closed fiber $\bar{\mathbb{F}}_B$ of an s -bush B is irredundantly described by

- an equality $x_i - x_j = \mu(B, i, j)$ for each hole (i, j) of B ,
- an inequality $x_i - x_j \leq \mu(B, i, j)$ for each ascent (i, j) of B ,
- an inequality $x_i - x_j \geq \nu(B, i, j)$ for each descent (i, j) of B .

Proof. Fix $j \in [n]$ and consider the $s_{\leq j-1}$ -bush $B_{\leq j-1}$ with gaps labeled according to the insertion $B(s_{\leq j-1}, \mathbf{x}_{\leq j-1})$ of any $\mathbf{x} \in \mathbb{F}_B$. Observe (by induction on j) that, if (i, σ) is the gap label immediately to the left (resp. right) of a leaf ℓ of $B_{\leq j-1}$, then

- The leftmost (resp. rightmost) increasing path from i to ℓ takes the leftmost (resp. rightmost) outgoing edge at each node, except at i . We say that i is the *left* (resp. *right*) *ancestor* of ℓ .
- $\sigma = r - 1 + \sum_{k \in K} \max(0, s_k - 1)$ where r is the number of children of i and K the set of nodes $i < k < j$, all located weakly (resp. strictly) to the right of the leftmost (resp. rightmost) increasing path in B from i to ℓ .

Assume now that j is attached to the two leaves ℓ, ℓ' around a gap label (w, τ) of $B_{\leq j-1}$. Then w is the greatest common ancestor of ℓ and ℓ' in B (by (a)), and $\tau = \mu(B, w, j) = \nu(B, w, j)$ (by (b)). Hence, the corresponding equation $x_j = x_w - \tau$ of \bar{F}_B is indeed of the form $x_i - x_j = \mu(B, i, j)$ for a hole (i, j) of B .

Assume now that j is attached to a leaf ℓ between two gap labels (u, ρ) and (v, σ) of $B_{\leq j-1}$. Then u is the left ancestor of j (by (a)), and $\rho = \mu(B, u, j)$ (by (b)). Moreover, if $s_j \neq 0$ and h lies on the left zigzag Z of j , then $x_u - \mu(B, u, j) - \zeta \leq x_h \leq x_j - \zeta$, with $\zeta = \sum_{k \in K} \max(0, s_k - 1)$ where K is the set of nodes $j \leq k < h$ on the right of Z , including the zig nodes of Z , but not the zag nodes of Z . If the node h has indegree 1, then both inequalities are strict on F_B , so that the inequality $x_u - \mu(B, u, j) \leq x_j$ is actually redundant. The same arguments hold for the inequality $x_j \leq x_v - \nu(B, v, j)$. We conclude that all facet defining inequalities of \bar{F}_B are of the form $x_i - x_j \leq \mu(B, i, j)$ for an ascent (i, j) of B , or $x_i - x_j \geq \nu(B, i, j)$ for a descent (i, j) of B .

Finally, we need to prove that our system of equalities and inequalities is irredundant. The equalities are irredundant because they are echeloned. For the inequalities, we choose for instance an ascent (i, j) of B , and we prove that there is $\mathbf{x} \in \bar{F}_B$ for which the inequality $x_i - x_j \leq \mu(B, i, j)$ is the only tight inequality in our system. For this, start with \mathbf{y} in the interior of F_B (so that all our inequalities are strict), and let $\delta = y_i - y_j - \mu(B, i, j)$. Let Z be the left zigzag of j , and J be the set of zig nodes of Z . Consider the point $\mathbf{x} := \mathbf{y} + \delta \sum_{j \in J} \mathbf{e}_j$. As $i \notin J$ while $j \in J$, we have $x_i - x_j = y_i - y_j - \delta = \mu(B, i, j)$. Finally, we let the reader check that \mathbf{x} satisfies the equalities given by all holes of B and strictly satisfies all inequalities given by the other ascents and descents of B . \square

Corollary 15. *The dimension of \bar{F}_B is the rank of B .*

Proof. By Proposition 14, the codimension of \bar{F}_B is the number of indegree 2 nodes of B . Hence the dimension is the number of indegree 1 nodes of B , thus the rank of B . \square

Example 16. Recall from Remark 2(6) that for $\mathbf{q} \in \Lambda_s$, we denote by $T_{\mathbf{q}}$ the s -trunk obtained by attaching node i to leaves q_i and q_i+1 (or to the only leaf if there is only one). Its insertion fiber $F_{T_{\mathbf{q}}}$ is the affine subspace of dimension $n+T_n-S_n$, defined by the equations $x_1 - x_j = \mu(T_{\mathbf{q}}, 1, j) = q_j - 1$ for all $j \in [n]$ such that $T_{j-1} \geq 2$. Hence, the insertion fibers of the s -trunks form a grid in the basis $x_1 - x_j$. This is visible in Figure 5.

1.5. **s -foam.** We now consider the collection of all s -insertion fibers.

Definition 17. The **s -foam** is the collection \mathcal{F}_s of closed fibers \bar{F}_B of all s -bushes B .

Some s -foams are illustrated in Figure 5. As $B(s, \mathbf{x} + \lambda \sum_{i \in [n]} \mathbf{e}_i) = B(s, \mathbf{x})$ for any $\lambda \in \mathbb{R}$, all fibers contain the line $\mathbb{R} \sum_{i \in [n]} \mathbf{e}_i$ in their lineality space, hence we intersect the s -foams with the hyperplane $\{\mathbf{x} \in \mathbb{R}^n \mid \sum_{i \in [n]} x_i = 0\}$ in all illustrations. We need the following property of the s -foam.

Proposition 18. *Any face of a closed fiber \bar{F}_B is a closed fiber $\bar{F}_{B'}$.*

Proof. Consider a facet G of a closed fiber \bar{F}_B . We will prove that $G = \bar{F}_{B'}$ where $B' := B(s, \mathbf{g})$ for an arbitrary \mathbf{g} in the relative interior of G . This shows the statement by induction on the dimension (since any face of \bar{F}_B is a face of a facet of \bar{F}_B).

Let H be the affine span of \bar{F}_B , let H' be the affine span of G , and let H^+ be the half-space of H defined by H' and containing \bar{F}_B (this is well-defined since G is a facet of \bar{F}_B). Pick a generic $\mathbf{x}' \in H'$ and then some $\mathbf{x} \in H^+$ close enough to \mathbf{x}' so that $x'_i < x'_j - \sigma$ implies $x_i < x_j - \sigma$ for any $i, j \in [n]$ and $0 \leq \sigma \leq S_n$ (this is possible as we have finitely many open conditions).

For $j \in [n]$, consider the $s_{\leq j}$ -bushes $B_j := B(s_{\leq j}, \mathbf{x}_{\leq j})$ and $B'_j := B(s_{\leq j}, \mathbf{x}'_{\leq j})$. Let i be the minimal index such that $B_i \neq B'_i$. Hence, there is a gap label (u, ρ) in $B_{i-1} = B'_{i-1}$ such that $x_i \neq x_u - \rho$ while $x'_i = x'_u - \rho$. Assume for instance $x_i < x_u - \rho$ (the other case is similar).

We claim that we can reconstruct the sequence B_1, \dots, B_n from the sequence B'_1, \dots, B'_n and *vice versa*. To see it, we prove by induction that, for any $j > i$,

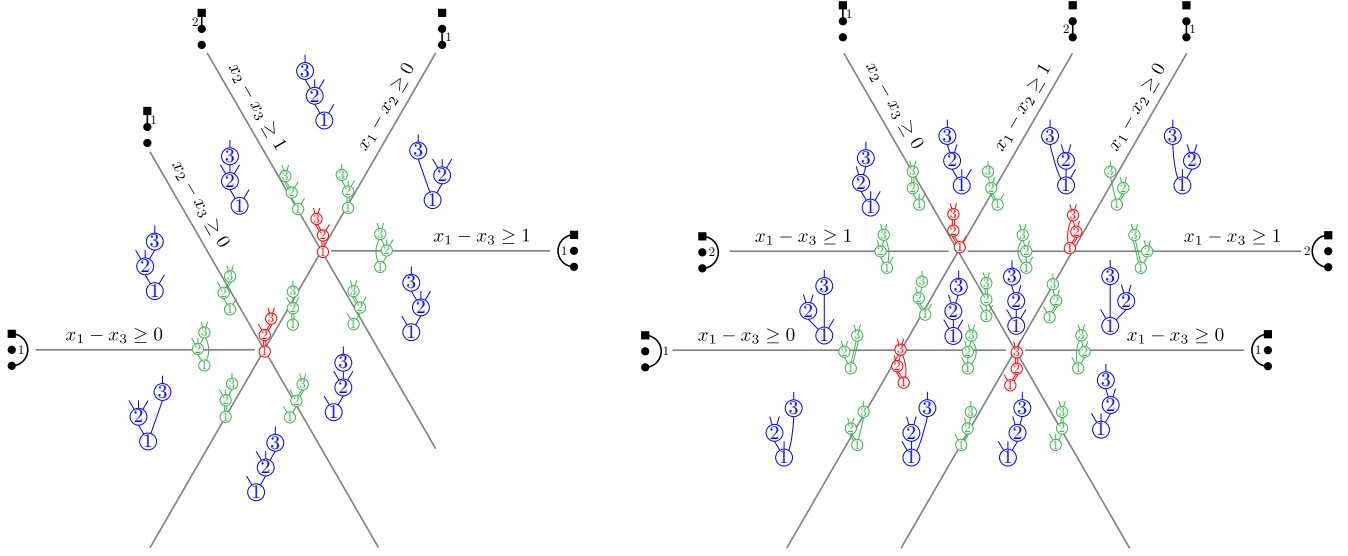


FIGURE 5. The \mathbf{s} -foam for $\mathbf{s} = (1, 2, 0)$ (left) and $\mathbf{s} = (2, 1, 0)$ (right).

- (a) the gap labels in \mathbf{B}_j are precisely the gap labels in \mathbf{B}'_j , except that one gap label of the form (u, ρ') in \mathbf{B}_j may disappear in \mathbf{B}'_j ,
- (b) if a gap label (u, ρ') of \mathbf{B}_j does not appear in \mathbf{B}'_j , then the gap label (v, σ) immediately to the left of (u, ρ') in \mathbf{B}_j is such that $x'_v - \sigma = x'_u - \rho'$,
- (c) the position of $j + 1$ in \mathbf{B}_{j+1} determines the position of $j + 1$ in \mathbf{B}'_{j+1} and *vice versa*.

Note that (a) and (b) hold for $j = i$. Indeed, the gap (u, ρ) of \mathbf{B}_i has disappeared in \mathbf{B}'_i , the gap immediately to its left is $(i, 0)$, and we have $x'_i - 0 = x'_u - \rho$. Assume now that (a) and (b) hold for some $j > i$. For any gap label (w, τ) common to \mathbf{B}_j and \mathbf{B}'_j , we have

- $x_{j+1} = x_w - \tau \iff x'_{j+1} = x'_w - \tau$. Indeed, let \mathbb{K} be the hyperplane of equation $y_{j+1} = y_w - \tau$. If $x_{j+1} = x_w - \tau$, then $\mathbb{H} \subseteq \mathbb{K}$, so that $x'_{j+1} = x'_w - \tau$. Conversely, if $x'_{j+1} = x'_w - \tau$, then $\mathbb{H}' \subseteq \mathbb{K}$, so that $\mathbb{H} \subseteq \mathbb{K}$ (otherwise, \mathbb{H}' would have codimension at least 2 in \mathbb{H} , since \mathbf{x}' is generic in \mathbb{H}'), hence $x_{j+1} = x_w - \tau$.
- $x_{j+1} < x_w - \tau \iff x'_{j+1} < x'_w - \tau$ by our assumption that \mathbf{x} is close enough to \mathbf{x}' .

Assume now that some gap label (u, ρ') in \mathbf{B}_j disappeared in \mathbf{B}'_j , and let (v, σ) be the gap label immediately to its left in \mathbf{B}_j , so that $x'_v - \sigma = x'_u - \rho'$ by (b). Assume that $x_v - \sigma \leq x_{j+1} \leq x_u - \rho'$. As \mathbf{x} is close enough to \mathbf{x}' , we also have $x'_v - \sigma \leq x'_{j+1} \leq x'_u - \rho'$. As $x'_v - \sigma = x'_u - \rho'$, we obtain that $x'_{j+1} = x'_v - \sigma$. Since (v, σ) is a common gap label in \mathbf{B}_j and \mathbf{B}'_j , this implies that $x_v - \sigma = x_u - \rho'$. We thus obtain that $j + 1$ cannot be attached only to the leaf between the gap labels (v, σ) and (u, ρ') , nor to the two leaves around the gap label (u, ρ') . We conclude that the position of $j + 1$ in \mathbf{B}_{j+1} determines the position of $j + 1$ in \mathbf{B}'_{j+1} and *vice versa*, so that (c) holds for j . This in turn implies that (a) and (b) hold for $j + 1$ since we shift a gap label common to \mathbf{B}_j and \mathbf{B}'_j by the same quantity to obtain the corresponding gap label common to \mathbf{B}_{j+1} and \mathbf{B}'_{j+1} .

We now consider the facet \mathbb{G} of $\bar{\mathbb{F}}_{\mathbf{B}}$. We pick an arbitrary \mathbf{g} in the relative interior of \mathbb{G} , and choose \mathbf{f} close enough to \mathbf{g} such that $\mathbf{f} \in \mathbb{F}_{\mathbf{B}}$. We prove that $\mathbb{G} = \bar{\mathbb{F}}_{\mathbf{B}'}$ where $\mathbf{B}' := \mathbf{B}(\mathbf{s}, \mathbf{g})$.

Observe first that, for any \mathbf{x}' in the interior of \mathbb{G} , we can choose \mathbf{x} close enough to \mathbf{x}' such that $\mathbf{x} \in \mathbb{F}_{\mathbf{B}}$. As we proved that $\mathbf{B}(\mathbf{s}, \mathbf{x}')$ is determined by $\mathbf{B}(\mathbf{s}, \mathbf{x}) = \mathbf{B} = \mathbf{B}(\mathbf{s}, \mathbf{f})$, we obtain that $\mathbf{B}(\mathbf{s}, \mathbf{x}') = \mathbf{B}(\mathbf{s}, \mathbf{g}) = \mathbf{B}'$. Hence, the interior of \mathbb{G} is contained in $\mathbb{F}_{\mathbf{B}'}$.

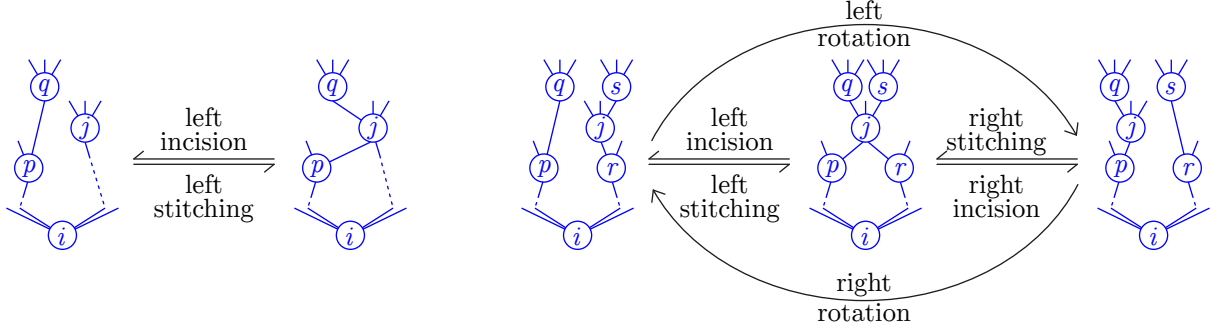


FIGURE 6. The left stitching and incision of Definitions 20 and 21 (left) and the left and right rotations of Definition 23.

Conversely, consider any \mathbf{x}' in $\mathbb{F}_{B'}$, and let \mathbf{x} in \mathbb{H}^+ be close enough to \mathbf{x}' . Since $B(\mathbf{s}, \mathbf{x})$ is determined by $B(\mathbf{s}, \mathbf{x}') = B' = B(\mathbf{s}, \mathbf{g})$, we obtain that $B(\mathbf{s}, \mathbf{x}) = B(\mathbf{s}, \mathbf{f}) = B$. Hence, \mathbf{x}' lies on the boundary of \mathbb{F}_B . We conclude that the interior of $\mathbb{F}_{B'}$ is contained in G . \square

Proposition 19. *The \mathbf{s} -foam \mathcal{F}_s is a **complete polyhedral complex** (i.e. a set of polyhedra closed under faces, pairwise intersecting along faces, and whose union completely covers \mathbb{R}^n).*

Proof. We already observed that the closed fibers are polyhedra (Lemma 7), and that their faces are closed fibers (Proposition 18). The fibers (and thus their closures) cover \mathbb{R}^n as the insertion algorithm is defined on \mathbb{R}^n . We thus just need to prove that the intersection X of two closed fibers $\bar{\mathbb{F}}_B$ and $\bar{\mathbb{F}}_{B'}$ is a face of both. For this, consider $\mathbf{x} \in X$, and let $B'' := B(\mathbf{s}, \mathbf{x})$. Since $\mathbf{x} \in \bar{\mathbb{F}}_B$, Proposition 18 implies that $\bar{\mathbb{F}}_{B''}$ is a face of $\bar{\mathbb{F}}_B$ (possibly $\bar{\mathbb{F}}_B$ itself). We thus obtain that $\bar{\mathbb{F}}_{B''}$ is contained in X . Hence, X is a union of faces of $\bar{\mathbb{F}}_B$. As it is convex, it is actually a face of $\bar{\mathbb{F}}_B$ (possibly $\bar{\mathbb{F}}_B$ itself). By symmetry, it is also a face of $\bar{\mathbb{F}}_{B'}$ (possibly $\bar{\mathbb{F}}_{B'}$ itself). \square

1.6. \mathbf{s} -rotations. We now describe the dual graph of the \mathbf{s} -foam \mathcal{F}_s . For this, we describe two operations, which are obviously inverse to each other, as illustrated in Figure 6 (left).

Definition 20. Let (i, j) be an ascent (resp. descent) in an \mathbf{s} -tree T . Let $p \rightarrow q$ be the last edge whose source is smaller than j along the rightmost (resp. leftmost) increasing path leaving i through the edge immediately to the left (resp. right) of the path from i to j (note that q might be a leaf). The **stitching** of (i, j) in T is the \mathbf{s} -bush B obtained from T by replacing the edge $p \rightarrow q$ by $p \rightarrow j$ and the leftmost (resp. rightmost) outgoing edge of j (which is a leaf) by $j \rightarrow q$.

Definition 21. Consider an \mathbf{s} -bush B with a single hole (i, j) . Let $p \rightarrow j$ and $j \rightarrow q$ denote the leftmost (resp. rightmost) incoming and outgoing edges at j (note that q can be a leaf). The **left** (resp. **right**) **incision** of B is the \mathbf{s} -tree T obtained from B by replacing the edge $p \rightarrow j$ by $p \rightarrow q$ and the edge $j \rightarrow q$ by a leaf at j .

Proposition 22. *If (i, j) is an ascent (resp. descent) in an \mathbf{s} -tree T , and B is the stitching of (i, j) in T , then $\bar{\mathbb{F}}_B$ is the facet of $\bar{\mathbb{F}}_T$ corresponding to (i, j) . If an \mathbf{s} -bush B has a single hole, and T and T' are the left and right incisions of B , then $\bar{\mathbb{F}}_T$ and $\bar{\mathbb{F}}_{T'}$ are the two facets of \mathcal{F}_s containing $\bar{\mathbb{F}}_B$.*

Proof. If B is the stitching of an ascent (resp. descent) (i, j) in an \mathbf{s} -tree T , then (i, j) is the only hole of B , so that $\bar{\mathbb{F}}_B$ satisfies the single equation $x_i - x_j = \mu(B, i, j) = \nu(B, i, j)$, and we have $\mu(B, i, j) = \mu(T, i, j)$ (resp. $\nu(B, i, j) = \nu(T, i, j)$). Moreover, as in the proof of Proposition 18, an immediate induction shows that, for any $k \geq j$, the gap labels in $T_{\leq k}$ and $B_{\leq k}$ are identical, except that a gap label (i, ρ) of T disappears in B . Hence, we obtain that $\bar{\mathbb{F}}_B$ satisfies the same inequalities as $\bar{\mathbb{F}}_T$. We conclude that $\bar{\mathbb{F}}_B$ is the facet of $\bar{\mathbb{F}}_T$ defined by $x_i - x_j = \mu(B, i, j)$.

Conversely, if an \mathbf{s} -bush B has a single hole, then $\bar{\mathbb{F}}_B$ is a codimension 1 polyhedron of the \mathbf{s} -foam \mathcal{F}_s . As \mathcal{F}_s is a complete polyhedral complex, $\bar{\mathbb{F}}_B$ is contained in precisely two full-dimensional polyhedra of \mathcal{F}_s . Since the stitching and incision operations are clearly inverse to

each other, the first part of the statement implies that $\bar{\mathbb{F}}_T$ and $\bar{\mathbb{F}}_{T'}$ are the two facets of \mathcal{F}_s containing $\bar{\mathbb{F}}_B$. \square

We now connect incisions and stitchings with the following operations, adapted from the description of [CP24a], and illustrated in Figure 6 (right).

Definition 23 ([CP24a, Def. 1.30]). Consider an ascent (resp. descent) (i, j) in an s -tree T . Let r be the parent of j (note that r might be i). Let $j \rightarrow s$ be the rightmost (resp. leftmost) outgoing edge of j (note that s might be a leaf). Let $p \rightarrow q$ be last edge whose source is smaller than j along the rightmost (resp. leftmost) increasing path leaving i through the edge immediately to the left (resp. right) of the path from i to j (note that q might be a leaf). The *left* (resp. *right*) *rotation* of (i, j) transforms T by replacing the edges $r \rightarrow j$, $j \rightarrow s$ and $p \rightarrow q$ by new edges $r \rightarrow s$, $j \rightarrow q$ and $p \rightarrow j$ respectively.

Lemma 24. A left (resp. right) rotation is the composition of an ascent (resp. descent) stitching of Definition 20 with a right (resp. left) incision of Definition 21.

Corollary 25. The dual graph of the s -foam is the rotation graph on s -trees. Its incidence graph is the incision (or equivalently stitching) graph.

Remark 26. More generally, given an s -bush B , the combinatorial description of the s -bushes B' such that $\mathbb{F}_{B'}$ is a face of \mathbb{F}_B is quite technical. Namely, the s -bushes B' such that $\mathbb{F}_{B'}$ is a facet of \mathbb{F}_B are obtained by selecting an ascent or a descent (i, j) of B and performing a technical sewing process along (i, j) .

In contrast, given an s -bush B' , the combinatorial description of which are the s -bushes B such that $\mathbb{F}_{B'}$ is a face of \mathbb{F}_B is easier. Let j be an indegree 2 node of B' , and let $i \rightarrow j$ and $j \rightarrow k$ denote the leftmost (resp. rightmost) incoming and outgoing edges at j (note that k can be leaf). A *left* (resp. *right*) *incision* of B' at j is an s -bush B obtained as follows:

- replace the edge $i \rightarrow j$ by $i \rightarrow k$,
- if the two leftmost (resp. rightmost) outgoing edges of j have a lowest common descendant ℓ , then perform a (left or right) incision at ℓ and replace the edge $j \rightarrow k$ by $j \rightarrow \ell$,
- otherwise, replace the edge $j \rightarrow k$ by a leaf.

Then $\mathbb{F}_{B'}$ is a facet of \mathbb{F}_B if and only if B is obtained by some incision at an indegree 2 node of B' . Hence, $\mathbb{F}_{B'}$ is a face of \mathbb{F}_B if and only if B is obtained by a sequence of incisions in B' . We skip the proof of this description as we will not need it in the remaining of the paper.

Remark 27. Given an s -bush B' , we denote by $T(B')$ the set of s -trees T such that $\mathbb{F}_{B'}$ is a face of \mathbb{F}_T . In other words, all s -trees obtained by performing left or right incisions at all indegree 2 nodes of B' . We distinguish two particular s -trees of $T(B')$: the *left tree* $L(B')$ obtained by performing only left incisions, and the *right tree* $R(B')$ obtained by performing only right incisions. In other words, if $\mathbf{x}' \in \mathbb{F}_{B'}$, then $L(B') = B(\mathbf{s}, \mathbf{x}' + \varepsilon \boldsymbol{\omega})$ and $R(B') = B(\mathbf{s}, \mathbf{x}' - \varepsilon \boldsymbol{\omega})$ for a sufficiently small $\varepsilon > 0$ and $\boldsymbol{\omega} := (1, 2, \dots, n) - (n, \dots, 2, 1) = \sum_{1 \leq i < j \leq n} \mathbf{e}_j - \mathbf{e}_i = \sum_{i \in [n]} (2i - n - 1) \mathbf{e}_i$. Note that the holes, ascents and descents of B' can be derived from the ascents and descents of $L(B')$ and $R(B')$. Namely, the holes of B' are the ascents of $L(B')$ that are also descents of $R(B')$, the ascents of B' are the ascents of $R(B')$, and the descents of B' are the descents of $L(B')$. In fact, $T(B')$ is actually the interval $[L(B'), R(B')]$ in the s -weak order (defined in the next section). These intervals are called pure intervals in [CP24b]. Such an interval is also determined by the s -tree $L(B')$ (resp. $R(B')$) together with a subset of its ascents (resp. descents). To sum up, there are bijections between the s -bushes, the faces of the s -foam, the pure intervals of [CP24b], and the pairs (T, A) where A is a subset of ascents (resp. descents) of an s -tree T .

2. THE s -WEAK ORDER AND FACIAL s -WEAK ORDER

In this section, we consider the s -weak order W_s on s -trees (directly adapted from the original definition of [CP24a]), and we extend it to the facial s -weak order FW_s on all s -bushes. We prove that these two posets are actually congruence uniform lattices by exhibiting a construction by interval doublings (recovering a result of [CP24a] for the s -weak order).

2.1. Recollections 2: The weak order and facial weak order. We first remind basic properties of the weak order on permutations of $[n]$ and the facial weak order on ordered set partitions of $[n]$.

2.1.1. Lattices and interval doublings. A *lattice* (L, \leq, \wedge, \vee) is a poset (L, \leq) where any subset X admits a *meet* $\bigwedge X$ (greatest lower bound) and a *join* $\bigvee X$ (least upper bound). Particularly interesting lattices are semidistributive and congruence uniform lattices, whose definitions are delayed to Sections 3.1 and 4.1, where we will have introduced more lattice theoretic background. We just note here that congruence uniformity implies semidistributivity.

The *doubling* of a subset X of a poset P is the poset $P[X]$ on $(P \setminus X) \sqcup (X \times \{0, 1\})$ defined by

- $a \leq b$ in $P[X]$ if $a, b \notin X$ and $a \leq b$ in P ,
- $(a, i) \leq b$ in $P[X]$ if $a \in X$, $b \notin X$, $i \in \{0, 1\}$, and $a \leq b$ in P ,
- $a \leq (b, j)$ in $P[X]$ if $a \notin X$, $b \in X$, $j \in \{0, 1\}$, and $a \leq b$ in P ,
- $(a, i) \leq (b, j)$ in $P[X]$ if $a, b \in X$, $i, j \in \{0, 1\}$, and $a \leq b$ in P and $i \leq j$.

Recall that $C \subseteq P$ is *order convex* if $x \leq y \leq z$ and $x, z \in C$ implies $y \in C$, and that an *interval* of P is a subset of the form $[x, z] := \{y \in P \mid x \leq y \leq z\}$. A. Day [Day94] observed that if L is a lattice and $C \subseteq L$ is order convex, then $L[C]$ is again a lattice. In fact, a lattice is congruence normal (resp. uniform) if and only if it can be obtained from a distributive lattice by a sequence of doublings of order convex sets (resp. of intervals).

2.1.2. The weak order. We now remind basic properties of the weak order on permutations and of the facial weak order on ordered partitions, and show that they are constructible by interval doublings. The *inversion set* of a permutation σ of $[n]$ is $\text{inv}(\sigma) := \{(\sigma_i, \sigma_j) \mid 1 \leq i < j \leq n \text{ and } \sigma_i > \sigma_j\}$. The *weak order* W_n is the partially ordered set of permutations of $[n]$ ordered by inclusion of their inversion sets. Its cover relations are given by transpositions of adjacent entries (meaning at two consecutive positions). See Figure 7. The weak order is known to be a congruence uniform lattice [GR63, DC94, LCdPB94].

As we will mimic it for the *s*-weak order and facial *s*-weak order, we now present a construction of the weak order by interval doublings, closely related to the insertion algorithm of Section 1. By induction, it suffices to exhibit a sequence of interval doublings from the weak order W_{n-1} to the weak order W_n . We denote by $\bar{\sigma}$ the permutation of $[n-1]$ obtained by deleting the entry n in a permutation σ of $[n]$. For any $i \in [n]$, we denote by W_n^i the poset obtained from the weak order W_n by identifying two permutations σ and σ' if and only if $\bar{\sigma} = \bar{\sigma}'$ and the relative position of k and n are the same in σ and σ' , for all $n-i < k < n$. Note that W_n^1 is isomorphic to the weak order W_{n-1} and W_n^n is just the weak order W_n . For instance, Figure 8 represents the

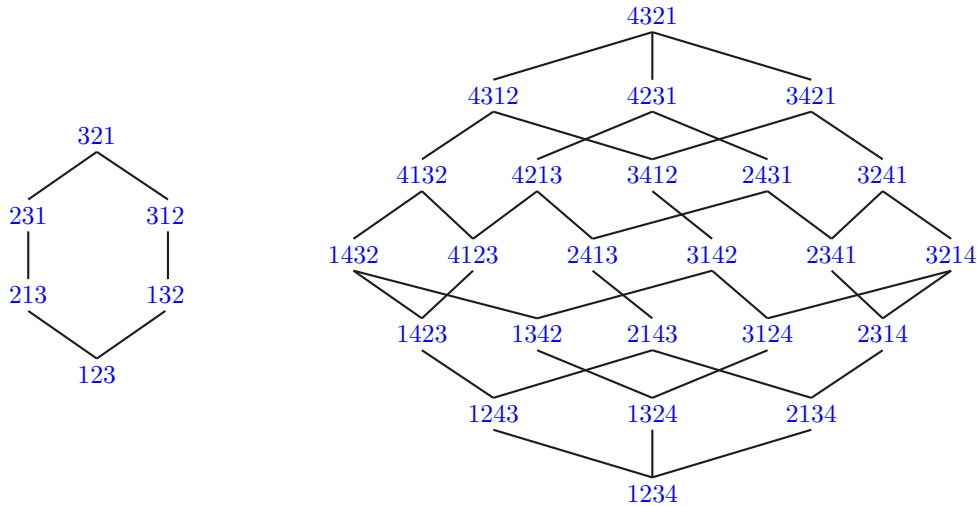


FIGURE 7. The weak order W_n for $n = 3$ (left) and $n = 4$ (right).

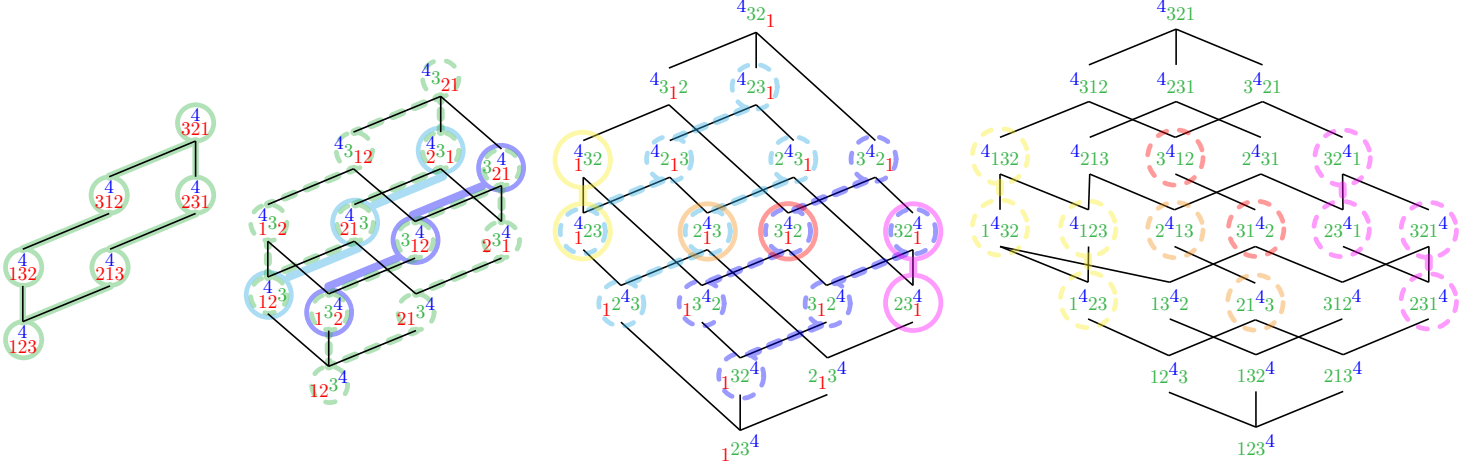


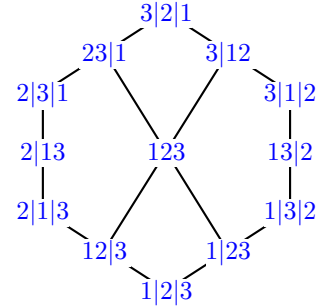
FIGURE 8. Interval doublings from the weak order W_3 (left) to the weak order W_4 (right). The four lattices are $W_3 \simeq W_4^1$, W_4^2 , W_4^3 , and $W_4^4 = W_4$. We bold some intervals of W_4^{i-1} and dash the corresponding doubled intervals in W_4^i .

posets W_4^i for $i = 1, \dots, 4$. In this picture, we represent an element of W_n^i , on three lines (red, green, blue). The red line contains $[n-i-1]$, the green line contains $[n-i, n]$, and the blue line just contains n . The red and green lines form the permutation $\bar{\sigma}$, the green and blue lines record the relative position of k and n for all $n-i < k \leq n$, while the red and blue lines are incomparable.

We claim that W_n^{i+1} is obtained from W_n^i by interval doublings. Consider $U := \{u_1 < \dots < u_p\}$ and $V := \{v_1 < \dots < v_q\}$ such that $U \sqcup V =]n-i, n[$. Let $\tilde{\sigma}_{U,V}^i$ (resp. $\tilde{\tau}_{U,V}^i$) denote the class in W_n^i of the permutations σ (resp. τ) of $[n]$ such that $\bar{\sigma} = [1, \dots, n-i-1, u_1, \dots, u_p, n-i, v_1, \dots, v_q]$ (resp. $\bar{\tau} = [u_p, \dots, u_1, n-i, v_q, \dots, v_1, n-i-1, \dots, 1]$) and where n is to the right of any $u \in U$ and to the left of any $v \in V$. We invite the reader to check that W_n^{i+1} is obtained from W_n^i by doubling, for all $U \sqcup V =]n-i, n[$, the interval $[\tilde{\sigma}_{U,V}^i, \tilde{\tau}_{U,V}^i]$ in W_n^i to the intervals $[\tilde{\sigma}_{U \cup \{n-i\}, V}^{i+1}, \tilde{\tau}_{U \cup \{n-i\}, V}^{i+1}]$ and $[\tilde{\sigma}_{U, V \cup \{n-i\}}^{i+1}, \tilde{\tau}_{U, V \cup \{n-i\}}^{i+1}]$ in W_n^{i+1} . These interval doublings are illustrated in Figure 8.

2.1.3. The facial weak order. Finally, we briefly describe the facial weak order. It is a lattice structure on all cones of the braid arrangement, or equivalently, on all faces of the permutahedron, which extends the weak order. It is illustrated on the right for $n = 3$. It was introduced for the braid arrangement in [KLN⁺01, BHKN01], studied for arbitrary Coxeter arrangements in [PR06, DHP18], and extended even further in [DHMP22, Han24]. The *facial weak order* FW_n is the partial order on ordered set partitions of $[n]$ where $\mu \leq \nu$ if the following equivalent assertions holds:

- $\min(\mu) \leq \min(\nu)$ and $\max(\mu) \leq \max(\nu)$, where $\min(\mu)$ and $\max(\mu)$ respectively denote the weak order minimal and maximal permutations refining μ ,
- $\text{inv}(\mu) \subseteq \text{inv}(\nu)$ and $\text{ninv}(\mu) \supseteq \text{ninv}(\nu)$, where $\text{inv}(\mu)$ (resp. $\text{ninv}(\mu)$) is the set of pairs $i < j$ such that the part of μ containing i is weakly after (resp. before) the part of μ containing j ,
- the corresponding cones C_μ and C_ν of the braid arrangement are connected by a path of pairs (F, G) , where either F is a facet of G with the same weak order maximum, or G is a facet of F with the same weak order minimum.



2.2. The s -weak order. We now define the s -weak order as introduced in [CP24a] (modulo our minor convention changes, see Remark 3).

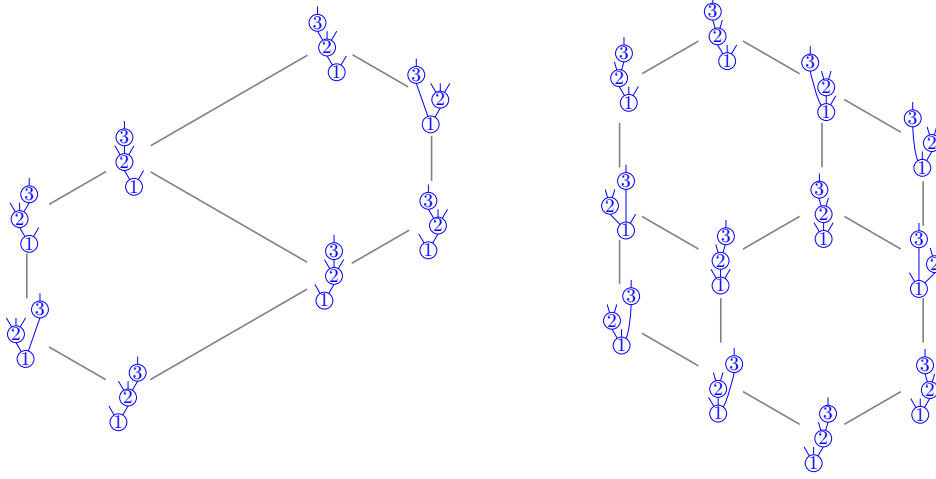


FIGURE 9. The \mathbf{s} -weak order $W_{\mathbf{s}}$ for $\mathbf{s} = (1, 2, 0)$ (left) and $\mathbf{s} = (2, 1, 0)$ (right).

Definition 28 ([CP24a, Def. 1.3]). For an \mathbf{s} -tree T and $1 \leq i < j \leq n$, the *position* $\text{pos}(T, i, j) \in \llbracket s_i \rrbracket$ is the minimum of s_i and the number of outgoing edges of i strictly to the right of the increasing path from the root of T to j .

Lemma 29. For any \mathbf{s} -tree T and $1 \leq i < j < k \leq n$,

$$\text{pos}(T, j, k) > 0 \Rightarrow \text{pos}(T, i, j) \leq \text{pos}(T, i, k) \quad \text{and} \quad \text{pos}(T, j, k) < s_j \Rightarrow \text{pos}(T, i, j) \geq \text{pos}(T, i, k).$$

Proof. If $\text{pos}(T, j, k) > 0$, then j is weakly right of the path from the root of T to k . Hence, the path from the root of T to j is weakly on the right of the path from the root of T to k . By definition, this yields $\text{pos}(T, i, j) \leq \text{pos}(T, i, k)$. The other inequality is similar. \square

Although not strictly necessary in this paper, we recall from [CP24a] that the inequalities of Lemma 29 actually characterize the position vectors of \mathbf{s} -trees.

Proposition 30 ([CP24a, Prop. 1.6]). The following are equivalent for a $\binom{n}{2}$ -tuple $(P_{i,j})_{1 \leq i < j \leq n}$:

- (1) there exists an \mathbf{s} -tree T such that $\text{pos}(T, i, j) = P_{i,j}$ for all $1 \leq i < j \leq n$,
- (2) $0 \leq P_{i,j} \leq s_i$ for all $1 \leq i < j \leq n$, and $P_{j,k} > 0 \Rightarrow P_{i,j} \leq P_{i,k}$ and $P_{j,k} < s_j \Rightarrow P_{i,j} \geq P_{i,k}$ for all $1 \leq i < j < k \leq n$.

The main object of [CP24a, CP24b] is the following order on \mathbf{s} -trees, illustrated in Figure 9.

Definition 31 ([CP24a, Def. 1.9]). The *\mathbf{s} -weak order* $W_{\mathbf{s}}$ is the partially ordered set of \mathbf{s} -trees given by $T \leq T'$ if and only if $\text{pos}(T, i, j) \leq \text{pos}(T', i, j)$ for all $1 \leq i < j \leq n$.

We now describe the cover relations in the \mathbf{s} -weak order in terms of ascents, descents, and rotations (see Definitions 10 and 23 and Remark 11).

Proposition 32 ([CP24a, Thm. 1.32]). If two \mathbf{s} -trees T and T' are related by the rotation of an ascent (i, j) of T to a descent (i, j) of T' , then T is the maximal (resp. T' is the minimal) \mathbf{s} -tree such that $T \leq T'$ and $\text{pos}(T, i, j) < \text{pos}(T', i, j)$.

Proposition 33 ([CP24a, Thm. 1.32]). The \mathbf{s} -trees which cover (resp. are covered by) an \mathbf{s} -tree T in the \mathbf{s} -weak order $W_{\mathbf{s}}$ are precisely those obtained by rotating an ascent (resp. descent) of T .

We obtain the following geometric consequence of Corollary 25 and Proposition 33.

Corollary 34. The Hasse diagram of the \mathbf{s} -weak order $W_{\mathbf{s}}$ is isomorphic to the dual graph of the \mathbf{s} -foam oriented in the direction $\omega := (1, 2, \dots, n) - (n, \dots, 2, 1) = \sum_{1 \leq i < j \leq n} \mathbf{e}_j - \mathbf{e}_i = \sum_{i \in [n]} (2i - n - 1) \mathbf{e}_i$.

Remark 35. We note that C. Ceballos and V. Pons also briefly mention the construction of the “ \mathbf{s} -braid arrangement” in [CP24b, end of Sect. 3.2 & Fig. 27] that seems to coincide with our \mathbf{s} -foam [Pon24]. Note that we prefer the term “foam” to “arrangement” as it is not anymore a hyperplane arrangement (not even affine).

Finally, we state to the key result of [CP24a].

Theorem 36 ([CP24a, Thms. 1.21 & 1.40]). *The \mathbf{s} -weak order $W_{\mathbf{s}}$ is a congruence uniform lattice.*

Remark 37. The proof of the lattice property in [CP24a] actually exploits the characterization of Proposition 30 to explicitly describe the join in the \mathbf{s} -weak order $W_{\mathbf{s}}$. Namely, the join $T \vee T'$ of two \mathbf{s} -trees T and T' satisfies $\text{pos}(T \vee T', i, j) = M_{i,j}^{tc}$ where $M_{i,j} := \max(\text{pos}(T, i, j), \text{pos}(T', i, j))$ and $M_{i,k}^{tc} := \max\{M_{j_0,j_1} \mid i = j_0 < \dots < j_q = k \text{ and } M_{j_p,j_{p+1}} > 0 \text{ for all } p \in [q]\}$ for $1 \leq i < j \leq n$. The congruence uniformity is proved in [CP24a] by showing semidistributivity, and exhibiting a certain edge labeling of the \mathbf{s} -weak order that ensures congruence uniformity. We now give an alternative argument for the congruence uniformity (and hence the semidistributivity) based on interval doublings, which naturally arise from our insertion algorithm, and will be extended to the facial \mathbf{s} -weak order in Section 2.3. We note that C. Ceballos and V. Pons also mention a proof by interval doublings in [CP24a, Rem. 1.41]. Their sequence of doublings can be found in [Pon22, function `lattice_doublings` at line 1489] and seems quite different from ours [Pon24].

Proposition 38. *The \mathbf{s} -weak order $W_{\mathbf{s}}$ is constructible by a sequence of interval doublings.*

Proof sketch. We just give a brief description of the sequence of doublings, generalizing the description of Section 2.1 for the interval doublings in the weak order. Let $\bar{\mathbf{s}} := \mathbf{s}_{\leq n-1} = (s_1, \dots, s_{n-1})$ and denote by \bar{T} the $\bar{\mathbf{s}}$ -tree obtained by deleting the node n in an \mathbf{s} -tree T . For any $i \in [n-1]$ and $j \in [s_{n-i}]$, we denote by $W_{\mathbf{s}}^{i,j}$ the poset obtained from the \mathbf{s} -weak order $W_{\mathbf{s}}$ by identifying two \mathbf{s} -trees T and T' if and only if $\bar{T} = \bar{T}'$, $\text{pos}(T, k, n) = \text{pos}(T', k, n)$ for all $n-i < k < n$, and $\text{pos}(T, n-i, n)$ and $\text{pos}(T', n-i, n)$ either coincide or are both at least j . Note that $W_{\mathbf{s}}^{1,0}$ is isomorphic to the $\bar{\mathbf{s}}$ -weak order $W_{\bar{\mathbf{s}}}$, that $W_{\mathbf{s}}^{n-1,s_1}$ is just the \mathbf{s} -weak order $W_{\mathbf{s}}$, and that $W_{\mathbf{s}}^{i,s_i} = W_{\mathbf{s}}^{i+1,0}$. See Figure 10 for illustrations.

We now observe that we can construct $W_{\mathbf{s}}^{i,j}$ from $W_{\mathbf{s}}^{i,j-1}$ by interval doublings. For $J \subseteq [n]$, the *left* (resp. *right*) *\mathbf{s} -comb* with nodes J is the increasing tree on J , where each node $j \in J$ has $s_j + 1$ outgoing edges, which are all leaves except the leftmost (resp. rightmost). Consider $U := \{u_1 < \dots < u_p\}$ and $V := \{v_1 < \dots < v_q\}$ such that $U \sqcup V =]n-i, n[$. We denote by $S_{U,V}^{i,j}$ the class in $W_{\mathbf{s}}^{i,j}$ of \mathbf{s} -trees S such that \bar{S} is obtained by attaching the right comb with nodes U to the $(j+1)$ -st rightmost outgoing edge of $n-i$ in the right comb with nodes $[n-i-1] \cup V$ and where the node n is attached either to the rightmost leaf of the right comb with nodes U or to leftmost leaf of the j -th rightmost subtree of $n-i$. We denote by $T_{U,V}^{i,j}$ the class in $W_{\mathbf{s}}^{i,j}$ of \mathbf{s} -trees T such that \bar{T} is obtained by attaching the left comb with nodes V to the j -th rightmost outgoing edge of $n-i$ in the left comb with nodes $[n-i-1] \cup U$ and where the node n is attached either to the leftmost leaf of the left comb with nodes V or to the rightmost leaf of the $(j+1)$ -st rightmost subtree of $n-i$. We let the reader check that $W_{\mathbf{s}}^{i,j}$ is obtain from $W_{\mathbf{s}}^{i,j-1}$ by doubling the intervals $[S_{U,V}^{i,j}, T_{U,V}^{i,j}]$ for all $U \sqcup V =]n-i, n[$. \square

2.3. The facial \mathbf{s} -weak order. We now extend the \mathbf{s} -weak order to all \mathbf{s} -bushes (hence, to all polyhedra of the \mathbf{s} -foam $\mathcal{F}_{\mathbf{s}}$). Although it is not required to read the remaining of the paper, we have included this section as the ideas are very similar to that of Section 2.2.

Definition 39. For an \mathbf{s} -bush B and $1 \leq i < j \leq n$, we define the *left* (resp. *right*) *position* $\text{lpos}(B, i, j)$ (resp. $\text{rpos}(B, i, j)$) as follows:

- If i is an ancestor of j , consider the rightmost (resp. leftmost) increasing path π from i to j such that any inner node of π with an incoming edge strictly left (resp. right) of π has an outgoing edge strictly left (resp. right) of π , and define $\text{lpos}(B, i, j)$ (resp. $\text{rpos}(B, i, j)$) as the number of outgoing edges of i strictly left (resp. right) of π .
- Otherwise, define $\text{lpos}(B, i, j) = s_i$ and $\text{rpos}(B, i, j) = 0$ if i is on the left of any increasing path from the root of B to j , and $\text{lpos}(B, i, j) = 0$ and $\text{rpos}(B, i, j) = s_i$ otherwise.

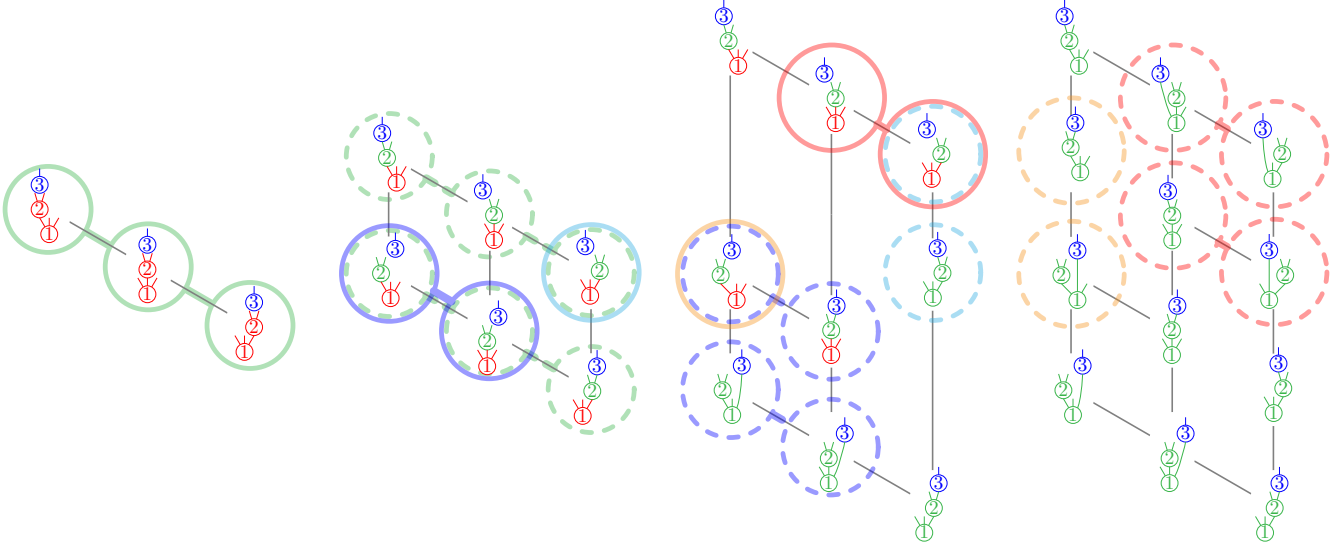


FIGURE 10. Interval doublings from the $(2, 1)$ -weak order (left) to the $(2, 1, 0)$ -weak order (right). The four lattices are $W_{(2,1)} \simeq W_{(2,1,0)}^{1,0}$, $W_{(2,1,0)}^{1,1} = W_{(2,1,0)}^{2,0}$, $W_{(2,1,0)}^{2,1}$, and $W_{(2,1,0)}^{2,2} = W_{(2,1,0)}$.

Remark 40. A few observations on Definition 39:

- Definition 39 contains Definition 28: for all $1 \leq i < j \leq n$, there is at most one increasing path from i to j in an \mathbf{s} -tree T , so that $\text{pos}(T, i, j) = \text{rpos}(T, i, j) = s_i - \text{lpos}(T, i, j)$.
- For any \mathbf{s} -bush B and any $1 \leq i < j \leq n$, we have $0 \leq \text{lpos}(B, i, j), \text{rpos}(B, i, j) \leq s_i$, and $\text{lpos}(B, i, j) + \text{rpos}(B, i, j) \leq s_i + 1$. Moreover, both $\text{lpos}(B, i, j)$ and $\text{rpos}(B, i, j)$ satisfy the conditions of Lemma 29. We conjecture that these conditions characterize the left and right positions of \mathbf{s} -bushes.
- For any two \mathbf{s} -bushes B and B' , one can check that the closed fiber $\bar{\mathbb{F}}_B$ is a face of the closed fiber $\bar{\mathbb{F}}_{B'}$ if and only if $\text{lpos}(B, i, j) \geq \text{lpos}(B', i, j)$ and $\text{rpos}(B, i, j) \geq \text{rpos}(B', i, j)$ for all $1 \leq i < j \leq n$.

We now use $\text{lpos}(B, i, j)$ and $\text{rpos}(B, i, j)$ to define a different order on \mathbf{s} -bushes, which extends the \mathbf{s} -weak order of Definition 31 and generalizes the facial weak order of [KLN⁺01]. It is illustrated in Figure 11.

Definition 41. The *facial \mathbf{s} -weak order* $FW_{\mathbf{s}}$ is the partially ordered set of \mathbf{s} -bushes given by $B \leq B'$ if and only if $\text{lpos}(B, i, j) \geq \text{lpos}(B', i, j)$ and $\text{rpos}(B, i, j) \leq \text{rpos}(B', i, j)$ for all $1 \leq i < j \leq n$.

Remark 42. As for the facial weak order on ordered set partitions of $[n]$, there are several equivalent perspectives on the facial \mathbf{s} -weak order. Namely,

- $B \leq B'$ if and only if $\min(B) \leq \min(B')$ and $\max(B) \leq \max(B')$, where $\min(B)$ and $\max(B)$ denote the \mathbf{s} -weak order minimal and maximal \mathbf{s} -trees refining the \mathbf{s} -bush B ,
- if an \mathbf{s} -bush B has an indegree 2 node j , then it covers (resp. is covered by) the \mathbf{s} -bush obtained from B by detaching the left (resp. right) incoming edge of j , and these are all cover relations of the facial \mathbf{s} -weak order (note that this simple description contrasts with the involved description of the cover relations of the refinement order, see Remark 26).

Proposition 43. The facial \mathbf{s} -weak order $FW_{\mathbf{s}}$ is constructible by interval doublings, so that it is a congruence uniform lattice.

Proof sketch. The proof follows the same lines as that of Proposition 38. Let $\bar{\mathbf{s}} := \mathbf{s}_{\leq n-1} = (s_1, \dots, s_{n-1})$ and denote by \bar{B} the $\bar{\mathbf{s}}$ -bush obtained by deleting the node n in an \mathbf{s} -bush B . For any $i \in [n-1]$ and $j \in [s_{n-i}]$, we denote by $FW_{\bar{\mathbf{s}}}^{i,j}$ the poset obtained from the facial \mathbf{s} -weak

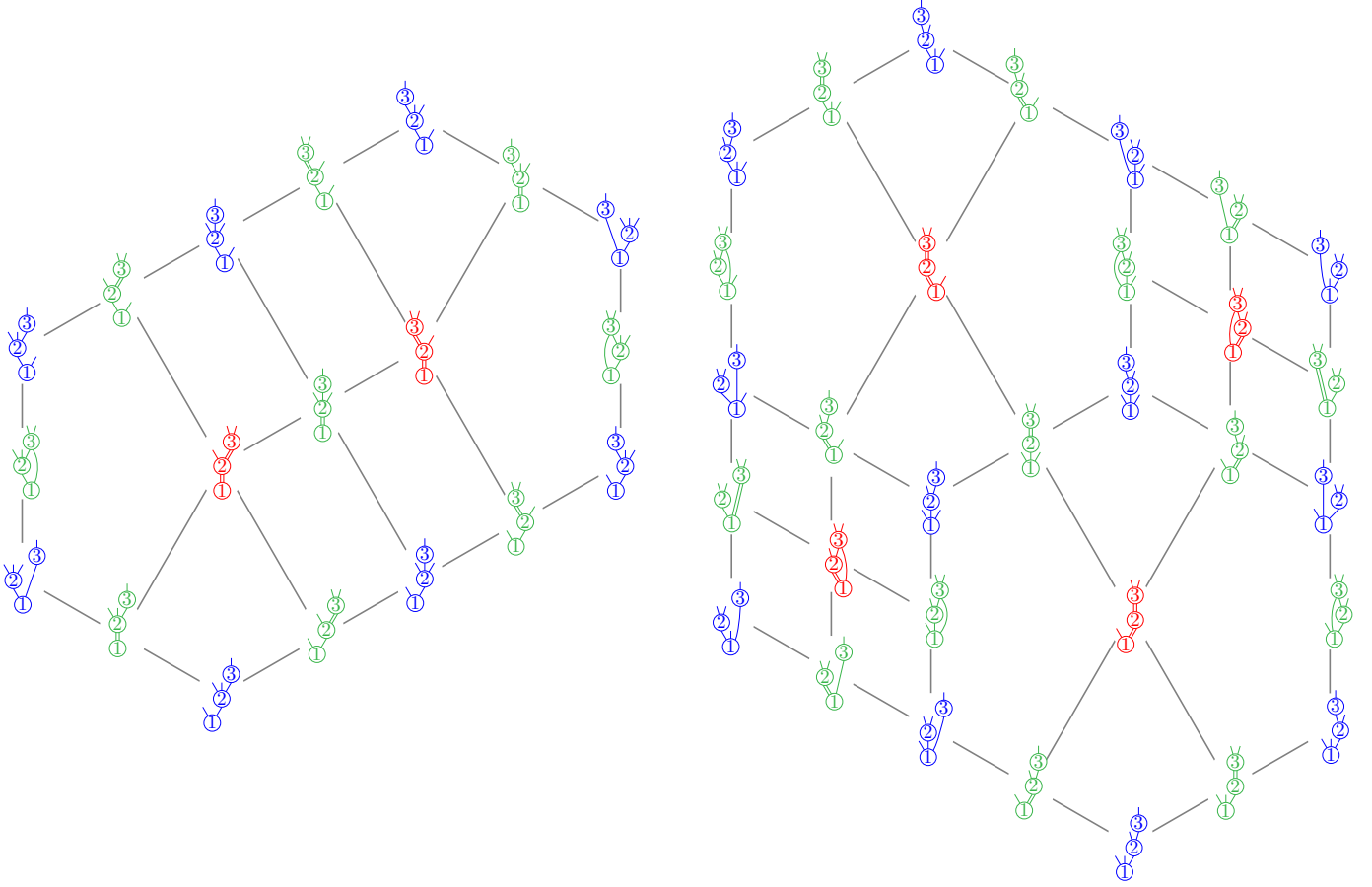


FIGURE 11. The facial \mathbf{s} -weak order $FW_{\mathbf{s}}$ for $\mathbf{s} = (1, 2, 0)$ (left) and $\mathbf{s} = (2, 1, 0)$ (right).

order $FW_{\mathbf{s}}$ by identifying two \mathbf{s} -bushes \mathbf{B} and \mathbf{B}' if and only if $\bar{\mathbf{B}} = \bar{\mathbf{B}}'$, $\text{lpos}(\mathbf{B}, k, n) = \text{lpos}(\mathbf{B}', k, n)$ and $\text{rpos}(\mathbf{B}, k, n) = \text{rpos}(\mathbf{B}', k, n)$ for all $n - i < k < n$, $\text{lpos}(\mathbf{B}, n - i, n)$ and $\text{lpos}(\mathbf{B}', n - i, n)$ either coincide or are both at most $s_i - j$, and $\text{rpos}(\mathbf{B}, n - i, n)$ and $\text{rpos}(\mathbf{B}', n - i, n)$ either coincide or are both at least j . As before, observe that $FW_{\mathbf{s}}^{1,0}$ is isomorphic to the facial $\bar{\mathbf{s}}$ -weak order $FW_{\bar{\mathbf{s}}}$, that $FW_{\mathbf{s}}^{n-1,s_1}$ is just the facial \mathbf{s} -weak order $FW_{\mathbf{s}}$, and that $FW_{\mathbf{s}}^{i,s_i} = FW_{\mathbf{s}}^{i+1,1}$. We then prove that we can construct $FW_{\mathbf{s}}^{i,j}$ from $FW_{\mathbf{s}}^{i,j-1}$ by a sequence of interval tripling (which are obtained by doubling twice each interval). \square

3. CANONICAL REPRESENTATIONS IN THE \mathbf{s} -WEAK ORDER

This section is devoted to the combinatorial description of the join irreducibles and canonical join representations in the \mathbf{s} -weak order $W_{\mathbf{s}}$.

3.1. Recollections 3: Canonical representations in the weak order. We first recall the combinatorics of canonical representations of permutations in terms of non-crossing arc diagrams [Rea15], and of weak order intervals in terms of semi-crossing arc bidiagrams [AP23].

3.1.1. Canonical representations in semidistributive lattices. We first recall the definition of canonical representations in a finite semi-distributive lattice (L, \leq, \wedge, \vee) . A *join representation* of $x \in L$ is a subset $J \subseteq L$ such that $x = \bigvee J$. Such a representation is *irredundant* if $x \neq \bigvee J'$ for any strict subset $J' \subsetneq J$. The irredundant join representations of an element $x \in L$ are ordered by containment of the down sets of their elements, *i.e.* $J \leq J'$ if and only if for any $y \in J$ there

exists $y' \in J'$ such that $y \leq y'$ in L . The *canonical join representation* of x is the minimal irredundant join representation of x for this order when it exists. Its elements are the *canonical joinands* of x . Note that by definition, the canonical joinands form an antichain of join irreducible elements of L (the elements that are their only irredundant join representation, or equivalently that cover a single element).

The lattice L is *join semidistributive* if the following equivalent assertions hold

- $x \vee y = x \vee z$ implies $x \vee (y \wedge z) = x \vee y$ for any $x, y, z \in L$,
- all elements of L admit a canonical join representation.

The *canonical join complex* of L is the simplicial complex whose vertices are the join irreducible elements of L and whose simplices are the canonical join representations of elements of L , see [Rea15, Bar19]. The *canonical meet representations*, the *canonical meetands*, and the *canonical meet complex* of a meet semidistributive lattice are defined dually.

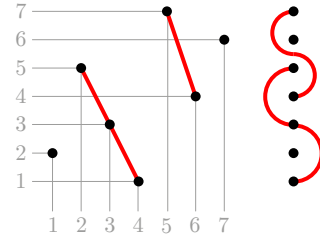
The lattice L is *semidistributive* if it is both join and meet semidistributive. In this situation, its canonical join and meet complexes are isomorphic flag simplicial complexes [Bar19]. The *canonical representation* of an interval $[x, y]$ of L is the disjoint union $J \sqcup M$, where J is the canonical join representation of x and M the canonical meet representation of y . The *canonical complex* of L is the flag simplicial complex whose vertex set is the disjoint union of the join irreducible elements of L and the meet irreducible elements of L , and whose simplices are the canonical representations of the intervals of L , see [AP23].

3.1.2. Canonical join representations of permutations and non-crossing arc diagrams. We now recall the combinatorial model of [Rea15] for the canonical join representations in the weak order. An *arc* on $[n]$ is a quadruple (i, j, A, B) where $1 \leq i < j \leq n$ and $A \sqcup B$ forms a partition of the interval $]i, j[:= \{i+1, \dots, j-1\}$. We represent an arc by a curve wiggling around the vertical axis, starting at height i and ending at height j , and passing to the right of the points of A and to the left of the points of B . Two arcs $\alpha := (i, j, A, B)$ and $\alpha' := (i', j', A', B')$ are *crossing* if they cross in their interior or have the same bottom endpoints or the same top endpoints. In other words, if there exist $u \neq v$ such that $u \in (A' \cup \{i', j'\}) \cap (B \cup \{i, j\})$ and $v \in (A \cup \{i, j\}) \cap (B' \cup \{i', j'\})$. A *non-crossing arc diagram* on $[n]$ is a collection of pairwise non-crossing arcs on $[n]$.

In [Rea15], N. Reading defined an elegant bijection between permutations of $[n]$ and non-crossing arc diagrams on $[n]$. It sends a permutation σ to the non-crossing arc diagram $\delta_\vee(\sigma)$ with an arc $(\sigma_{j+1}, \sigma_j, A_j, B_j)$ for each descent $j \in [n-1]$ of σ (i.e. with $\sigma_j > \sigma_{j+1}$), where

$$A_j := \{\sigma_i \mid 1 \leq i < j \text{ and } \sigma_{j+1} < \sigma_i < \sigma_j\}$$

and $B_j := \{\sigma_k \mid j+1 < k \leq n \text{ and } \sigma_{j+1} < \sigma_k < \sigma_j\}.$



As illustrated on the right with $\sigma = 2531746$, the non-crossing arc diagram $\delta_\vee(\sigma)$ can also be visualized by representing the table (j, σ_j) of the permutation σ , drawing the segments corresponding to the descents of σ , and collapsing the picture vertically, allowing the segments to bend but not to cross each other nor to pass through a point.

The single arcs correspond to permutations with a single descent, that is, to join irreducible permutations of the weak order. More generally, the non-crossing arc diagram $\delta_\vee(\sigma)$ of a permutation σ encodes the canonical join representation of σ in the weak order.

Theorem 44 ([Rea15]). *The map δ_\vee is a bijection from the permutations of $[n]$ to the non-crossing arc diagrams on $[n]$. The canonical join representation σ is precisely the set of join irreducible permutations corresponding to the arcs of the non-crossing arc diagram $\delta_\vee(\sigma)$. In other words, the canonical join complex of the weak order W_n is isomorphic to the non-crossing arc complex on $[n]$.*

See Figure 12 for the weak order on non-crossing arc diagrams and [Rea15] for details. The canonical meet representation of a permutation is obtained similarly, using ascents instead of descents to define the non-crossing arc diagram $\delta_\wedge(\sigma)$.

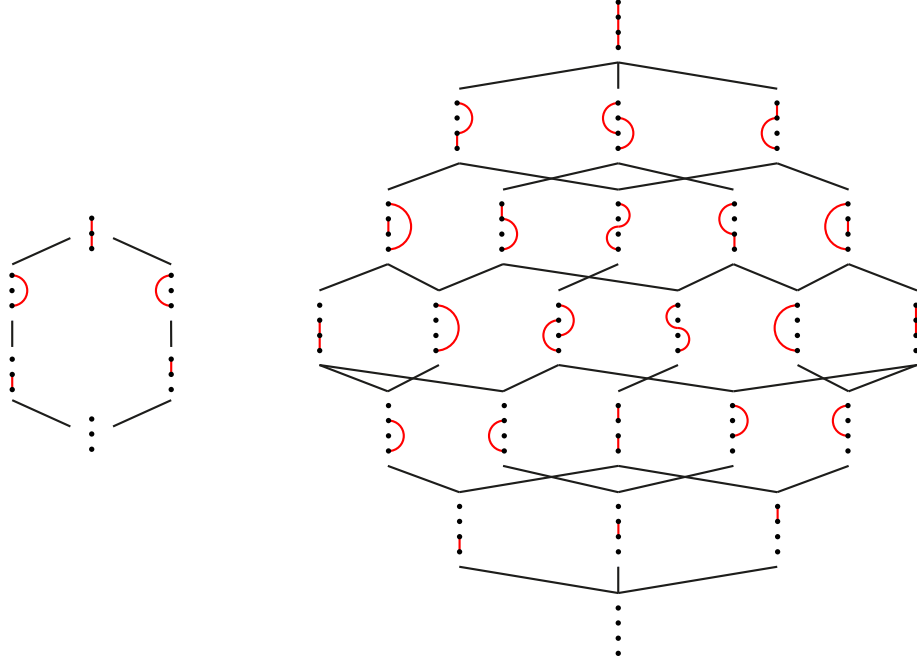


FIGURE 12. The weak order for $n = 3$ (left) and $n = 4$ (right), where each permutation σ is replaced by its non-crossing arc diagram $\delta_V(\sigma)$.

3.1.3. Canonical representations of weak order intervals and semi-crossing arc bideagrams. Two arcs $\alpha_V := (i_V, j_V, A_V, B_V)$ and $\alpha_\Lambda := (i_\Lambda, j_\Lambda, A_\Lambda, B_\Lambda)$ are **semi-crossing** if they do not cross in their interiors with α_V going in the diagonal direction and α_Λ in the anti-diagonal direction at the crossing, and do not start at the same point with α_V leaving right of α_Λ at this point, and do not end at the same point with α_V arriving left of α_Λ at this point. In other words, if there exists no $u < v$ with $u \in (A_\Lambda \cup \{i_\Lambda\}) \cap (B_V \cup \{i_V\})$ and $v \in (A_V \cup \{j_V\}) \cap (B_\Lambda \cup \{j_\Lambda\})$. A **semi-crossing arc bideagram** is a disjoint union $\delta_V \sqcup \delta_\Lambda$ of two non-crossing arc diagrams δ_V and δ_Λ such that any $\alpha_V \in \delta_V$ and $\alpha_\Lambda \in \delta_\Lambda$ are semi-crossing. The following statement is illustrated in Figure 13 and details can be found in [AP23].

Theorem 45 ([AP23]). *The map $[x, y] \mapsto \delta_V(\sigma) \sqcup \delta_\Lambda(\sigma)$ is a bijection from the weak order intervals to the semi-crossing arc bideagrams, which encodes the canonical representations of the weak order. In other words, the canonical complex of the weak order W_n is isomorphic to the semi-crossing arc complex on $[n]$.*

3.2. Join irreducibles of the s -weak order, s -arcs, s -shards. We first define the main characters of this paper, generalizing the arcs of [Rea15].

Definition 46. An **s -arc** is a quintuple (i, j, A, B, r) where $1 \leq i < j \leq n$, the sets A and B form a partition of $\{k \in]i, j[\mid s_k \neq 0\}$, and $r \in [s_i]$.

Note that the first entry i of an s -arc must satisfy $s_i \neq 0$ (otherwise, we have no choice for r). We represent s -arcs graphically as follows. We place n points on the vertical axis, where the point at level i is round if $s_i \neq 0$ and square if $s_i = 0$. The s -arc (i, j, A, B, r) is represented by a curve wiggling around the vertical axis, starting from the point at level i and ending at the point at level j , passing on the right of the points in A and on the left of the points in B (we do not care if it passes on the left or right of the square points), and with an additional label r written close to it.

Remark 47. The number of s -arcs is $\sum_{1 \leq i < j \leq n} s_i 2^{\#\{k \in]i, j[\mid s_k \neq 0\}}$.

We now associate two specific s -trees to each s -arc.

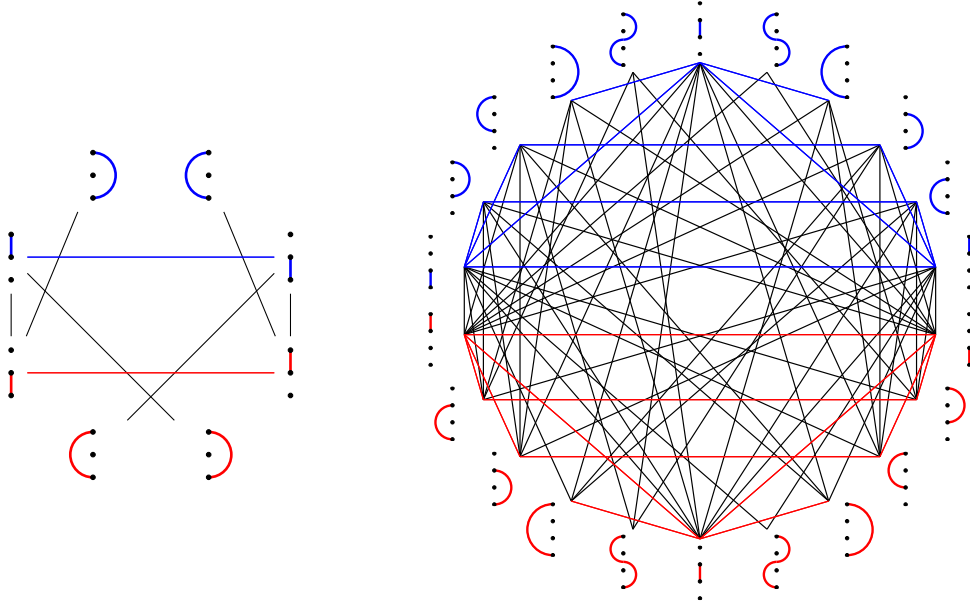
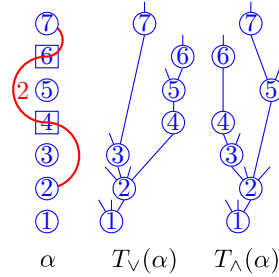


FIGURE 13. The canonical complex of the weak order for $n = 3$ (left) and $n = 4$ (right), interpreted as the semi-crossing arc complex. The canonical join and meet complexes of the weak order, interpreted as non-crossing arc complexes, appear in red and blue respectively. Adapted from [AP23, Fig. 8 & 9].

Definition 48. For $J \subseteq [n]$, the *left* (resp. *right*) *s-comb* with nodes J is the increasing tree on J , where each node $j \in J$ has $s_j + 1$ outgoing edges, which are all leaves except the leftmost (resp. rightmost). For an *s-arc* $\alpha := (i, j, A, B, r)$, we define $T_V(\alpha)$ (resp. $T_\wedge(\alpha)$) as the *s-tree* obtained by attaching the right (resp. left) *s-comb* with nodes $A \cup \{j\}$ (resp. $B \cup \{j\}$) to the $(r + 1)$ -st (resp. r -th) rightmost leaf of i in the right (resp. left) *s-comb* with nodes $[n] \setminus (A \cup \{j\})$ (resp. $[n] \setminus (B \cup \{j\})$). See examples of $T_V(\alpha)$ and $T_\wedge(\alpha)$ on the right for $\mathbf{s} = (2, 3, 1, 0, 1, 0, 0)$ and $\alpha = (2, 7, \{3\}, \{5\}, 2)$.



Lemma 49. For any *s-arc* $\alpha := (i, j, A, B, r)$, and any $1 \leq k < \ell \leq n$, we have

$$\text{pos}(T_V(\alpha), k, \ell) = \begin{cases} r & \text{if } k = i \text{ and } \ell \in A \cup \{j\} \\ s_k & \text{if } k \in B \text{ and } \ell \in A \cup \{j\} \\ 0 & \text{otherwise} \end{cases},$$

$$\text{and } \text{pos}(T_\wedge(\alpha), k, \ell) = \begin{cases} r - 1 & \text{if } k = i \text{ and } \ell \in B \cup \{j\} \\ 0 & \text{if } k \in A \text{ and } \ell \in B \cup \{j\} \\ s_k & \text{otherwise} \end{cases}.$$

Proof. Immediate from Definitions 28 and 48. \square

Corollary 50. For any two *s-arcs* $\alpha := (i, j, A, B, r)$ and $\alpha' := (i', j', A', B', r')$, we have

- (i) $T_V(\alpha) \leq T_V(\alpha')$ if and only if $A \cup \{j\} \subseteq A' \cup \{j'\}$ and $B \cup \{i\} \subseteq B' \cup \{i'\}$ and $i = i' \Rightarrow r \leq r'$,
- (ii) $T_\wedge(\alpha) \leq T_\wedge(\alpha')$ if and only if $A \cup \{i\} \supseteq A' \cup \{i'\}$ and $B \cup \{j\} \supseteq B' \cup \{j'\}$ and $i = i' \Rightarrow r < r'$,
- (iii) $T_V(\alpha) \leq T_\wedge(\alpha')$ if and only if there is no $1 \leq k < \ell \leq n$ such that $k \in (A' \cup \{i'\}) \cap (B \cup \{i\})$ and $\ell \in (A \cup \{j\}) \cap (B' \cup \{j'\})$ except if $k = i'$ and $r < r'$.

Proof. Straightforward from Definition 31 and Lemma 49. \square

Recall that an element of a lattice (L, \leq, \wedge, \vee) is *join* (resp. *meet*) *irreducible* if it covers (resp. is covered by) a single element of L .

Proposition 51. *The map T_\vee (resp. T_\wedge) is a bijection from the s -arcs to the join (resp. meet) irreducible s -trees in the s -weak order.*

Proof. Consider an s -tree T that is a join irreducible in the s -weak order. By Proposition 33, this means that T has a unique descent (i, j) . This implies that T is a right s -comb, to which we have attach on some leaf of node i a right s -comb with top vertex j . Let $r := \text{pos}(T, i, j) \in [s_i]$, let A denote the set of nodes along the path from i to j (but distinct from i and j), and let B be the complement of A in $\{k \in]i, j[\mid s_k \neq 0\}$. Define the s -arc $\alpha_\vee(T) := (i, j, A, B, r)$. Then T_\vee and α_\vee are obviously inverse to each other. \square

We now provide the geometric counterpart of the s -arcs, generalizing the shards of [Rea03] (see also [Rea16, Sect. 9.7]).

Definition 52. The s -shard of an s -arc $\alpha := (i, j, A, B, r)$ is the polyhedron Σ_α of \mathbb{R}^n defined by

- the equality $x_i - x_j = r - 1 + \sum_{k \in B} \max(0, s_k - 1)$,
- the inequalities $x_i - x_a \geq r - 1 + \sum_{k \in B \cap]i, a[} \max(0, s_k - 1)$ for all $a \in A$, and
- the inequalities $x_i - x_b \leq r - 1 + \sum_{k \in B \cap]i, b[} \max(0, s_k - 1)$ for all $b \in B$.

Lemma 53. *For any s -arc $\alpha := (i, j, A, B, r)$, the s -shard Σ_α is the union of the closed fibers \bar{F}_B over all s -bushes B in which (i, j) is a hole and the rightmost path from i to the left incoming edge at j has the nodes of A weakly on its left, and the nodes of B and r children of i strictly on its right.*

Proof. We prove both inclusions.

Consider an s -bush B where (i, j) is a hole and the rightmost path from i to the left incoming edge at j has the nodes of A weakly on its left, and the nodes of B and r children of i strictly on its right. Consider \mathbf{x} in the fiber F_B . As in the proof of Proposition 14, we check that \mathbf{x} must satisfy the equality $x_i - x_j = r - 1 + \sum_{k \in B} \max(0, s_k - 1)$ since (i, j) is a hole of B and the inequalities $x_i - x_a \geq r - 1 + \sum_{k \in B \cap]i, a[} \max(0, s_k - 1)$ for $a \in A$ and $x_i - x_b \leq r - 1 + \sum_{k \in B \cap]i, b[} \max(0, s_k - 1)$ for $b \in B$.

Conversely, consider $\mathbf{x} \in \Sigma_\alpha$ and let $B := B(\mathbf{s}, \mathbf{x})$. Follow the steps of the insertion algorithm described in Definition 4, and construct inductively the rightmost path π leaving through the $(r + 1)$ -st leaf of node i . Since $\mathbf{x} \in \Sigma_\alpha$, we obtain by induction that all nodes of A are weakly on the left of π while all nodes of B are strictly on its right, and finally that (i, j) is a hole of B . It follows from the description of the insertion algorithm in Definition 4 that B is an s -bush where (i, j) is a hole and the rightmost path from i to the left incoming edge at j has the nodes of A weakly on its left, and the nodes of B and r children of i strictly on its right. \square

Corollary 54. *The union of all codimension 1 closed fibers in \mathcal{F}_s is precisely the union of the shards Σ_α for all s -arcs α .*

3.3. Canonical join representations in the s -weak order and non-crossing s -arc diagrams. We now generalize Theorem 44 to the s -weak order, exploiting its semidistributivity established in Theorem 36 and [CP24a, Thms. 1.21 & 1.40].

Definition 55. Consider two s -arcs $\alpha := (i, j, A, B, r)$ and $\alpha' := (i', j', A', B', r')$. Assume without loss of generality that $j \leq j'$ (otherwise, exchange α and α'). Then α and α' are *non-crossing* if $j < j'$, and one of the following conditions hold

- (1) $j \leq i'$,
- (2) $i < i' < j$ and $i' \in A$ and $j \notin A'$ and $A' \cap]i, j[\subseteq A \cap]i', j'[$,
- (3) $i < i' < j$ and $i' \in B$ and $j \notin B'$ and $A' \cap]i, j[\supseteq A \cap]i', j'[$,
- (4) $i = i'$ and $r < r'$ and $j \notin A'$ and $A' \cap]i, j[\subseteq A \cap]i', j'[$,
- (5) $i = i'$ and $r = r'$ and $s_j = 0$ and $A' \cap]i, j[= A \cap]i', j'[$,
- (6) $i = i'$ and $r > r'$ and $j \notin B'$ and $A' \cap]i, j[\supseteq A \cap]i', j'[$,
- (7) $i' < i$ and $i \in A'$ and $j \notin B'$ and $A' \cap]i, j[\supseteq A \cap]i', j'[$,
- (8) $i' < i$ and $i \in B'$ and $j \notin A'$ and $A' \cap]i, j[\subseteq A \cap]i', j'[$.

A *non-crossing s -arc diagram* is a set δ of pairwise non-crossing s -arcs. The *non-crossing s -arc complex* is the (flag) simplicial complex of non-crossing s -arc diagrams.

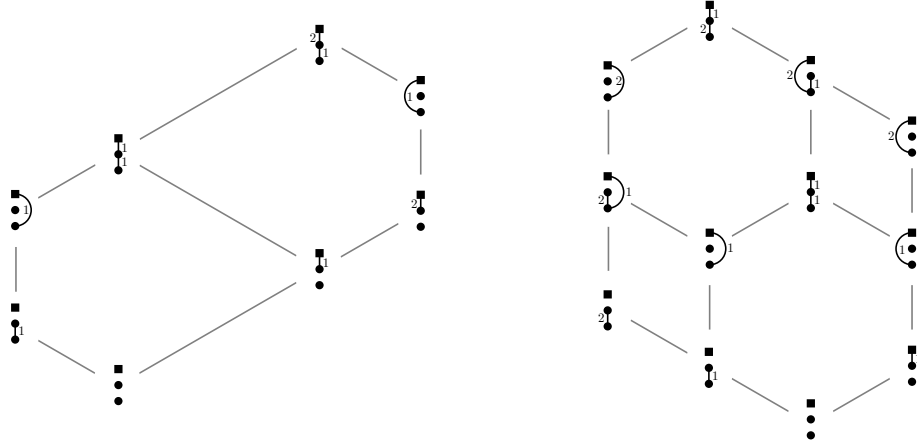


FIGURE 14. The s -weak order W_s for $s = (1, 2, 0)$ (left) and $s = (2, 1, 0)$ (right), where each s -tree T is replaced by its non-crossing s -arc diagram $\delta_\vee(T)$.

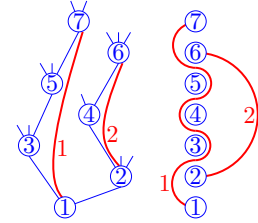
Lemma 56. *If α and α' are non-crossing, then $T_\vee(\alpha)$ and $T_\vee(\alpha')$ are incomparable in s -weak order.*

Proof. Write $\alpha := (i, j, A, B, r)$ and $\alpha' := (i', j', A', B', r')$, and assume that $T_\vee(\alpha) \leq T_\vee(\alpha')$. By Corollary 50 (i), we have $A \cup \{j\} \subseteq A' \cup \{j'\}$ and $B \cup \{i\} \subseteq B' \cup \{i'\}$ and $i = i' \Rightarrow r \leq r'$. The two inclusions imply in particular that $i' \leq i < j \leq j'$. If $j = j'$, then α and α' are crossing. Otherwise, $j < j'$ and the first inclusion implies $j \in A'$. If $i' = i$, then $r \leq r'$, and since $j \in A'$, we obtain by Condition (5) and (6) of Definition 55 that α and α' are crossing. Otherwise, $i' < i$, and the second inclusion implies $i \in B'$, which together with $j \in A'$ implies by Condition (8) of Definition 55 that α and α' are crossing. \square

Definition 57. For a descent (i, j) of an s -tree T , let $r := \text{pos}(T, i, j)$ and A (resp. B) be the set of nodes $i < k < j$ with $s_k \neq 0$ and weakly on the left (resp. strictly on the right) of the path from i to j . Define $\alpha_\vee(T, i, j) := (i, j, A, B, r)$ and $\delta_\vee(T) := \{\alpha_\vee(T, i, j) \mid (i, j) \text{ descent of } T\}$. Define similarly $\alpha_\wedge(T, i, j)$ for an ascent (i, j) of T , and $\delta_\wedge(T) := \{\alpha_\wedge(T, i, j) \mid (i, j) \text{ ascent of } T\}$.

Remark 58. The maps δ_\vee and δ_\wedge have both a graphical and a geometric interpretation. Namely, the non-crossing s -arc diagram $\delta_\vee(T)$ (resp. $\delta_\wedge(T)$) of an s -tree T is obtained

- by drawing the path joining i to j in T for each descent (resp. ascent) (i, j) of T , perturbing all these paths so that they pass slightly to the right (resp. left) of their intermediate nodes, and flattening the picture horizontally, allowing the arcs to bend but not to cross nor to pass a node, see on the right,
- as the set of all s -arcs α whose corresponding s -shard Σ_α supports a lower facet of the maximal cell $\bar{\mathbb{F}}_T$ of the s -foam corresponding to T .



The following statement is illustrated by Figure 14.

Proposition 59. *The maps δ_\vee and δ_\wedge are bijections from s -trees to non-crossing s -arc diagrams.*

Proof. By symmetry, we only prove it for δ_\vee . First, for a descent (i, j) of an s -tree T , $\alpha_\vee(T, i, j)$ is indeed an s -arc, and it is not difficult to see that the s -arcs of $\delta_\vee(T)$ are non-crossing by Remark 58. We now define the inverse map of δ_\vee . Consider a non-crossing s -arc diagram δ . We construct an s -tree $T_\vee(\delta)$ inductively as follows:

- start with the rooted tree with just a root 1 and $s_1 + 1$ leaves,

- at step $k \geq 2$, attach a node k with $s_k + 1$ leaves to the rightmost leaf of the $(r + 1)$ -st subtree of node i where i and r are defined by:
 - if there exists an \mathbf{s} -arc (i', k, A, B, r') in δ , then $i := i'$ and $r := r'$ (such an arc is necessarily unique),
 - otherwise, if there exists an \mathbf{s} -arc (i', j, A, B, r') in δ with $k \in A$, then

$$i := \max \{i' \mid \exists (i', j, A, B, r') \in \delta \text{ with } k \in A\}$$
 and

$$r := \max \{r' \mid \exists (i, j, A, B, r') \in \delta \text{ with } k \in A\},$$
 - otherwise $i := 1$ and $r := 0$.

Let us check that $\delta_V(\mathsf{T}_V(\delta)) = \delta$. It is clear that any arc (i, j, A, B, r) of δ will correspond to a descent (i, j) in T_V , created at step j . Reciprocally, let (i, j) be a descent of $\mathsf{T}_V(\delta)$. The construction of $\mathsf{T}_V(\delta)$ implies that there is an arc (i, j, A, B, r) in δ with $\text{pos}(\mathsf{T}_V(\delta), i, j) = r$. We show by induction on $k \in]i, j[$ and i that A (resp. B) corresponds to the nodes of T weakly on the left (resp. strictly on the right) of the path from i to j in $\mathsf{T}_V(\delta)$.

Suppose that $k \in A$. During the construction of $\mathsf{T}_V(\delta)$, the node k was attached to the rightmost leaf of the $(r' + 1)$ -st subtree of a node i' with $i' > i$ or $i' = i$ and $r' \geq r$. This implies that k is weakly on the left of the path from i to j . Indeed, this is clear if $i' = i$ and $r' \geq r$. Suppose that $i' > i$. Then we are in the case (7) of Definition 55 since $i < i' < k < j$ and $k \in A$. Thus $i' \in A$ and we conclude by induction.

Now, suppose that $k \in B$. During the construction of $\mathsf{T}_V(\delta)$, the node k was attached either to the rightmost available leaf at step k , in which case it is clear that k is strictly on the right of the path from i to j in $\mathsf{T}_V(\delta)$, or to the rightmost leaf of the $(r' + 1)$ -st subtree of a node i' such that there is an \mathbf{s} -arc (i', j', A', B', r') in δ , with $k \in A' \cup \{j'\}$. In this case, assume that $j < j'$. Then the only possible cases of Definition 55 are (3), which implies $i' \in B$, (6), which implies $i = i'$ and $r' < r$, or (7), which implies $i \in A'$. In all these cases we can conclude either directly or by induction that k is strictly on the right of the path from i to j in $\mathsf{T}_V(\delta)$. Similarly, if $j' < j$ the only possible cases of Definition 55 are (2), (4), or (8) and we arrive to the same conclusion.

We have proven that $\delta_V \circ \mathsf{T}_V$ is the identity function on the set of non-crossing \mathbf{s} -arc diagrams.

To finish the proof of the bijection, we show that δ_V is injective. Let T and T' be two \mathbf{s} -trees and denote by j the first step where their inductive construction differs. Up to exchanging T and T' we can assume that the leaf of $\mathsf{T}_{\leq j-1}$ where j is attached to build T is on the left of the leaf where j is attached to build T' . In particular j is not on the rightmost path from the root in T . If $s_j = 0$, then j forms an ascent (i, j) in T , which gives an \mathbf{s} -arc $\alpha_V(\mathsf{T}, i, j)$ that is in $\delta_V(\mathsf{T})$ but not in $\delta_V(\mathsf{T}')$. Assume that $s_j \neq 0$. Then there is an \mathbf{s} -arc (i, k, A, B, r) with $j \in A$ that is in $\delta_V(\mathsf{T})$ but not in $\delta_V(\mathsf{T}')$ (we take i and k to be the smallest and greatest nodes such that j is on the rightmost path from i to k in T). This proves that δ_V is injective and we have the desired bijection. \square

Lemma 60. *For a descent (i, j) of an \mathbf{s} -tree T , the tree $\mathsf{T}_V(\alpha_V(\mathsf{T}, i, j))$ is the unique minimal element of the set $\{\mathsf{T}' \leq \mathsf{T} \mid \text{pos}(\mathsf{T}', i, j) = \text{pos}(\mathsf{T}, i, j)\}$.*

Proof. Let $(i, j, A, B, r) := \alpha_V(\mathsf{T}, i, j)$. Note that $\text{pos}(\mathsf{T}, i, a) \geq r$ and $\text{pos}(\mathsf{T}, a, j) = 0$ for all $a \in A$, while $\text{pos}(\mathsf{T}, i, b) < r$ and $\text{pos}(\mathsf{T}, b, j) = s_b$ for all $b \in B$. For any \mathbf{s} -tree $\mathsf{T}' \leq \mathsf{T}$ with $\text{pos}(\mathsf{T}', i, j) = r$,

- for $a \in A$, we have $\text{pos}(\mathsf{T}', a, j) \leq \text{pos}(\mathsf{T}, a, j) = 0 < s_a$ (because $s_a \neq 0$), so that we get $\text{pos}(\mathsf{T}', i, a) \geq \text{pos}(\mathsf{T}', i, j) = r$ (by Lemma 29),
- for $a \in A \cup \{j\}$ and $b \in B$ with $b < a$, we have $\text{pos}(\mathsf{T}', i, b) \leq \text{pos}(\mathsf{T}, i, b) < r \leq \text{pos}(\mathsf{T}', i, a)$, so that $\text{pos}(\mathsf{T}', b, a) = s_b$ (by Lemma 29).

We conclude that $\text{pos}(\mathsf{T}', k, \ell) \geq \text{pos}(\mathsf{T}_V(\alpha_V(\mathsf{T}, i, j)), k, \ell)$ for all $1 \leq k < \ell \leq n$ by Lemma 49, so that $\mathsf{T}' \geq \mathsf{T}_V(\alpha_V(\mathsf{T}, i, j))$. This concludes the proof since $\text{pos}(\mathsf{T}_V(\alpha_V(\mathsf{T}, i, j)), i, j) = r = \text{pos}(\mathsf{T}, i, j)$ by Definitions 48 and 57, and $\mathsf{T} \geq \mathsf{T}_V(\alpha_V(\mathsf{T}, i, j))$ by setting $\mathsf{T}' = \mathsf{T}$. \square

Proposition 61. *The canonical join (resp. meet) representation of an \mathbf{s} -tree T is $\mathsf{T} = \bigvee_{\alpha \in \delta_V(\mathsf{T})} \mathsf{T}_V(\alpha)$ (resp. $\mathsf{T} = \bigwedge_{\alpha \in \delta_\wedge(\mathsf{T})} \mathsf{T}_\wedge(\alpha)$). In other words, the map α_V (resp. α_\wedge) induces an isomorphism from the canonical join (resp. meet) complex of the \mathbf{s} -weak order $W_\mathbf{s}$ to the non-crossing \mathbf{s} -arc complex.*

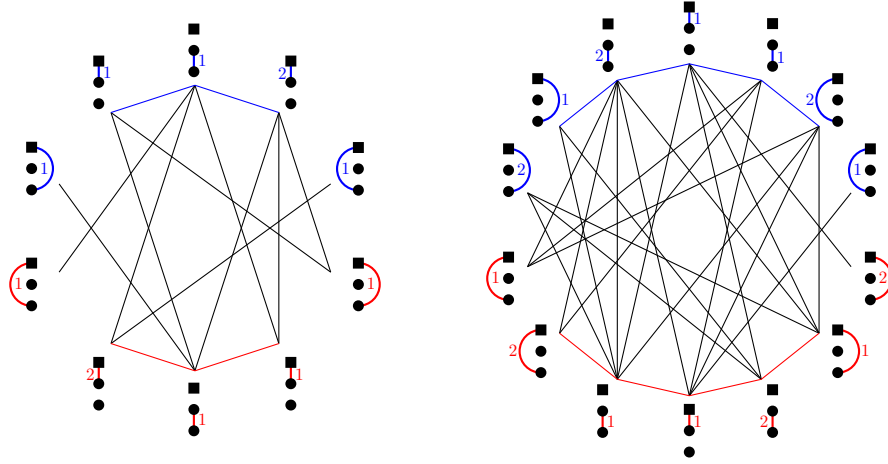


FIGURE 15. The canonical complex of the s -weak order W_s for $s = (1, 2, 0)$ (left) and $s = (2, 1, 0)$ (right), interpreted as the semi-crossing arc complex. The canonical join and meet complexes of the s -weak order, interpreted as non-crossing arc complexes, appear in red and blue respectively.

Proof. We only prove the result for the canonical join representation.

We first show that $T = \bigvee_{\alpha \in \delta_V(T)} T_V(\alpha)$. Indeed, Lemma 60 implies that $T \geq T_V(\alpha_V(T, i, j))$ for any descent (i, j) of T , so that $T \geq \bigvee_{\alpha \in \delta_V(T)} T_V(\alpha)$. Moreover, as any T' covered by T is obtained by rotating a descent (i, j) of T , we have $\text{pos}(T', i, j) = \text{pos}(T, i, j) - 1 < \text{pos}(T_V(\alpha_V(T, i, j)), i, j)$, so that $T' \not\geq \bigvee_{\alpha \in \delta_V(T)} T_V(\alpha)$.

It follows from Lemma 56 and Proposition 59 that the s -trees $T_V(\alpha)$ for $\alpha \in \delta_V(T)$ form an antichain in the s -weak order, thus the join representation $T = \bigvee_{\alpha \in \delta_V(T)} T_V(\alpha)$ is irredundant.

Consider now any join representation $T = \bigvee \mathcal{J}$, and assume by contradiction that there is a descent (i, j) of T such that there is no $J \in \mathcal{J}$ with $T_V(\alpha_V(T, i, j)) \leq J$. Let T' be the s -tree obtained by rotating the descent (i, j) of T . For all $J \in \mathcal{J}$, we thus obtain that $\text{pos}(J, i, j) < \text{pos}(T, i, j)$ by Lemma 60, so that $J \leq T'$ by Proposition 32. Hence, we conclude that $\bigvee \mathcal{J}' \leq T' < T$, a contradiction. \square

For instance, Figure 15 contains the canonical join (red) and meet (blue) complexes of the s -weak order for $s = (1, 2, 0)$ and $s = (2, 1, 0)$.

3.4. Canonical complex of the s -weak order and semi-crossing s -arc bidiagrams. We finally generalize Theorem 45 to the s -weak order. This section is not required in the sequel.

Definition 62. A *semi-crossing s -arc bidiagram* is a disjoint union $\delta_V \sqcup \delta_\wedge$ of non-crossing s -arc diagrams such that for any $\alpha_V := (i_V, j_V, A_V, B_V, r_V) \in \delta_V$ and $\alpha_\wedge := (i_\wedge, j_\wedge, A_\wedge, B_\wedge, r_\wedge)$, there is no $1 \leq k < \ell \leq n$ such that $k \in (A_\wedge \cup \{i_\wedge\}) \cap (B_V \cup \{i_V\})$ and $\ell \in (A_V \cup \{j_V\}) \cap (B_\wedge \cup \{j_\wedge\})$ except if $k = i_\wedge$ and $r_V < r_\wedge$. The *semi-crossing s -arc complex* is the (flag) simplicial complex whose ground set contains two copies α_V and α_\wedge of each s -arc α and whose simplices are all semi-crossing s -arc bidiagrams.

Proposition 63. *The map $[T, T'] \rightarrow \delta_V(T) \sqcup \delta_\wedge(T')$ is a bijection from intervals of the s -weak order to semi-crossing s -arc diagrams. The canonical representation of an interval $[T, T']$ in the s -weak order is given by $\bigvee_{\alpha \in \delta_V(T)} T_V(\alpha) \sqcup \bigwedge_{\alpha \in \delta_\wedge(T')} T_\wedge(\alpha)$. In other words, the canonical complex of the s -weak order W_s is isomorphic to the semi-crossing s -arc complex.*

Proof. According to Proposition 61 and Corollary 50 (iii), this is a direct application of the ideas of [AP23]. \square

See Figure 15 for illustrations.

4. LATTICE CONGRUENCES OF THE \mathbf{s} -WEAK ORDER

In this section, we describe the combinatorics of the congruence lattice of the \mathbf{s} -weak order, and we explore a few relevant families of these congruences.

4.1. Recollections 4: Lattice congruences of the weak order. We first recall the combinatorics of lattice congruences of the weak order. We refer to [Rea16] for an enlightening survey on the topic.

4.1.1. Lattice congruences and quotients. Consider a finite lattice (L, \leq, \wedge, \vee) . A *congruence* \equiv on L is an equivalence relation on L that respects the lattice operations, *i.e.* such that $x \equiv x'$ and $y \equiv y'$ implies $x \vee y \equiv x' \vee y'$ and $x \wedge y \equiv x' \wedge y'$. Equivalently, the equivalence classes are intervals, and the maps $\pi_{\downarrow}^{\equiv}$ and π_{\uparrow}^{\equiv} sending an element to the minimum and maximum elements in its congruence class are order preserving. The *lattice quotient* L/\equiv is the lattice structure on the congruence classes of \equiv , where for any two congruence classes X and Y , the order is given by $X \leq Y$ if and only if $x \leq y$ for some representatives $x \in X$ and $y \in Y$, and the join $X \vee Y$ (resp. meet $X \wedge Y$) is the congruence class of $x \vee y$ (resp. $x \wedge y$) for any representatives $x \in X$ and $y \in Y$. Intuitively, the quotient L/\equiv is obtained by contracting the equivalence classes of \equiv in the lattice L . More precisely, we say that an element x is *contracted* by \equiv if it is not minimal in its equivalence class of \equiv , *i.e.* if $x \neq \pi_{\downarrow}^{\equiv}(x)$. As each class of \equiv is an interval of L , it contains a unique uncontracted element, and the quotient L/\equiv is isomorphic to the subposet of L induced by its uncontracted elements $\pi_{\downarrow}^{\equiv}(L)$.

The prototypical example of congruence of the weak order W_n is the *sylvestre congruence* \equiv_{sylv} [Ton97, LR98, HNT05]. Its congruence classes are the fibers of the binary tree insertion algorithm, or equivalently the sets of linear extensions of binary trees (labeled in inorder and considered as posets oriented from bottom to top). It can also be seen as the transitive closure of the rewriting rule $UuwVvW \equiv_{\text{sylv}} UwuVvW$ where $u < v < w$ are letters and U, V, W are words on $[n]$. The uncontracted permutations for \equiv_{sylv} are those avoiding the pattern 312. The quotient W_n/\equiv_{sylv} is (isomorphic to) the classical *Tamari lattice* [Tam51], whose elements are the binary trees on n nodes and whose cover relations are right rotations in binary trees. See Figure 16.

4.1.2. Canonical representations in lattice quotients. If a lattice L is semidistributive, then any lattice quotient L/\equiv is also semidistributive. Moreover, via the identification between congruence classes of \equiv and their minimal elements, the canonical join representations in the quotient $L/\equiv \simeq \pi_{\downarrow}^{\equiv}(L)$ are precisely the canonical join representations of L that only involve join-irreducibles of L uncontracted by \equiv . In other words, the canonical join complex of the quotient L/\equiv is isomorphic to the subcomplex of the canonical complex of L induced by the join-irreducibles of L uncontracted by \equiv .

Recall from Section 3.1 that the weak order W_n is semidistributive, the join-irreducible permutations correspond to arcs on $[n]$, and the canonical join representations of permutations correspond to non-crossing arc diagrams. This yields the following statement.

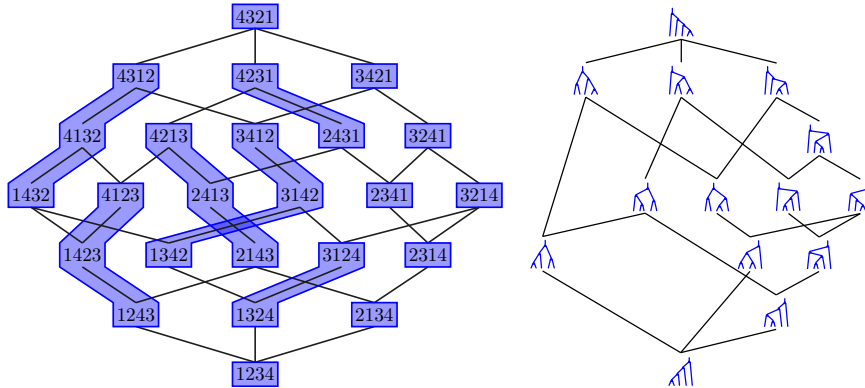


FIGURE 16. The sylvestre congruence \equiv_{sylv} (left), and the Tamari lattice (right). [PS19, Fig. 2]

Theorem 64 ([Rea15, Thm. 4.1]). *For any lattice congruence \equiv of the weak order W_n , the set of join-irreducibles of W_n uncontracted by \equiv corresponds to a set of arcs \mathcal{A}_\equiv , and the canonical join representations in the lattice quotient W_n/\equiv correspond to non-crossing arc diagrams using only arcs of \mathcal{A}_\equiv .*

For instance, the uncontracted join-irreducibles of the sylvester congruence \equiv_{syly} are given by the set $\mathcal{A}_{\text{syly}} = \{(i, j,]i, j[, \emptyset) \mid 1 \leq i < j \leq n\}$ of right arcs, *i.e.* those which pass on the right of all dots in between their endpoints. Therefore, the sylvester congruence classes are in bijection with non-crossing arc diagrams with arcs in $\mathcal{A}_{\text{syly}}$, also known as non-crossing partitions.

4.1.3. The congruence lattice and the forcing relation. The **congruence lattice** $\text{con}(L)$ is the set of all congruences of L ordered by refinement. It is a lattice where the meet is the intersection of relations and the join is the transitive closure of union of relations. Consider a join irreducible element j of L , and let j_\star be the unique element covered by j . We say that \equiv **contracts** j if $j \equiv j_\star$ and we denote by $\text{con}(j)$ the unique minimal congruence of L that contracts j . It turns out that $\text{con}(j)$ is join irreducible in $\text{con}(L)$ and that all join irreducible congruences in $\text{con}(L)$ are of this form. Hence, any congruence of L is completely determined by the subset J_\equiv of join irreducible elements of L that it contracts. For j and j' join irreducible in L , we say that j **forces** j' , and write $j \succcurlyeq j'$, if $\text{con}(j) \geq \text{con}(j')$, that is, if any congruence contracting j also contracts j' . The relation \succcurlyeq is a preorder (*i.e.* a transitive and reflexive, but not necessarily antisymmetric, relation) on the join irreducible elements of L . Moreover, the down sets of \succcurlyeq (*i.e.* the subsets J such that $j \succcurlyeq j'$ and $j \in J$ implies $j' \in J$) are precisely the subsets J_\equiv of join irreducible elements of L that are contracted by some congruence \equiv on L . We sum up with the following statement.

Theorem 65 ([Rea16, Prop. 9.5.16]). *The congruence lattice $\text{con}(L)$ is isomorphic to the lattice of down sets of the forcing relation \succcurlyeq (hence, it is a distributive lattice).*

When \succcurlyeq is a poset (meaning antisymmetric), then there is a bijection between its join irreducible elements and its join irreducible congruences. The lattice L is **congruence uniform** if and only if it satisfies this property and the dual property (*i.e.* the meet irreducible elements are in bijection with the meet irreducible congruences). As already mentioned in Section 2.1, this is equivalent to constructibility by interval doublings, and it implies semidistributivity.

The weak order W_n is a congruence uniform lattice, and the forcing order on join-irreducible permutations can be described visually on arcs as follows. We say that an arc $\alpha := (i, j, A, B)$ is a subarc of an arc $\alpha' := (i', j', A', B')$, if $i' \leq i < j \leq j'$ and $A \subseteq A'$ and $B \subseteq B'$. Visually, α is a subarc of α' if the endpoints of α are located in between those of α' and α agrees with α' in between its endpoints (meaning, α and α' pass on the left and on the right of the same points in between the endpoints of α). See Figure 17. Then α is a subarc of α' if and only if the join irreducible permutation corresponding to α forces the join irreducible permutation corresponding to α' . We thus obtain the following description of the lattice congruences of the weak order W_n .

Theorem 66 ([Rea15, Thm. 4.4 & Coro. 4.5]). *The map $\equiv \mapsto \mathcal{A}_\equiv$ is a bijection between the lattice congruences of the weak order and the down sets of the subarc poset.*

For instance, we have represented in Figure 19 the upper set of the congruence lattice $\text{con}(W_4)$ generated by the recoil congruence (these are precisely the congruences whose quotient fan is essential, see [PS19] and Figure 25).

4.1.4. Forcing in polygonal lattices. A **polygon** in L is an interval $[x, y]$ that is the union of two maximal chains joining x to y , which are disjoint except at x and y . The **edges** are the order relations appearing in the polygon. The two edges incident to x are called the **bottom edges** of the polygon, the two edges incident to y are called the **top edges** of the polygon, and the other edges are called the **side edges** of the polygon. The lattice L is **polygonal** if

- for any y, y' covering the same element x , the interval $[x, y \vee y']$ is a polygon, and
- for any x, x' covered by the same element y , the interval $[x \wedge x', y]$ is a polygon.

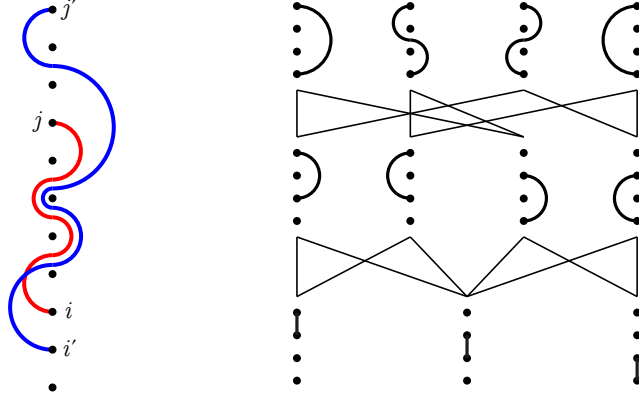


FIGURE 17. The subarc relation (left) and the subarc poset for $n = 4$ (right). The red arc (i, j, A, B) is a subarc of the blue arc (i', j', A', B') . [PS19, Fig. 5]

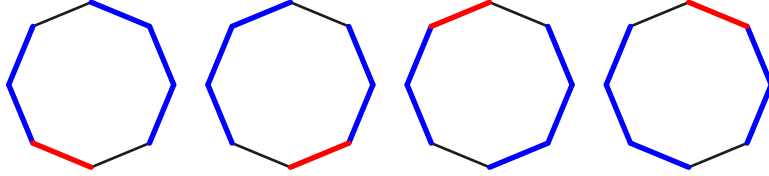


FIGURE 18. Forcing in a polygon. In each picture, the red edge forces all the blue edges.

Polygonal lattices behave particularly nicely with respect to congruence relations. To be precise, let us define two notions of forcing on all cover relations of L (not only on the relations $j_\star < j$ as before). We say that a congruence \equiv of L *contracts* a cover relation $x < y$ in L if $x \equiv y$. We say that $x < y$ *forces* $x' < y'$ if any congruence contracting $x < y$ also contracts $x' < y'$. We say that $x < y$ *forces* $x' < y'$ *in a polygon* if there is some polygon in L containing $x < y$ and $x' < y'$ such that one of the following holds:

- (1) $x < y$ is a bottom edge of the polygon and $x' < y'$ is the opposite top edge,
- (2) $x < y$ is a bottom edge of the polygon and $x' < y'$ is a side edge,
- (3) $x < y$ is a top edge of the polygon and $x' < y'$ is the opposite bottom edge,
- (4) $x < y$ is a top edge of the polygon and $x' < y'$ is a side edge.

See Figure 18. Note that these are the only forcing relations in a polygon, and the following holds.

Theorem 67 ([Rea16, Thm. 9-6.5]). *If L is a finite polygonal lattice, then the forcing relation (on cover relations of L) is the transitive closure of the forcing in polygons relation.*

It is known that the weak order W_n is polygonal [CLCdPBM04]. More generally, the polygonality of posets of regions of hyperplane arrangements was studied in details in [Rea16, Sect. 9-6].

4.1.5. *Special congruences of the weak order.* We conclude this recollection with some particularly relevant congruences of the weak order W_n :

- (1) the *recoil congruence* \equiv_{rec} is defined by the down set $\mathcal{A}_{\text{rec}} = \{(i, i+1, \emptyset, \emptyset) \mid i \in [n-1]\}$ of basic arcs. It has a congruence class for each subset $I \subseteq [n-1]$ given by the permutations whose recoils (descents of the inverse) are at positions in I . It can also be seen as the transitive closure of the rewriting rule $UuvV \equiv_{\text{rec}} UvuV$ for $|u-v| > 1$. The quotient $W_n / \equiv_{\text{rec}}$ is the boolean lattice.
- (2) for an arc $\alpha := (i, j, A, B)$, the *α -Cambrian congruence* \equiv_α is defined by the down set of subarcs of α . It was introduced by N. Reading [Rea06] as a generalization of the sylvester

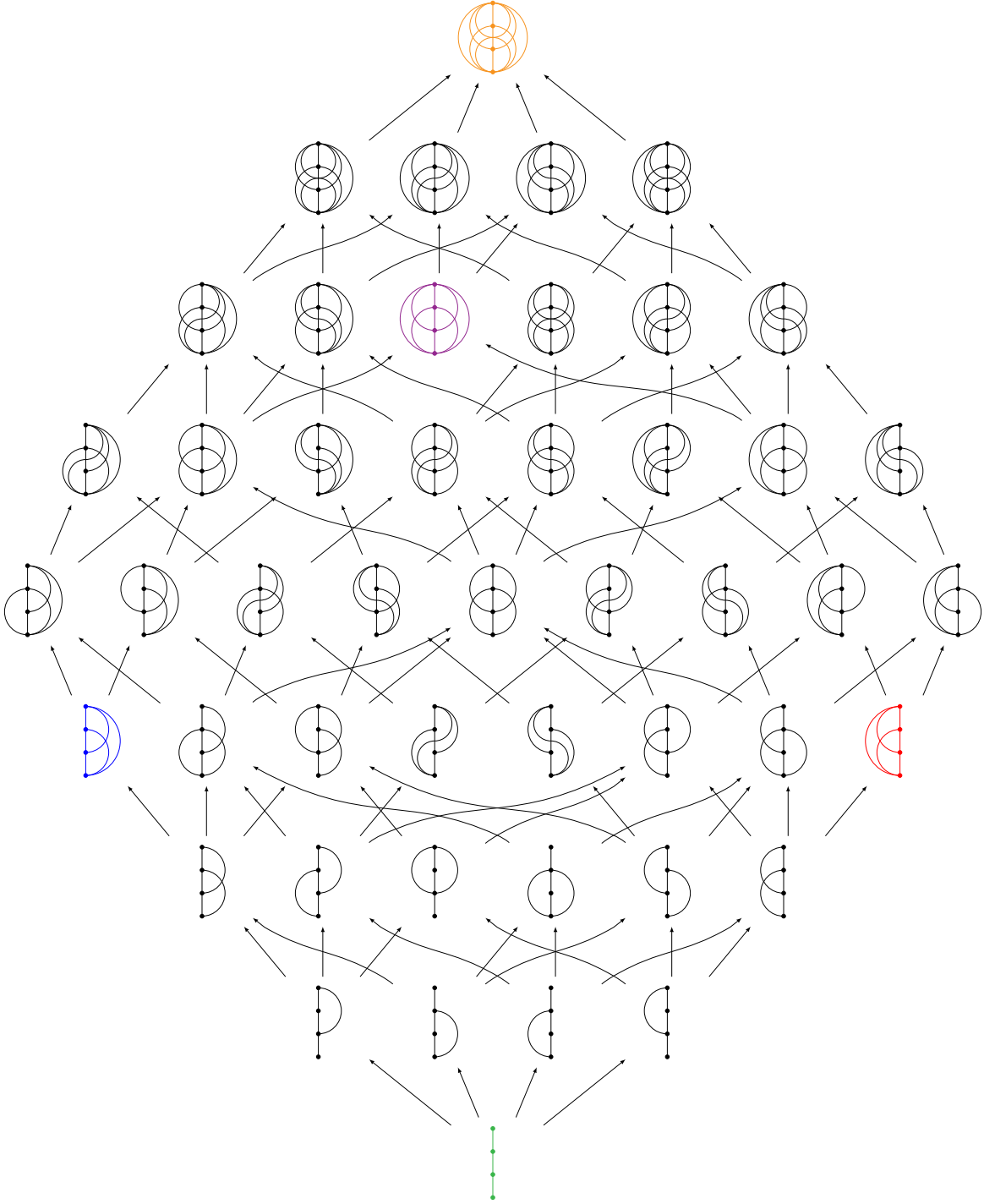


FIGURE 19. The congruence lattice of the weak order W_4 , where each congruence \equiv is replaced by its down set \mathcal{A}_{\equiv} . We have colored in green / blue / red / purple / orange the recoil / sylvester / anti-sylvester / Baxter / trivial (also generic rectangulation) congruence. See also Figure 25. Adapted from [PS19, Fig. 6]

- congruence, obtained for $\alpha = (1, n, 1, n, \emptyset)$. The α -Cambrian congruence classes are fibers of the α -Cambrian tree insertion, or equivalently linear extensions of α -Cambrian trees, see [LP18, CP17, PP18]. An α -Cambrian tree is a tree on $[i, j]$ such that the node $b \in \{i\} \cup A$ (resp. $b \in B \cup \{j\}$) has one ancestor (resp. descendant) subtree and two descendant (resp. ancestor) subtrees, and $a < b < c$ for any nodes a in the left descendant (resp. ancestor) subtree of b and c in the right descendant (resp. ancestor) subtree of b . The α -Cambrian congruence can also be seen as the transitive closure of the three rewriting rules $UuvV \equiv_{\alpha} UvuV$ for $u < i$ or $v > j$, $UuwVvW \equiv_{\alpha} UwuVvW$ for $u < v < w$ with $v \in A$, and $UvVuwW \equiv_{\alpha} UvVwuW$ for $u < v < w$ with $v \in B$.
- (3) for $\delta \in \{\otimes, \oplus, \odot, \boxtimes\}^n$, the δ -permutree congruence \equiv_{δ} is defined by the down set \mathcal{A}_{δ} of arcs that do not pass on the right the points j with $\delta_j \in \{\odot, \boxtimes\}$ nor on the left of the points j with $\delta_j \in \{\oplus, \boxtimes\}$. Its congruence classes correspond to δ -permutrees [PP18]. It can also be seen as the transitive closure of the rewriting rules $UuwVvW \equiv_{\delta} UwuVvW$ for $u < v < w$ with $\delta_v \in \{\oplus, \boxtimes\}$ and $UvVuwW \equiv_{\delta} UvVwuW$ for $u < v < w$ with $\delta_v \in \{\odot, \boxtimes\}$.
 - (4) the *Baxter congruence* \equiv_{Bax} is defined by the down set of arcs that do not cross the vertical axis, i.e. $\mathcal{A}_{\text{Bax}} = \{(i, j, A, B) \mid A = \emptyset \text{ or } B = \emptyset\}$. Its congruence classes correspond to diagonal rectangulations [LR12] or equivalently pairs of twin binary trees [Gir12], which are counted by the Baxter numbers. It can also be seen as the transitive closure of the rewriting rule $UvVuxWwX \equiv_{\text{Bax}} UvVxuWwX$ for $u < v, w < x$. See also [CP25].
 - (5) the *generic rectangulation congruence* \equiv_{Rec} is defined by the down set of arcs that do not cross twice the vertical axis, i.e. $\mathcal{A}_{\text{Rec}} = \{(i, j, A, B) \mid A \text{ and } B \text{ are empty or intervals}\}$. Its congruence classes correspond to generic rectangulations [Rea12] up to wall slides. See also [ACFF25, CP25].
 - (6) for $p \geq 1$, the *p-twist congruence* $\equiv_{p\text{-twist}}$ is defined by the down set of arcs passing on the left of at most p points, i.e. $\mathcal{A}_{p\text{-twist}} = \{(i, j, A, B) \mid |B| \leq p\}$. Its congruence classes correspond to certain acyclic pipe dreams [Pil18]. It can also be seen as the transitive closure of the rewriting rule $UuwV_1v_1 \dots V_pv_pW \equiv_{p\text{-twist}} UwuV_1v_1 \dots V_pv_pW$ for $u < v_1, \dots, v_p < w$.
 - (7) a congruence \equiv of the weak order W_n is *regular* if the cover graph of the quotient W_n/\equiv is regular (or equivalently if the quotient fan \equiv is simplicial and the quotientope \mathbb{Q}_{\equiv} is simple, see Section 5.1). It was proved in [HM21, DIR⁺23, BNP25] that \equiv is regular if and only if any minimal (in subarc order) arc in the complement of the down set \mathcal{A}_{\equiv} is either a left arc $(i, j, \emptyset, [i, j])$ or a right arc $(i, j, [i, j], \emptyset)$. For instance, the sylvester, Cambrian, and permutree congruences are regular, while the Baxter, generic rectangulation, and p -twist (for $p > 1$) congruences are not regular.

4.2. Forcing order and subarc order. The goal of this section is to describe the forcing order on the join irreducible elements of the \mathbf{s} -weak order. Our approach is similar to the one developed for the weak order in [Rea15, Thm. 4.4] and relies on the property that the \mathbf{s} -weak order is a polygonal lattice with well-understood polygons, described in [Lac22, Lems. 3.16 & 3.18 and Thm. 3.19] and [CP24a, Prop. 1.35].

Proposition 68 ([CP24a, Prop. 1.35], from [Lac22, Lems. 3.16 & 3.18 and Thm. 3.19]). *The \mathbf{s} -weak order is a polygonal lattice. More precisely, let T be an \mathbf{s} -tree such that T is covered by R and S by left rotations of the ascents (a, b) and (c, d) respectively, with $a < c$. Then the interval $[T, R \vee S]$ is either a square, a pentagon, or a hexagon depending on the following cases:*

- (1) *If (a, b) is an ascent of S and (c, d) is an ascent of R , then $[T, R \vee S]$ is a square depicted in the first case of Figure 20.*
- (2) *If (a, b) is an ascent of S but (c, d) is not an ascent of R , then $b = c$ and $[T, R \vee S]$ is a pentagon depicted in the second case of Figure 20.*
- (3) *If (a, b) is not an ascent of S and (c, d) is an ascent of R , then $b = c$ and $[T, R \vee S]$ is a pentagon depicted in the third case of Figure 20.*
- (4) *If (a, b) is not an ascent of S and (c, d) is not an ascent of R , then $b = c$, $s_b = 1$, and $[T, R \vee S]$ is a hexagon depicted in the fourth case of Figure 20.*

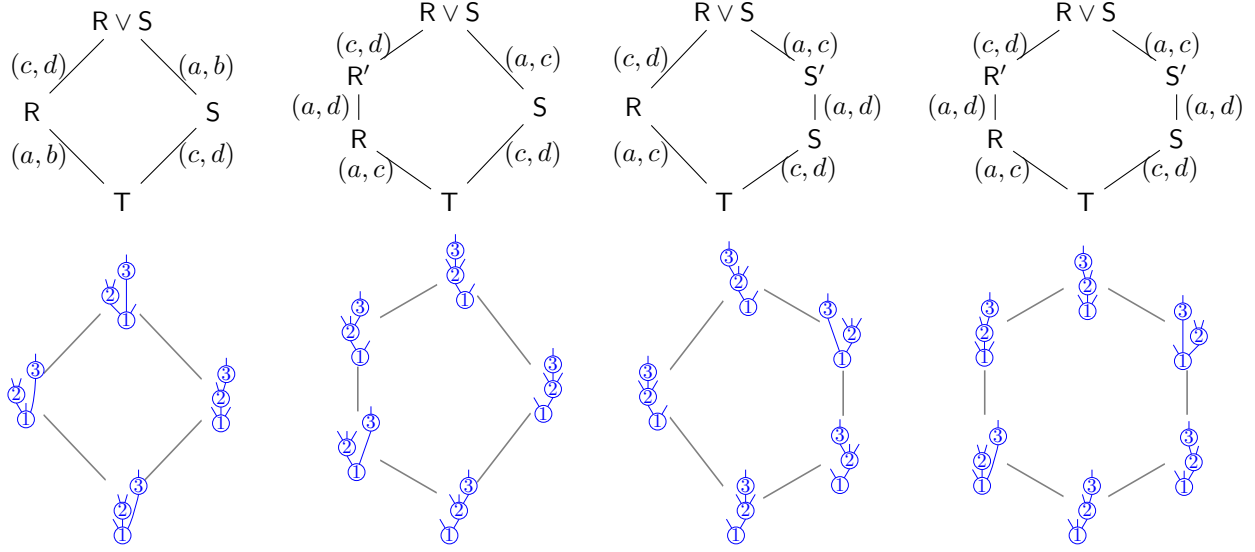


FIGURE 20. The four possible intervals between T and $R \vee S$ where $T \leq R$ and $T \leq S$ in the s -weak order. Figure adapted from [CP24a].

Lemma 69. Let $\alpha := (i, j, A, B, r)$ be an s -arc and δ be a non-crossing s -arc diagram such that $\alpha \in \delta$. Denote by $T_V(\alpha)_*$ the only s -tree covered by $T_V(\alpha)$, and by $T_V(\delta)_*$ the s -tree obtained by rotating the descent (i, j) of $T_V(\delta)$. Then, for any congruence \equiv of the s -weak order, $T_V(\alpha)_* \equiv T_V(\alpha)$ if and only if $T_V(\delta)_* \equiv T_V(\delta)$.

Proof. Assume first that $T_V(\alpha)_* \equiv T_V(\alpha)$. Then $T_V(\delta) = \bigvee_{\beta \in \delta} T_V(\beta) \equiv \bigvee_{\beta \in \delta \setminus \{\alpha\}} T_V(\beta) \vee T_V(\alpha)_*$. Let us denote $T' := \bigvee_{\beta \in \delta \setminus \{\alpha\}} T_V(\beta) \vee T_V(\alpha)_*$. It is clear that $T_V(\alpha) \not\leq T'$ in the s -weak order. Thus it follows from Lemma 60 (where we take $T := T_V(\delta)$) that $\text{pos}(T', i, j) < \text{pos}(T_V(\alpha), i, j)$, and Proposition 32 implies that $T' \leq T_V(\delta)_*$. Hence $T_V(\delta)_*$ is contained in the interval $[T', T_V(\delta)]$, and $T_V(\delta)_* \equiv T_V(\delta)$ since congruence classes are intervals.

Assume now that $T_V(\delta)_* \equiv T_V(\delta)$. Then we have $T_V(\alpha) = T_V(\alpha) \wedge T_V(\delta) \equiv T_V(\alpha) \wedge T_V(\delta)_*$. But since $T_V(\alpha) \not\leq T_V(\delta)_*$ in the s -weak order, we have that $T_V(\alpha) \wedge T_V(\delta)_* \leq T_V(\alpha)_*$. We conclude that $T_V(\alpha) \equiv T_V(\alpha)_*$. \square

Definition 70. Consider two s -arcs $\alpha := (i, j, A, B, r)$ and $\alpha' := (i', j', A', B', r')$. We say that α is a *subarc* of α' if all the following conditions hold:

- $i' \leq i < j \leq j'$,
- $A \subseteq A'$ and $B \subseteq B'$,
- if $s_j = 0$ then $j = j'$,
- if $i' = i$ then $r = r'$,
- if $i' < i$ then either $i \in A'$ and $r = 1$, or $i \in B'$ and $r = s_i$.

Definition 71. We say that an s -arc $\alpha := (i, j, A, B, r)$ is *extended* by an s -arc $\alpha' := (i', j', A', B', r')$ if one of the following conditions holds:

- (1) $s_j \neq 0$ and $\alpha' = (i, j + 1, A \cup \{j\}, B, r)$,
- (2) $s_j \neq 0$ and $\alpha' = (i, j + 1, A, B \cup \{j\}, r)$,
- (3) $r = s_i$ and $\alpha' = (i - 1, j, A, B \cup \{i\}, r')$,
- (4) $r = 1$ and $\alpha' = (i - 1, j, A \cup \{i\}, B, r')$.

It is clear that the subarc relation is the transitive closure of the extension relation. The subarc order is illustrated in Figure 21 (note that when $n = 3$, the subarc and the extension orders coincide).

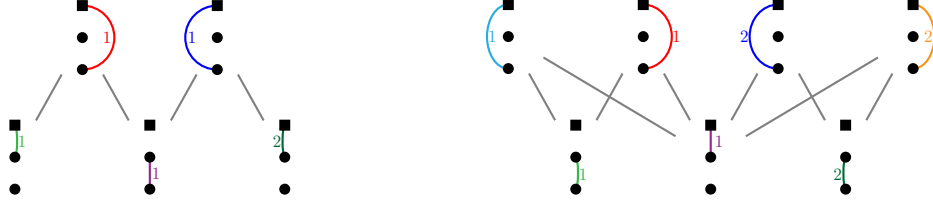


FIGURE 21. The subarc order on s -arcs for $s = (1, 2, 0)$ (left) and $s = (2, 1, 0)$ (right).

Theorem 72. *The forcing order on join irreducible s -trees coincide with the subarc order on s -arcs: if α and α' are two s -arcs, then $T_V(\alpha)$ forces $T_V(\alpha')$ if and only if α is a subarc of α' .*

Definition 73. Consider two s -arcs $\alpha := (i, j, A, B, r)$ and $\alpha' := (i', j', A', B', r')$. We write $\alpha \rightarrow \alpha'$ if there are non-crossing s -arc diagrams δ and δ' such that $\alpha \in \delta$, $\alpha' \in \delta'$ and the edge $T_V(\delta)_* \leq T_V(\delta)$ forces the edge $T_V(\delta')_* \leq T_V(\delta')$ in a polygon of the s -weak order, where we denote by $T_V(\delta)_*$ the s -tree obtained by rotating the descent (i, j) of $T_V(\delta)$ and by $T_V(\delta')_*$ the s -tree obtained by rotating the descent (i', j') of $T_V(\delta')$.

Proof of Theorem 72. It follows from Theorem 67, Lemma 69 and Definition 73 that the forcing order on the s -arcs is the transitive closure of the relation \rightarrow .

We can assume that α and α' are distinct.

First, we suppose that $\alpha \rightarrow \alpha'$ with $\delta, \delta', T_V(\delta)_*, T_V(\delta')_*$ as in Definition 73 and we show that α is a subarc of α' . By considering the polygon in which the edge $T_V(\delta)_* \leq T_V(\delta)$ forces the edge $T_V(\delta')_* \leq T_V(\delta')$, Proposition 68 shows that we are in one of the following cases:

- (1) $T_V(\delta) = R$ and $T_V(\delta') = R'$ (cases (2) or (4) of Proposition 68), then $i = i'$, $s_j \neq 0$. The s -tree $R = T_V(\delta) = T_V(\delta')_*$ has a descent (i, j) and an ascent (i, j') around a same gap of the node i (so that (j, j') is an ascent of $R' = T_V(\delta')$). This implies that $r = r'$. Moreover, all the nodes $i < k < j$ that are weakly on the left, resp. strictly on the right, of the path from i to j in R are weakly on the left, resp. strictly on the right, of the path from i to j' in R' , thus $A \subseteq A'$ and $B \subseteq B'$. (In this case we moreover have $j \in A'$).
- (2) $T_V(\delta) = R$ and $T_V(\delta') = S'$ (cases (3) or (4) of Proposition 68), then $i = i'$ and $s_j \neq 0$. The s -tree T has an ascent (i, j) and an ascent (j, j') around the leftmost gap of node j , so that (i, j') is an ascent of the s -tree S . This implies that $r = r'$. Moreover, all the nodes $i < k < j$ that are weakly on the left, resp. strictly on the right, of the path from i to j in R are weakly on the left, resp. strictly on the right, of the path from i to j' in S' , thus $A \subseteq A'$ and $B \subseteq B'$. (In this case we moreover have $j \in B'$).
- (3) $T_V(\delta) = S$ and $T_V(\delta') = S'$ (cases (3) or (4) of Proposition 68), then $j = j'$. The tree S has an ascent (i', j) and a descent (i, j) . This implies that $r = s_i$. Moreover, it follows from the fact that (i, j) is an ascent of S' that there are no nodes $i < k < j$ on the path from i to j in S . Hence, all the nodes $i < k < j$ that are weakly on the left, resp. strictly on the right, of the path from i to j in S are weakly on the left, resp. strictly on the right, of the path from i' to j in S' , thus $A \subseteq A'$ and $B \subseteq B'$. The node i is on the right of the path from i' to j in S' , thus $i \in B'$.
- (4) $T_V(\delta) = S$ and $T_V(\delta') = R'$ (cases (2) or (4) of Proposition 68), then $j = j'$. The s -tree T has an ascent (i', i) and an ascent (i, j) . The fact that (i', j) is an ascent of R implies that $r = 1$ (so that j is not moved during the rotation of (i', i) from T to R). The nodes $i < k < j$ that are weakly on the left, resp. strictly on the right, of the path from i to j in S are weakly on the left, resp. strictly on the right, of the path from i' to j in R' , thus $A \subseteq A'$ and $B \subseteq B'$. The node i is on the path from i' to j on R' , thus $i \in A'$.

Then, we suppose that α is extended by α' and we show that $\alpha \rightarrow \alpha'$. For each of the four cases of Definition 71 we indicate which δ and δ' we can use to recover the four previously studied cases.

- (1) $s_j \neq 0$ and $\alpha' = (i, j+1, A \cup \{j\}, B, r)$. We take $\delta = \{\alpha\}$ if $r = 1$ or $\delta = \{\alpha, (i, j+1, A \cup \{j\}, B, r-1)\}$ if $r > 1$, and $\delta' = \{\alpha'\}$. Then we have $T_V(\delta) = R$ and $T_V(\delta') = R'$ in case (2) of Proposition 68 if $s_j > 1$ or case (4) if $s_j = 1$.
- (2) $s_j \neq 0$ and $\alpha' = (i, j+1, A, B \cup \{j\}, r)$. If $s_j > 1$, we take $\delta = \{\alpha, (j, j+1, \emptyset, \emptyset, s_j)\}$, and $\delta' = \{\alpha'\}$ if $r = 1$ or $\delta' = \{\alpha', (i, j, A, B, r-1)\}$ if $r > 1$. Then we have $T_V(\delta) = R$ and $T_V(\delta') = S'$ in case (3) of Proposition 68. If $s_j = 1$, we take $\delta = \{\alpha\}$ and $\delta' = \{\alpha'\}$ if $r = 1$ or $\delta = \{\alpha, (i, j+1, A \cup \{j\}, B, r-1)\}$ and $\delta' = \{\alpha', (i, j, A, B, r-1)\}$ if $r > 1$. Then we have $T_V(\delta) = R$ and $T_V(\delta') = S'$ in case (4) of Proposition 68.
- (3) $r = s_i$ and $\alpha' = (i-1, j, A, B \cup \{i\}, r')$. If $A = \emptyset$, we take $\delta = \{\alpha\}$ and $\delta' = \{\alpha'\}$ if $r' = 1$, or $\delta = \{\alpha, (i-1, i, \emptyset, \emptyset, r'-1)\}$ and $\delta' = \{\alpha', (i-1, i, \emptyset, \emptyset, r'-1)\}$ if $r' > 1$. If $A \neq \emptyset$, we denote by $k \in]i, j[$ the maximum element of A and we add the s -arc $(i-1, k, A \setminus \{k\}, (B \cap]i, k[) \cup \{i\}, r')$ to the diagrams δ previously defined. Then we have $T_V(\delta) = S$ and $T_V(\delta') = S'$ in case (3) of Proposition 68 if $s_i > 1$ or case (4) if $s_i = 1$.
- (4) $r = 1$ and $\alpha' = (i-1, j, A \cup \{i\}, B, r')$. If $A = \emptyset$, we take $\delta = \{\alpha\}$ if $r' = 1$, or $\delta = \{\alpha, (i-1, i, \emptyset, \emptyset, r'-1)\}$ if $r' > 1$, and $\delta' = \{\alpha'\}$. If $A \neq \emptyset$, we denote by $k \in]i, j[$ the maximum element of A and we add the s -arc $(i-1, k, A \setminus \{k\}, (B \cap]i, k[) \cup \{i\}, r')$ to the diagram δ and we add $(i, k, A \setminus \{k\}, B \cap]i, k[, s_i)$ to δ' . Then we have $T_V(\delta) = S$ and $T_V(\delta') = R'$ in case (2) of Proposition 68 if $s_i > 1$ or case (4) if $s_i = 1$. \square

From Theorems 65 and 72, we immediately deduce the following statement, illustrated in Figure 22.

Corollary 74. *The congruence lattice of the s -weak order W_s is isomorphic to the lattice of down sets of the subarc order on s -arcs.*

For a congruence \equiv of W_s , we denote by \mathcal{A}_{\equiv} the corresponding down set of the subarc order on s -arcs.

4.3. Some relevant congruences of the s -weak order. In this section, we exploit Corollary 74 to define particularly relevant congruences, mimicking some congruences of Section 4.1.5. We present a few conjectures that echo the situation of the similar congruences in the classical weak order.

4.3.1. The s -sylvester congruence and the s -Tamari lattice. A *right s -arc* is an s -arc of the form $(i, j, \{k \in]i, j[\mid s_k \neq 0\}, \emptyset, r)$ for some $1 \leq i < j \leq n$ and $r \in [s_i]$. The set of right s -arcs clearly forms a down set $\mathcal{A}_{\text{sylv}}$ of the subarc order. The corresponding congruence of the s -weak order is the *s -sylvester congruence* \equiv_{sylv} , and the quotient $W_s / \equiv_{\text{sylv}}$ of the s -weak order by the s -sylvester congruence is the *s -Tamari lattice*. An s -tree T is minimal in its s -sylvester congruence class if and only if $\text{pos}(T, a, b) \leq \text{pos}(T, a, c)$ for all $1 \leq a < b < c \leq n$ with $s_b \neq 0$.

When s contains no 0, and up to our convention modifications (see Remark 3), these s -trees are called *s -Tamari trees* in [CP24a, CP24b]. We thus directly obtain that the subposet of the s -weak order induced by the s -Tamari trees is (isomorphic to) the s -Tamari lattice $W_s / \equiv_{\text{sylv}}$. This immediately recovers [CP24a, Thm. 2.20]. We refer to [CP24a, Sect. 2.4] for the connection to the ν -Tamari lattice of [PRV17, CPS19].

When s contains some 0, the s -trees that are minimal in their s -sylvester congruence classes actually differ from the s -Tamari trees of [CP24a], because they drop the condition $s_b \neq 0$. It was proved in [CP24a, Thm. 2.2] that the subposet of the s -weak order induced by the s -Tamari trees is still a sublattice of the s -weak order, but is not anymore a lattice quotient of the s -weak order. (We note that even when s contains no 0, it follows from the theory of lattice congruences that this subposet is a join sublattice, but it could a priori fail to be a meet sublattice.) They still call this sublattice the s -Tamari lattice. We insist that, in the situation that s contains some 0, our s -Tamari lattice differs from that of [CP24a, Sect. 2].

4.3.2. The s -Cambrian congruences. For any s -arc α , the *α -Cambrian congruence* \equiv_{α} is defined by the down set of subarcs of α , and the quotient W_s / \equiv_{α} is the *α -Cambrian lattice*. Note that the s -sylvester congruence is not anymore an s -Cambrian congruence (as some right arcs are not subarcs of the arc $(1, n, \{k \in]1, n[\mid s_k \neq 0\}, \emptyset, 1)$). Our main conjecture on s -Cambrian congruences is the following.

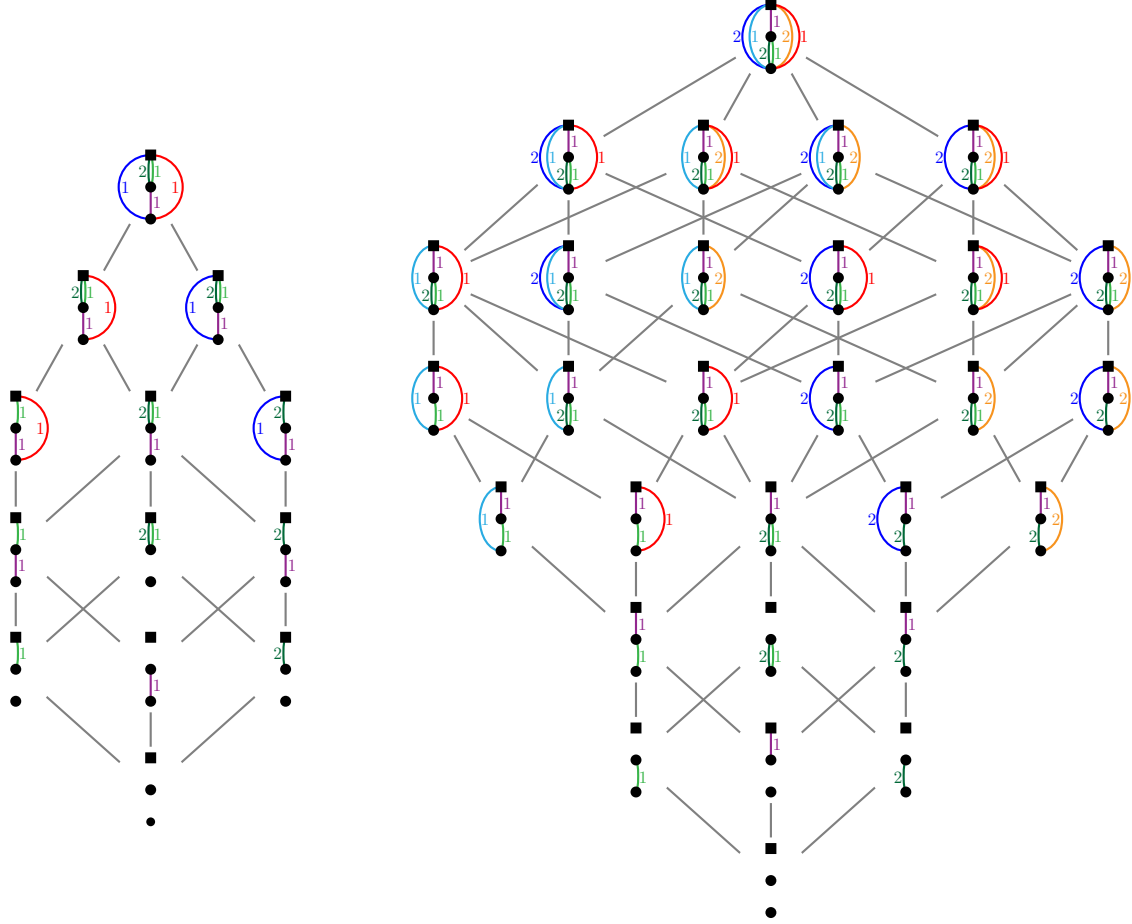


FIGURE 22. The congruence lattice of the s -weak order W_s for $s = (1, 2, 0)$ (left) and $s = (2, 1, 0)$ (right), where each congruence \equiv is replaced by its s -arc down set \mathcal{A}_{\equiv} . See also Figures 27 and 29.

Conjecture 75. *For any fixed s , the following only depend on the endpoints of α :*

- the cardinality of the α -Cambrian lattice,
- the f -vector of the canonical join complex of the α -Cambrian lattice,
- the (isomorphism class of the) undirected cover graph of the α -Cambrian lattice,
- the (isomorphism class of the) face lattice of the α -Cambrian foam $\mathcal{F}_{\equiv_\alpha}$ or equivalently of the α -Cambrian quotientopex $\mathbb{Q}_{\equiv_\alpha}$ (see Section 5 for the definitions of \mathcal{F}_{\equiv} and \mathbb{Q}_{\equiv}).

4.3.3. *The s -permutree congruences.* For a map $\delta : \{i \in [n] \mid s_i \neq 0\} \rightarrow \{\ominus, \otimes, \oplus, \boxtimes\}$, the δ -permutree congruence \equiv_δ is defined by the down set of arcs that do not pass on the right of a point j with $\delta(j) \in \{\oplus, \boxtimes\}$ nor on the left of the points j with $\delta(j) \in \{\otimes, \ominus\}$. The δ -permutree lattice is the quotient W_s / \equiv_δ . For these congruences, we observed the following behavior.

Conjecture 76. *For any fixed s , changing any \oplus to \otimes in δ does not affect*

- the cardinality of the δ -permutree lattice,
- the f -vector of the canonical join complex of the δ -permutree lattice.

Note that in contrast to Conjecture 75, the undirected cover graph of the δ -permutree lattice and the face lattice of the δ -permutree foam $\mathcal{F}_{\equiv_\delta}$ and of the δ -permutree quotientopex $\mathbb{Q}_{\equiv_\delta}$ all depend on the positions of \oplus and \otimes . For instance, for $s := (1, 1, 2, 2, 1, 1)$, and $\delta := (\oplus, \oplus, \oplus, \oplus, \oplus, \oplus)$ and $\delta' := (\oplus, \oplus, \oplus, \otimes, \oplus, \oplus)$, the δ - and δ' -permutree lattices both have cardinality 331, the

f -vector of their canonical complex is $(1, 20, 93, 139, 69, 9)$, but their undirected cover graphs are not isomorphic.

4.3.4. Regular congruences. An interval of a lattice L is *cellular* if it is of the form $[x, \bigvee Y]$ for $x \in L$ and a non-empty subset Y of elements of L covering x , or dually $[\bigwedge X, y]$ for any $y \in L$ and a non-empty subset X of elements of L covered by y . We say that L is *cellularly regular* if the cover graph of any cellular interval of L is regular. Note that it obviously does not imply that the cover graph of the lattice L itself is regular. The result of [HM21, DIR⁺23, BNP25] on regular congruences of the weak order motivates the following conjecture.

Conjecture 77. *The following conditions are equivalent for a congruence \equiv of the \mathbf{s} -weak order $W_{\mathbf{s}}$:*

- *the quotient $W_{\mathbf{s}}/\equiv$ is cellularly regular,*
- *any minimal (in subarc order) arc of the complement of the down set \mathcal{A}_{\equiv} is either a left arc (i.e. with $A = \emptyset$) or a right arc (i.e. with $B = \emptyset$).*

5. QUOTIENT FOAMS AND QUOTIENTOPLEXES

In this section, we construct polyhedral complexes realizing all lattice quotients of the \mathbf{s} -weak order $W_{\mathbf{s}}$. Most proofs of the results of this section actually require some basic tropical geometry, and are therefore delayed to Section 6.

5.1. Recollections 5: Quotient fans and quotientopes. As usual now, we start with a recollection of the geometric realizations of the lattice quotients of the classical weak order [Rea05, PS19, PPR23].

5.1.1. Quotient fan. We start with polyhedral fan realizations.

Definition 78 ([Rea05, Thm. 1.1]). The *quotient fan* of a congruence \equiv of the weak order is the polyhedral fan \mathcal{F}_{\equiv} where

- the maximal cones are obtained by gluing together the chambers of the braid arrangement corresponding to permutations in the same congruence class of \equiv ,
- the union of the codimension 1 cones is the union of the shards of the arcs of \mathcal{A}_{\equiv} .

By construction, the braid fan refines the quotient fan \mathcal{F}_{\equiv} , and the dual graph of the quotient fan \mathcal{F}_{\equiv} , oriented in the direction ω , is isomorphic to the Hasse graph of the quotient W_n/\equiv . For instance, Figure 23 (left) represents the *sylvester fan*, the quotient fan of the sylvester congruence of Figure 16 (left), whose dual graph is the cover graph of the Tamari lattice of Figure 16 (right).

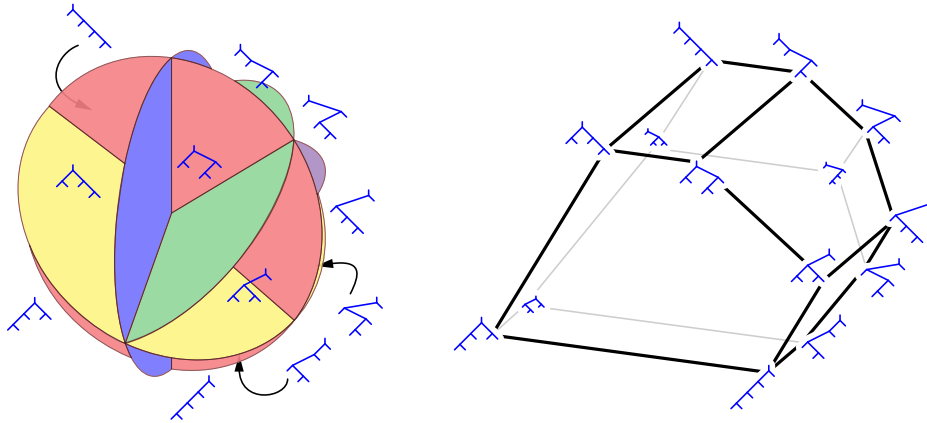


FIGURE 23. The sylvester fan (left) and the associahedron $\text{Asso}(4)$ (right). [PPR23, Fig. 5]

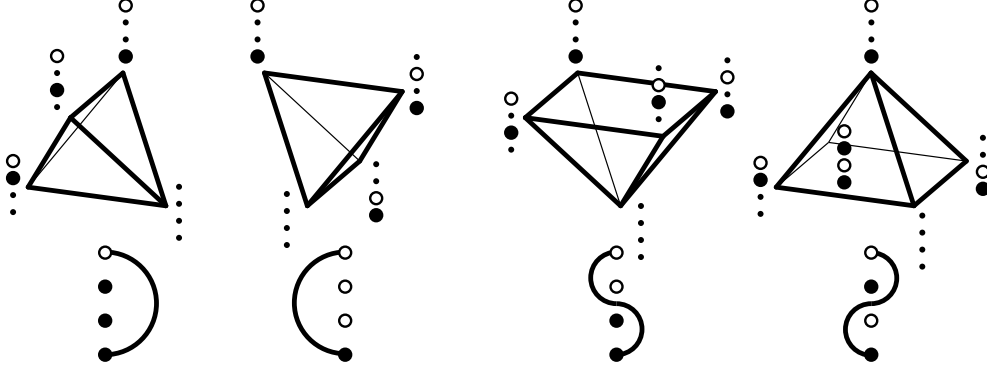


FIGURE 24. The shard polytopes of the four arcs of the form $(1, 4, A, B)$. The vertices of the shard polytope of $\alpha := (i, j, A, B)$ are labeled by the corresponding α -alternating matchings, where we use solid dots \bullet for elements in $\{i\} \cup A$ and hollow dots \circ for elements in $B \cup \{j\}$. The corresponding vertex coordinates are directly read replacing \bullet by 1 and \circ by -1 . For instance, the vertex labeled $\begin{smallmatrix} \circ & \bullet & \circ & \bullet \\ \bullet & \circ & \bullet & \circ \end{smallmatrix}$ has coordinates $(1, 0, 0, -1)$. Adapted from [PPR23, Fig. 10].

5.1.2. *Shard polytopes and quotientopes.* We now recall the definition and main property of the shard polytopes of [PPR23], which are illustrated in Figure 24.

Definition 79 ([PPR23, Defs. 39 & 40]). Fix a classical arc $\alpha := (i, j, A, B)$. An α -alternating matching μ is a sequence $i \leq i_1 < j_1 < i_2 < j_2 < \dots < i_q < j_q \leq j$ such that $i_p \in \{i\} \cup A$ and $j_p \in \{j\} \cup B$ for all $p \in [q]$. Its characteristic vector is $\chi_\mu := \sum_{p \in [q]} e_{i_p} - e_{j_p}$. We denote by \mathcal{M}_α the set of all α -alternating matchings. The *shard polytope* of α is the convex hull \mathbb{SP}_α of the characteristic vectors of all α -alternating matchings μ in \mathcal{M}_α .

For instance, the shard polytope \mathbb{SP}_α corresponding to a right arc $\alpha := (i, j, [i, j], \emptyset)$ is just the simplex $\Delta_{[i, j]} := \text{conv}\{e_k \mid i \leq k \leq j\}$ translated by the vector $-e_j$.

Proposition 80 ([PPR23, Prop. 48]). *For any arc α , the union of the walls of the normal fan of the shard polytope \mathbb{SP}_α*

- *contains the shard Σ_α corresponding to α ,*
- *is contained in the union of the shards Σ_β over all subarcs β of α .*

The shard polytopes are the building blocks to construct polytopal realizations of lattice quotients of the weak order. We note that alternative realizations were constructed by V. Pilaud and F. Santos in [PS19] using direct but slightly obscure right hand sides to define their inequalities.

Theorem 81 ([PPR23, Coro. 50]). *For any congruence \equiv of the weak order, the quotient fan \mathcal{F}_\equiv is the normal fan of the quotientope \mathbb{Q}_\equiv , obtained as the Minkowski sum of (any positive scaling of) the shard polytopes \mathbb{SP}_α , over all arcs α in \mathcal{A}_\equiv .*

By construction, the quotientope \mathbb{Q}_\equiv is a deformed permutahedron (or generalized permutahedron [Pos09, PRW08], or polymatroid [Edm70]), whose skeleton, oriented in the direction ω , is isomorphic to the Hasse diagram of the quotient W_n/\equiv . For instance, Figure 23 (right) represents the associahedron $\text{Asso}(4)$, a quotientope for the sylvester congruence of Figure 16 (left), whose normal fan is the sylvester fan of Figure 23 (left), and whose skeleton is the cover graph of the Tamari lattice of Figure 16 (right). It is obtained as the Minkowski sum of the shard polytopes of all right arcs, that is, up to translation, of the faces $\Delta_{[i, j]}$ of the standard simplex corresponding to all intervals $1 \leq i < j \leq n$.

If we want to make explicit the scaling coefficients, we denote by $\mathbb{Q}_\equiv(\lambda)$ the quotientope obtained as the Minkowski sum $\sum_{\alpha \in \mathcal{A}_\equiv} \lambda_\alpha \mathbb{SP}_\alpha$ for $\lambda := (\lambda_\alpha)_{\alpha \in \mathcal{A}_\equiv}$ with $\lambda_\alpha > 0$ for all $\alpha \in \mathcal{A}_\equiv$.

Remark 82. In general, the quotient fan \mathcal{F}_\equiv is not simplicial, and the quotientope \mathbb{Q}_\equiv is not simple. It is the case for regular congruences, see Section 4.1.5 (5) and [HM21, DIR⁺23, BNP25].

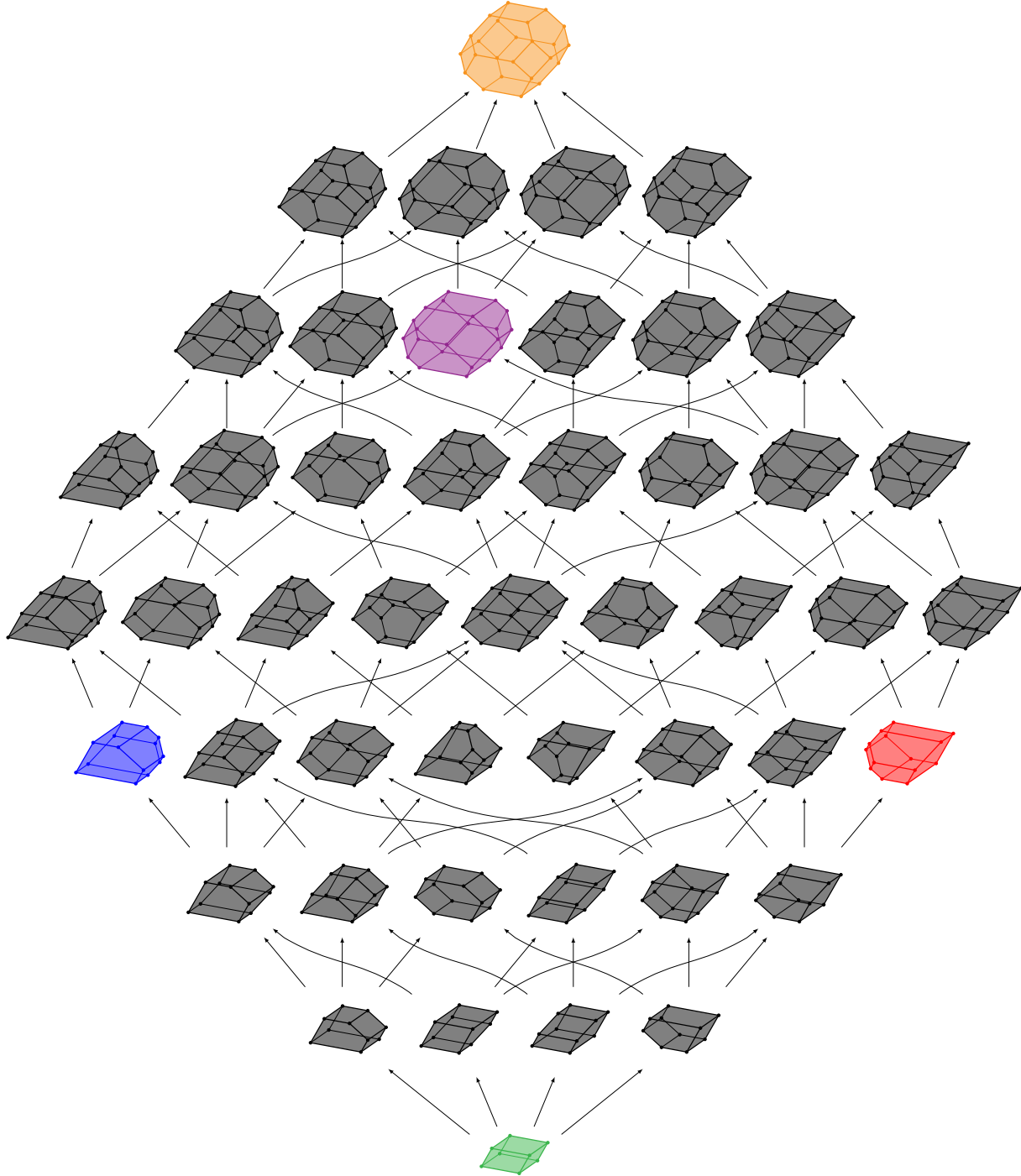


FIGURE 25. The congruence lattice of the weak order W_4 , where each congruence \equiv is replaced by its quotientope Q_{\equiv} . We have colored in green / blue / red / purple / orange the cube / associahedron / anti-associahedron / Baxter polytope / permutahedron. See also Figure 19. Adapted from [PS19, Fig. 9]

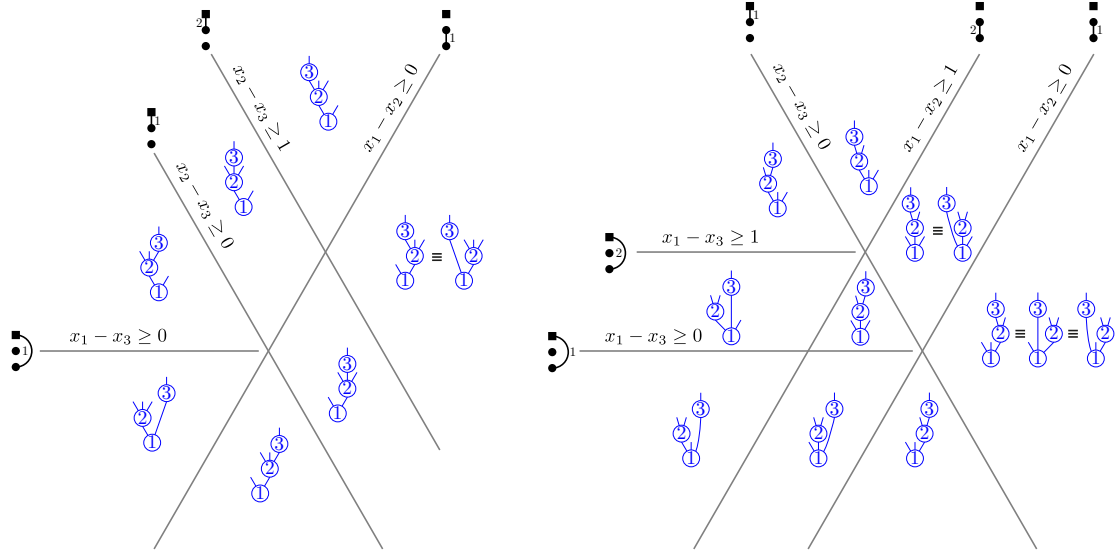


FIGURE 26. The quotient foam $\mathcal{F}_{\equiv_{\text{sylyv}}}$ for the \mathbf{s} -sylvester congruence of the \mathbf{s} -weak order of Section 4.3.1, for $\mathbf{s} = (1, 2, 0)$ (left) and $\mathbf{s} = (2, 1, 0)$ (right).

5.2. Quotient foams. We now generalize Definition 78 to the \mathbf{s} -weak order. For a congruence of the \mathbf{s} -weak order $W_{\mathbf{s}}$, we construct a polyhedral complex \mathcal{F}_{\equiv} coarsening the \mathbf{s} -foam $\mathcal{F}_{\mathbf{s}}$, and whose oriented dual graph is isomorphic to the Hasse diagram of the quotient $W_{\mathbf{s}}/\equiv$. See Figures 26 and 27 for some illustrations. Recall from Definition 52 that we have associated to each \mathbf{s} -arc α a codimension 1 polyhedral cone called the \mathbf{s} -shard Σ_{α} of α .

Definition 83. For any congruence \equiv of the \mathbf{s} -weak order $W_{\mathbf{s}}$, the *quotient foam* \mathcal{F}_{\equiv} is the complete polyhedral complex defined by the following equivalent descriptions:

- (i) its maximal cells are obtained by gluing together the maximal cells of the \mathbf{s} -foam corresponding to \mathbf{s} -trees in the same congruence class of \equiv ,
- (ii) the union of its codimension 1 cells is the union of the \mathbf{s} -shards Σ_{α} of the \mathbf{s} -arcs α in \mathcal{A}_{\equiv} .

Definition 83 requires some justifications, that we give in the following statements.

Proposition 84. For any congruence \equiv of the \mathbf{s} -weak order $W_{\mathbf{s}}$, the two descriptions of Definition 83 coincide.

Proof. Consider a cover relation $T \triangleleft T'$ in the \mathbf{s} -weak order, let (i, j) denote the ascent of T and descent of T' corresponding to this flip, and let $\alpha := (i, j, A, B, r)$ denote the corresponding \mathbf{s} -arc in $\delta_{\vee}(T')$. Consider now the \mathbf{s} -bush B obtained by stitching (i, j) in T (or equivalently in T'), that is, such that $\mathbb{F}_T \cap \mathbb{F}_{T'} = \mathbb{F}_B$ by Proposition 22. Then \mathbb{F}_B is contained in the shard Σ_{α} by Lemma 53. As $T \equiv T'$ if and only if $\alpha \notin \mathcal{A}_{\equiv}$, we thus obtain that $T \triangleleft T'$ is contracted in the description of Definition 83 (i) if and only if it is contracted in the description of Definition 83 (ii). \square

Proposition 85. For any congruence \equiv of the \mathbf{s} -weak order $W_{\mathbf{s}}$, the quotient foam \mathcal{F}_{\equiv} of Definition 83 is indeed a polyhedral complex.

Proof. The proof uses tropical geometry to show that the quotient foam is the polyhedral complex induced by a certain arrangement of tropical hypersurfaces, see Theorem 106. \square

Proposition 86. The Hasse diagram of the quotient $W_{\mathbf{s}}/\equiv$ is isomorphic to the dual graph of the quotient foam \mathcal{F}_{\equiv} , oriented in the direction ω .

Proof. By Definition 83 (i), the maximal cells of the quotient foam \mathcal{F}_{\equiv} are labeled by the equivalence classes of \equiv . Consider now two maximal cells C and C' corresponding to two equivalent classes C and C' of \equiv . Then the following are equivalent:

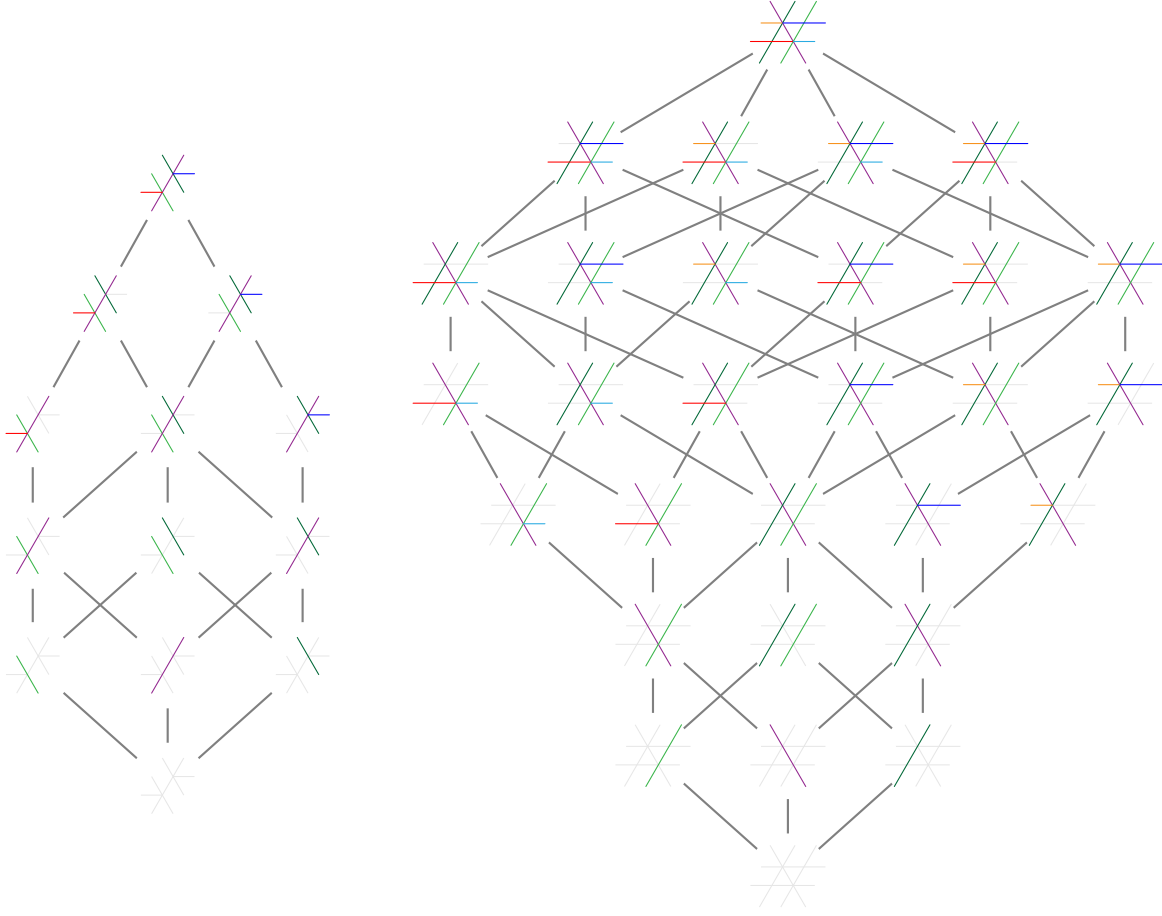


FIGURE 27. The congruence lattice of the \mathbf{s} -weak order $W_{\mathbf{s}}$ for $\mathbf{s} = (1, 2, 0)$ (left) and $\mathbf{s} = (2, 1, 0)$ (right), where each congruence \equiv is replaced by its quotient foam \mathcal{F}_{\equiv} . See also Figures 22 and 29.

- $\mathbb{C} \leq \mathbb{C}'$ in the quotient $W_{\mathbf{s}}/\equiv$,
- there exist two \mathbf{s} -trees $\mathbb{T} \in \mathbb{C}$ and $\mathbb{T}' \in \mathbb{C}'$ such that $\mathbb{T} \leq \mathbb{T}'$ in the \mathbf{s} -weak order,
- there exist two \mathbf{s} -trees $\mathbb{T} \in \mathbb{C}$ and $\mathbb{T}' \in \mathbb{C}'$ such that $\bar{\mathbb{F}}_{\mathbb{T}}$ and $\bar{\mathbb{F}}_{\mathbb{T}'}$ are adjacent, and ω points from $\bar{\mathbb{F}}_{\mathbb{T}}$ to $\bar{\mathbb{F}}_{\mathbb{T}'}$,
- \mathbb{C} and \mathbb{C}' are adjacent, and ω points from \mathbb{C} to \mathbb{C}' . □

5.3. Shardoplexes. Generalizing Definition 79, we now associate to each \mathbf{s} -arc α a polytopal complex \mathbb{S}_{α} , that we call the *α -shardoplex*. To construct this polytopal complex, we associate a polytope (not necessarily full-dimensional) to each \mathbf{s} -arc and \mathbf{s} -trunk, in such a way that the polytopes corresponding to the same \mathbf{s} -arc but different \mathbf{s} -trunks glue nicely. These polytopes are constructed as certain faces of shard polytopes of [PPR23], see Definition 79. Recall from Remark 2(6) our labeling of the \mathbf{s} -trunks by $\Lambda_{\mathbf{s}}$, and from Example 16 the geometric description of the corresponding minimal cells of the \mathbf{s} -foam $\mathcal{F}_{\mathbf{s}}$.

Definition 87. Fix an \mathbf{s} -arc $\alpha := (i, j, A, B, r)$, let $\tilde{\alpha} := (i, j, A, B)$ denote the corresponding classical arc, and let $\mathbf{q} \in \Lambda_{\mathbf{s}}$. The *local shard polytope* $\mathbb{S}_{\alpha}^{\mathbf{q}}$ is the face of the shard polytope $\mathbb{SP}_{\tilde{\alpha}}$ maximizing the scalar product with the vector $\sum_{\ell \in [i, j]} (q_i - q_{\ell} + r - 1 + \sum_{k \in B \cap]i, \ell[} \max(0, s_k - 1)) \mathbf{e}_{\ell}$.

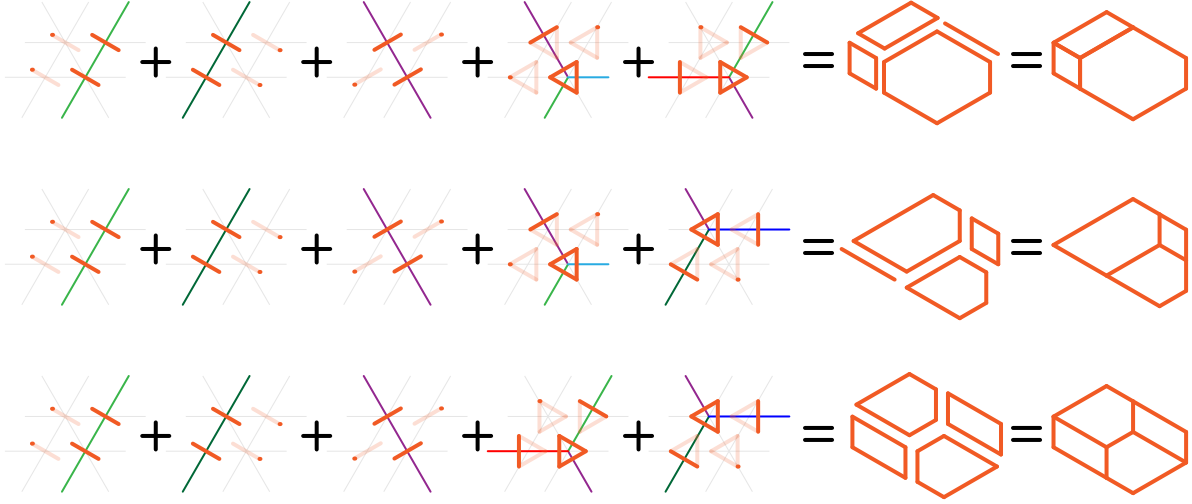


FIGURE 28. Some quotientpolytopes of the $(2,1,0)$ -weak order, obtained as Minkowski sums of shardpolytopes.

Remark 88. In Definition 87, note that $\tilde{\alpha} := (i, j, A, B)$ is strictly speaking not really an arc since $A \sqcup B = \{k \in]i, j[\mid s_k \neq 0\}$ may differ from $]i, j[$ if \mathbf{s} contains some 0. However, Definition 79 for the shard polytope $\mathbb{SP}_{\tilde{\alpha}}$ still holds, and was already considered in [PPR23, Rem. 43] as “pseudoshard polytope”.

Proposition 89. For any \mathbf{s} -arc α , the collection of all local shard polytopes $\mathbb{S}_{\alpha}^{\mathbf{q}}$ for $\mathbf{q} \in \Lambda_{\mathbf{s}}$, together with all their faces, form a polyhedral complex \mathbb{S}_{α} that we call the *shardpolyplex* of α .

Proof. The union of the sets of faces of the local shard polytopes $\mathbb{S}_{\alpha}^{\mathbf{q}}$ for $\mathbf{q} \in \Lambda_{\mathbf{s}}$ is a set of faces of the shard polytope $\mathbb{SP}_{\tilde{\alpha}}$ that contains $\mathbb{SP}_{\tilde{\alpha}}$ itself. Indeed, we can take for example $\mathbf{q} \in \Lambda_{\mathbf{s}}$ such that $q_{\ell} = 1$ for all $\ell \in [i] \cup]j, n]$ and $q_{\ell} = r + \sum_{k \in B \cap]i, \ell[} \max(0, s_k - 1)$ for all $\ell \in]i, j]$ to have $\mathbb{S}_{\alpha}^{\mathbf{q}} = \mathbb{SP}_{\tilde{\alpha}}$. Hence the collection of local shard polytopes with their faces indeed form a polytopal complex. \square

Generalizing Proposition 80, the main feature of the α -shardpolyplex \mathbb{S}_{α} is that the union of the walls of its dual polyhedral complex contains the \mathbf{s} -shard Σ_{α} and is contained in the union of the \mathbf{s} -shards Σ_{β} over all subarcs β of the \mathbf{s} -arc α . This property is properly stated in Proposition 105 in terms of tropical geometry.

5.4. Quotientpolytopes. We now generalize Theorem 81 to the \mathbf{s} -weak order. For a congruence \equiv of the \mathbf{s} -weak order, we define a polytopal complex \mathbb{Q}_{\equiv} using Minkowski sums of the α -shardpolyplexes of Proposition 89, such that the oriented graph of \mathbb{Q}_{\equiv} is isomorphic to the Hasse diagram of the quotient $W_{\mathbf{s}}/\equiv$. See Figures 28 to 33 for some illustrations. We first need to explain what we mean by Minkowski sums here, even if it will be clear from Section 6.

Lemma 90. Let $\mathbb{S} := (\mathbb{S}^{\mathbf{q}})_{\mathbf{q} \in \Lambda_{\mathbf{s}}}$ and $\mathbb{T} := (\mathbb{T}^{\mathbf{q}})_{\mathbf{q} \in \Lambda_{\mathbf{s}}}$ be such that for any $\mathbf{p} \neq \mathbf{q} \in \Lambda_{\mathbf{s}}$, there is $\mu, \nu \in \mathbb{R}$ such that $\langle \mathbf{q} - \mathbf{p} \mid \mathbf{s} \rangle - \mu$ (resp. $\langle \mathbf{q} - \mathbf{p} \mid \mathbf{t} \rangle - \nu$) is non-negative for all $\mathbf{s} \in \mathbb{S}^{\mathbf{p}}$ (resp. $\mathbf{t} \in \mathbb{T}^{\mathbf{p}}$) and non-positive for all $\mathbf{s} \in \mathbb{S}^{\mathbf{q}}$ (resp. $\mathbf{t} \in \mathbb{T}^{\mathbf{q}}$). If \mathbb{S} and \mathbb{T} , together with all their faces, form two polytopal complexes, then so does their *Minkowski sum* $\mathbb{S} + \mathbb{T} := (\mathbb{S}^{\mathbf{q}} + \mathbb{T}^{\mathbf{q}})_{\mathbf{q} \in \Lambda_{\mathbf{s}}}$.

Proof. Let \mathbb{X} and \mathbb{Y} be two faces of $\mathbb{S} + \mathbb{T}$ whose intersection is non-empty. Let $\mathbf{p}, \mathbf{q} \in \Lambda_{\mathbf{s}}$ be such that \mathbb{X} (resp. \mathbb{Y}) is a face of $\mathbb{S}^{\mathbf{p}} + \mathbb{T}^{\mathbf{p}}$ (resp. of $\mathbb{S}^{\mathbf{q}} + \mathbb{T}^{\mathbf{q}}$). Let $\mu, \nu \in \mathbb{R}$ be as in the statement. Then $\langle \mathbf{q} - \mathbf{p} \mid \mathbf{s} + \mathbf{t} \rangle - (\mu + \nu)$ is non-negative for any $\mathbf{s} + \mathbf{t} \in \mathbb{S}^{\mathbf{p}} + \mathbb{T}^{\mathbf{p}}$ and non-positive for $\mathbf{s} + \mathbf{t} \in \mathbb{S}^{\mathbf{q}} + \mathbb{T}^{\mathbf{q}}$. Hence, this dot product must vanish on the intersection $\mathbb{X} \cap \mathbb{Y}$. We conclude

that the intersection $\mathbb{X} \cap \mathbb{Y}$ lies in the face of \mathbb{X} , hence of $\mathbb{S}^{\mathbf{p}} + \mathbb{T}^{\mathbf{p}}$ (resp. of \mathbb{Y} , hence of $\mathbb{S}^{\mathbf{q}} + \mathbb{T}^{\mathbf{q}}$) maximizing the direction $\mathbf{q} - \mathbf{p}$ (resp. $\mathbf{p} - \mathbf{q}$). By standard properties of Minkowski sums, the latter is the Minkowski sum of the faces of $\mathbb{S}^{\mathbf{p}}$ and $\mathbb{T}^{\mathbf{p}}$ (resp. of $\mathbb{S}^{\mathbf{q}}$ and $\mathbb{T}^{\mathbf{q}}$) maximizing the direction $\mathbf{q} - \mathbf{p}$ (resp. $\mathbf{p} - \mathbf{q}$). Since \mathbb{S} (resp. \mathbb{T}) form polytopal complexes, these faces of $\mathbb{S}^{\mathbf{p}}$ and $\mathbb{S}^{\mathbf{q}}$ (resp. of $\mathbb{T}^{\mathbf{p}}$ and $\mathbb{T}^{\mathbf{q}}$) intersect along a face \mathbb{F} (resp. \mathbb{G}) of both. We conclude that $\mathbb{X} \cap \mathbb{Y} = \mathbb{F} + \mathbb{G}$ is a face of both \mathbb{X} and \mathbb{Y} . \square

As the shardodplexes clearly satisfy the conditions of Lemma 90, we can apply Lemma 90 to define Minkowski sums of shardodplexes. Note that we will see in Theorem 107 an alternative and more direct definition for the quotientplex \mathbb{Q}_{\equiv} in terms of tropical geometry.

Definition 91. For a congruence \equiv of the \mathbf{s} -weak order $W_{\mathbf{s}}$, the *quotientplex* \mathbb{Q}_{\equiv} is the Minkowski sum of (any positive scaling of) the shardodplexes \mathbb{S}_{α} over all \mathbf{s} -arcs α in \mathcal{A}_{\equiv} .

If we want to make explicit the scaling coefficients, we denote by $\mathbb{Q}_{\equiv}(\boldsymbol{\lambda})$ the quotientplex obtained as the Minkowski sum $\sum_{\alpha \in \mathcal{A}_{\equiv}} \lambda_{\alpha} \mathbb{S}_{\alpha}$ for $\boldsymbol{\lambda} := (\lambda_{\alpha})_{\alpha \in \mathcal{A}_{\equiv}}$ with $\lambda_{\alpha} > 0$.

We now state a generalization of Theorem 81. A more refined version will be stated in Theorem 106 and Theorem 107 using tropical geometry.

Proposition 92. *There is an inclusion reversing bijection ψ from the faces of the quotient foam \mathcal{F}_{\equiv} to the faces of the quotientplex \mathbb{Q}_{\equiv} such that \mathbb{F} and $\psi(\mathbb{F})$ are orthogonal.*

Proof. See Remark 108. \square

Proposition 93. *For any congruence \equiv of the \mathbf{s} -weak order $W_{\mathbf{s}}$, the Hasse diagram of the quotient $W_{\mathbf{s}}/\equiv$ is isomorphic to the skeleton of the quotientplex \mathbb{Q}_{\equiv} .*

Proof. This follows from Propositions 86 and 92. \square

Proposition 94. *For an \mathbf{s} -arc $\alpha := (i, j, A, B, r)$, denote by $\tilde{\alpha} := (i, j, A, B)$ the corresponding classical arc. For a congruence \equiv of the \mathbf{s} -weak order $W_{\mathbf{s}}$, denote by $\tilde{\equiv}$ the corresponding congruence of the weak order W_n , with down set of arcs $\mathcal{A}_{\tilde{\equiv}} := \{\tilde{\alpha} \mid \alpha \in \mathcal{A}_{\equiv}\}$. Consider $\boldsymbol{\lambda} := (\lambda_{\alpha})_{\alpha \in \mathcal{A}_{\equiv}}$ with $\lambda_{\alpha} > 0$, and let $\tilde{\boldsymbol{\lambda}} := (\tilde{\lambda}_{\tilde{\alpha}})_{\tilde{\alpha} \in \mathcal{A}_{\tilde{\equiv}}}$ with $\tilde{\lambda}_{\tilde{\alpha}} := \sum_{\alpha \in \mathcal{A}_{\equiv}} \lambda_{\alpha}$ where the sum ranges over all \mathbf{s} -arcs α which project to $\tilde{\alpha}$. Then the quotientplex $\mathbb{Q}_{\equiv}(\boldsymbol{\lambda})$ is a polytopal subdivision of (a translate of) the quotientope $\mathbb{Q}_{\tilde{\equiv}}(\tilde{\boldsymbol{\lambda}})$.*

Proof. For each \mathbf{s} -arc α , the support of the α -shardodplex \mathbb{S}_{α} is (a translate of) the shard polytope $\mathbb{SP}_{\tilde{\alpha}}$. Hence, the support of the Minkowski sum $\mathbb{Q}_{\equiv}(\boldsymbol{\lambda}) := \sum_{\alpha \in \mathcal{A}_{\equiv}} \lambda_{\alpha} \mathbb{S}_{\alpha}$ is (a translate of) the Minkowski sum $\sum_{\alpha \in \mathcal{A}_{\equiv}} \lambda_{\alpha} \mathbb{SP}_{\tilde{\alpha}} = \sum_{\tilde{\alpha} \in \mathcal{A}_{\tilde{\equiv}}} \left(\sum_{\alpha \in \mathcal{A}_{\equiv}} \lambda_{\alpha} \right) \mathbb{SP}_{\tilde{\alpha}} = \sum_{\tilde{\alpha} \in \mathcal{A}_{\tilde{\equiv}}} \tilde{\lambda}_{\tilde{\alpha}} \mathbb{SP}_{\tilde{\alpha}} =: \mathbb{Q}_{\tilde{\equiv}}(\tilde{\boldsymbol{\lambda}})$. \square

Remark 95. In Proposition 94, note that $\tilde{\equiv}$ is strictly speaking not really a congruence of the weak order, for the same reason as Remark 88. However, the definition of $\mathbb{Q}_{\tilde{\equiv}}(\tilde{\boldsymbol{\lambda}})$ as a Minkowski sum of pseudoshard polytopes $\sum_{\tilde{\alpha}} \tilde{\lambda}_{\tilde{\alpha}} \mathbb{SP}_{\tilde{\alpha}}$ is still valid.

Applying Propositions 93 and 94 to the trivial congruence (where each congruence class contains a single \mathbf{s} -tree), we obtain the following statement, answering a question of C. Ceballos and V. Pons [CP24a, CP24b]. We note that this question was partially solved in [DMP⁺23] in the case when \mathbf{s} contains no 0 entry, with a very different method based on a combination of flow polytopes, tropical geometry, and Cayley embedding.

Corollary 96. *For any \mathbf{s} , the Hasse diagram of the \mathbf{s} -weak order $W_{\mathbf{s}}$ is isomorphic to the oriented skeleton of a polytopal subdivision of a polytope combinatorially equivalent to the zonotope $\text{Zono}(\mathbf{s}) := \sum_{1 \leq i < j \leq n} s_i \text{conv}\{e_i, e_j\}$.*

Proof. By Propositions 93 and 94, the Hasse diagram of the \mathbf{s} -weak order $W_{\mathbf{s}}$ is isomorphic to a polyhedral subdivision of $\mathbb{Q}_{\equiv}(\tilde{\boldsymbol{\lambda}})$, where $\tilde{\equiv}$ is the projection of the trivial congruence \equiv of the \mathbf{s} -weak order. The normal fan of $\mathbb{Q}_{\equiv}(\tilde{\boldsymbol{\lambda}})$ is the arrangement of the hyperplanes $\{\mathbf{x} \in \mathbb{R}^n \mid x_i = x_j\}$ for all $1 \leq i < j \leq n$ such that there exists an \mathbf{s} -arc of the form (i, j, A, B, r) , that is, such that $s_i \neq 0$. We conclude that $\mathbb{Q}_{\equiv}(\tilde{\boldsymbol{\lambda}})$ and $\text{Zono}(\mathbf{s})$ are normally equivalent, hence combinatorially equivalent. \square

Remark 97. In fact, the Minkowski sum of the shardoxes S_α for all \mathbf{s} -arcs α , with coefficients $\lambda_\alpha = 1$ is a polytopal subdivision of the zonotope

$$\sum_{1 \leq i < j \leq n} \mathbf{1}_{s_i \neq 0} \left(\sum_{1 \leq g \leq i} s_g 2^{\#\{h \in [g, i] \mid s_h \neq 0\}} \right) \left(1 + \mathbf{1}_{s_j \neq 0} \sum_{j < \ell \leq n} 2^{\#\{k \in [j, \ell] \mid s_k \neq 0\}} \right) \text{conv}\{\mathbf{0}, \mathbf{e}_i - \mathbf{e}_j\}.$$

For instance, when $\mathbf{s} = (1, \dots, 1)$, this zonotope

$$\sum_{1 \leq i < j \leq n} 2^{n-j+i-1} \text{conv}\{\mathbf{0}, \mathbf{e}_i - \mathbf{e}_j\}$$

is the sum of all the shard polytopes illustrated in [PPR23, Fig. 14].

Figure 29 illustrates the quotientplexes of all congruences of the $(1, 2, 0)$ - and $(2, 1, 0)$ -weak orders. In Figures 30 to 33, we have represented the quotientplexes for the trivial and the sylvester congruences of some \mathbf{s} -weak orders.

Remark 98. Consider $\mathbf{s} \in \{0, 1\}^n$, and define the directed graph $D_\mathbf{s}$ with vertices $[n]$ and arcs $\{(i, j) \mid 1 \leq i < j \leq n \text{ and } s_i \neq 0\}$. As $T_j \leq 2$ for all $j \in [n]$, we have $\prod_{j \in [n]} \max(1, T_{j-1} - 1) = 1$, hence a single \mathbf{s} -trunk. Consequently

- the \mathbf{s} -weak order is the acyclic reorientation lattice of $D_\mathbf{s}$ studied in [Pil24] (one can check that $D_\mathbf{s}$ is indeed a vertebrate and skeletal acyclic directed graph as defined in [Pil24]),
- the \mathbf{s} -arcs correspond to the ropes of $D_\mathbf{s}$, the non-crossing \mathbf{s} -arc diagrams correspond to the non-crossing rope diagrams of $D_\mathbf{s}$, and the subarc order coincide with the subrope order of $D_\mathbf{s}$ (see [Pil24] for the definitions),
- the \mathbf{s} -foam is the graphical arrangement of $D_\mathbf{s}$, and the \mathbf{s} -permutahedron is a graphical zonotope of $D_\mathbf{s}$ (a Minkowski sum of positive dilates of the segments $[e_i, e_j]$ for all arcs (i, j) of $D_\mathbf{s}$, where the dilation factors are directly obtained from Remark 97).

6. TROPICAL GEOMETRY

In this section, we prove the results of Section 5 via tropical geometry.

6.1. Recollection 6: Polytopal subdivisions and tropical duality. Tropical geometry offers a convenient setting to dualize regular polyhedral subdivisions, in a sense that we define below. This section is based on the work of Joswig in [Jos21, Chap. 1] and [Jos17] (except that we define the tropical addition with max rather than min).

The *tropical semiring* is the set $\mathbb{T} := \mathbb{R} \cup \{\infty\}$ equipped with the *tropical addition* $x \oplus y := \max(x, y)$ and the *tropical multiplication* $x \odot y := x + y$. A *tropical polynomial* on d variables is any function $F : \mathbb{R}^d \rightarrow \mathbb{R}$ of the form

$$F(\mathbf{x}) = \bigoplus_{i \in [n]} c_i \odot \mathbf{x}^{\mathbf{a}_i} = \max \{c_i + \langle \mathbf{a}_i, \mathbf{x} \rangle \mid i \in [n]\},$$

where $n \in \mathbb{N}$ and for all $i \in [n]$, $c_i \in \mathbb{T}$ and $\mathbf{a}_i \in \mathbb{Z}^d$. This is a convex piecewise affine function. Note that F is not uniquely determined by the exponents \mathbf{a}_i and the coefficients c_i .

The *tropical hypersurface* defined by F , or *vanishing locus* of F , is the set

$$\mathcal{T}(F) := \{\mathbf{x} \in \mathbb{R}^d \mid \text{the maximum of } F(\mathbf{x}) \text{ is attained at least twice}\}.$$

It is the image codimension-2-skeleton of the *dome*

$$\mathcal{D}(F) := \{(\mathbf{x}, y) \in \mathbb{R}^{d+1} \mid \mathbf{x} \in \mathbb{R}^d, y \in \mathbb{R}, y \geq F(\mathbf{x})\}$$

under the orthogonal projection that omits the last coordinate [Jos21, Coro. 1.6].

The *cells* of $\mathcal{T}(F)$ are the projections of the faces of $\mathcal{D}(F)$ (here we include the regions of \mathbb{R}^d delimited by $\mathcal{T}(F)$ as its d -dimensional cells. In fact we are considering the normal complex $NC(F)$ defined in [Jos21, after Exm. 1.7]).

Note that the cells of $\mathcal{T}(F)$ are invariant under multiplying all c_i and \mathbf{a}_i by a same scalar $\lambda \in \mathbb{R}$.

Let $\mathbf{A} = \{\mathbf{a}_1, \dots, \mathbf{a}_n\}$ be a point configuration in \mathbb{R}^d with integer coordinates vertices, and $\ell : [n] \rightarrow \mathbb{R}$ a *lifting function*. Such a point configuration together with its lifting function ℓ define:

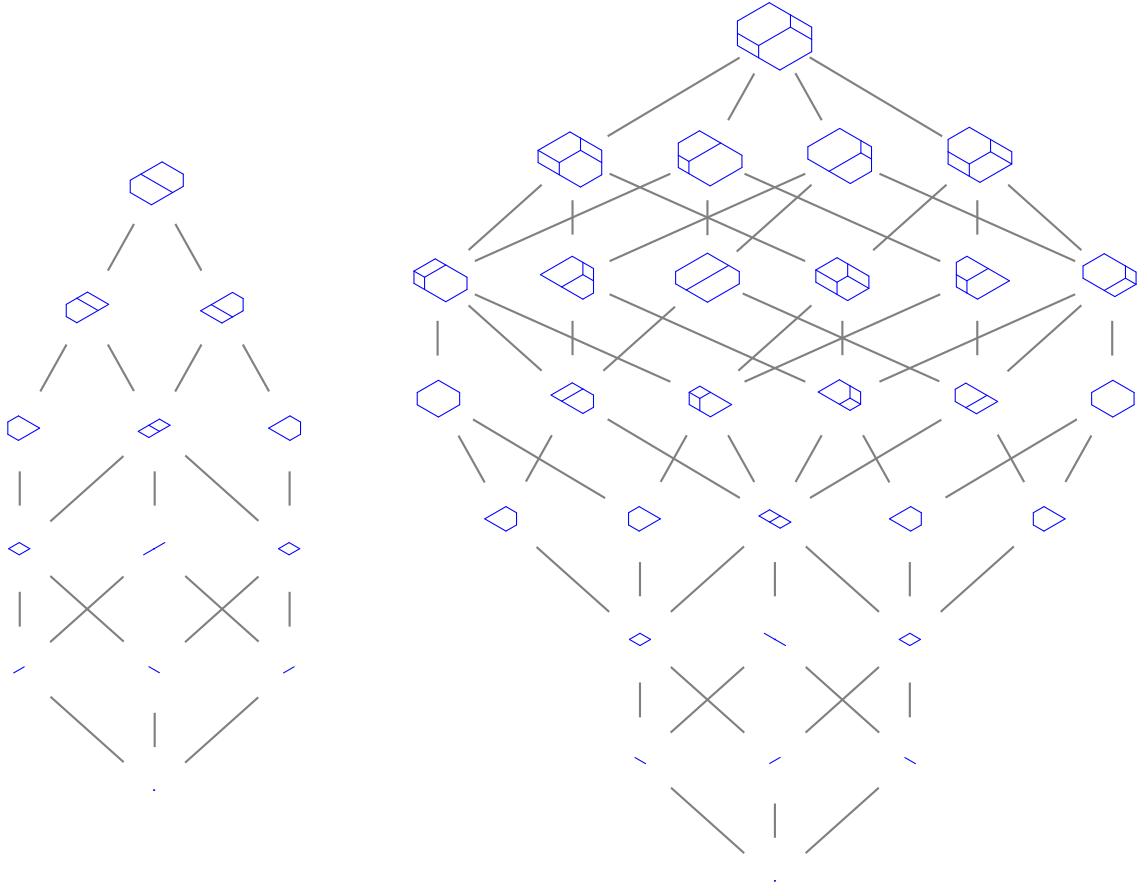


FIGURE 29. The congruence lattice of the s -weak order W_s for $s = (1, 2, 0)$ (left) and $s = (2, 1, 0)$ (right), where each congruence \equiv is replaced by its quotienttoplex Q_{\equiv} . See also Figures 22 and 27.

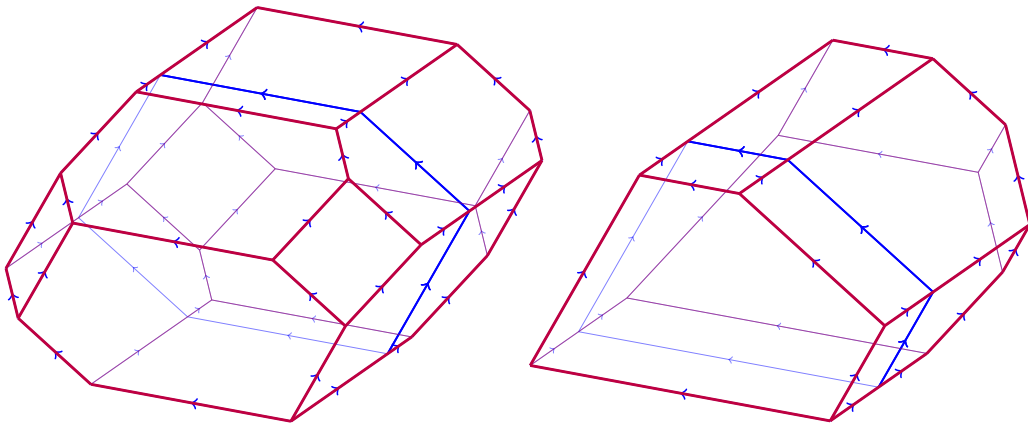


FIGURE 30. The $(1, 1, 2, 1)$ -permutahedron and the $(1, 1, 2, 1)$ -associahedron.

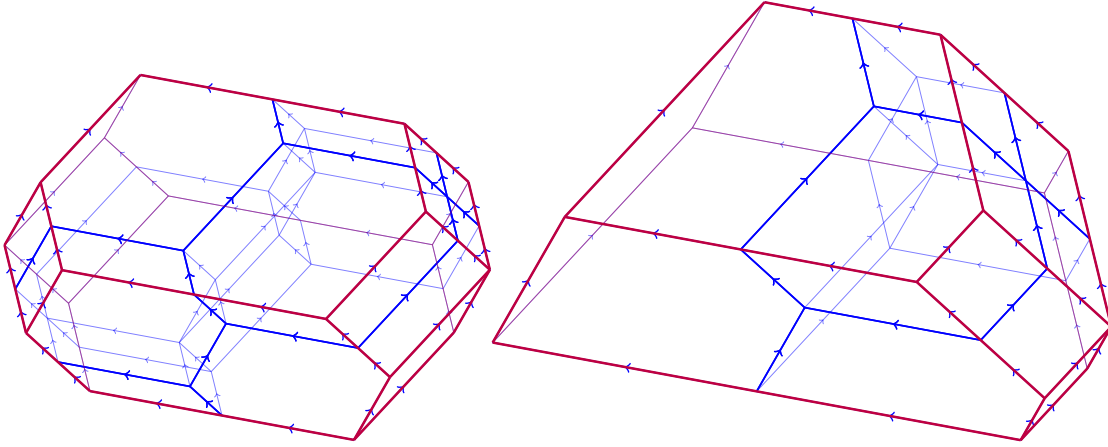


FIGURE 31. The $(2, 1, 0, 1)$ -permutahedron and the $(2, 1, 0, 1)$ -associahedron.

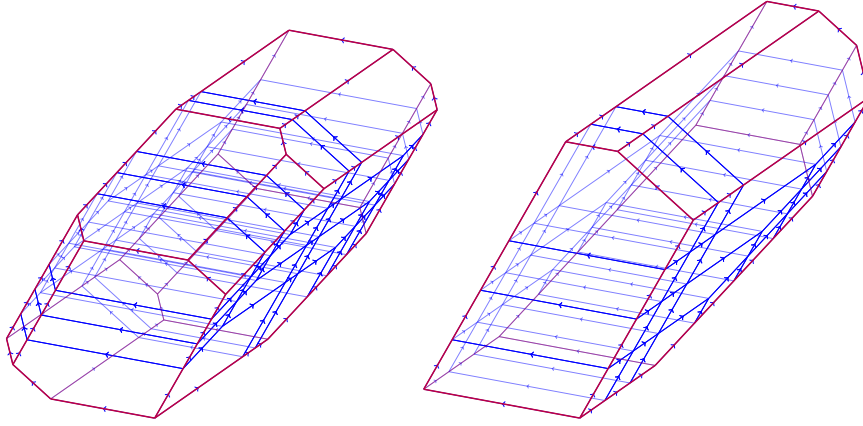


FIGURE 32. The $(1, 4, 3, 2)$ -permutahedron and the $(1, 4, 3, 2)$ -associahedron.

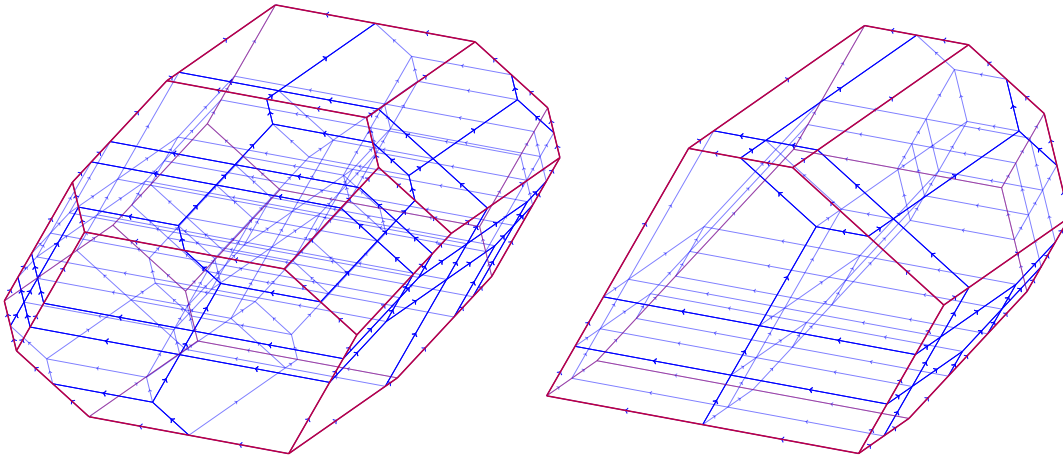


FIGURE 33. The $(2, 3, 2, 1)$ -permutahedron and the $(2, 3, 2, 1)$ -associahedron.

- the *regular* subdivision \mathcal{S} of \mathbf{A} obtained by taking the image of the upper faces of $\text{conv}(\{(\mathbf{a}_1, \ell(1)), \dots, (\mathbf{a}_n, \ell(n))\})$ by the projection that forgets the last coordinate,
- the *tropical polynomial*

$$F(\mathbf{x}) = \bigoplus_{i \in [n]} \ell(i) \odot \mathbf{x}^{\mathbf{a}_i} = \max \{ \ell(i) + \langle \mathbf{a}_i, \mathbf{x} \rangle \mid i \in [n] \},$$

where $\mathbf{x} \in \mathbb{R}^d$.

We say that $\mathcal{T}(F)$ is the *tropical dual* of the subdivision \mathcal{S} with lifting function ℓ since we have the following theorem.

Theorem 99 ([Jos21, Theorem 1.13]). *There is a bijection between the k -dimensional cells of \mathcal{S} and the $(d - k)$ -dimensional cells of $\mathcal{T}(F)$, which reverses the inclusion order.*

Remark 100. This duality corresponds to what P. McMullen calls *strong duality* in [McM03, Sects. 6 & 7] (see in particular [McM03, Thm. 7.1]). It implies that the affine spans of dual cells are orthogonal.

We now look at the case of Minkowski sum. We consider a family of point configurations $\mathbf{A}_1, \dots, \mathbf{A}_k$ in \mathbb{R}^d such that for all $j \in [k]$, $\mathbf{A}_j = \{\mathbf{a}_{j,1}, \dots, \mathbf{a}_{j,m_j}\}$ is a point configuration in \mathbb{R}^d with integer coordinate vertices and $\ell_j : [m_j] \rightarrow \mathbb{R}$ is an associated lifting function. Their Minkowski sum is the point configuration $\mathbf{A} := \sum \mathbf{A}_i = \{\mathbf{a}_{1,i_1} + \dots + \mathbf{a}_{k,i_k} \mid (i_1, \dots, i_k) \in [m_1] \times \dots \times [m_k]\}$ in \mathbb{R}^d with the lifting function $\ell : [m_1] \times \dots \times [m_k] \rightarrow \mathbb{R}$ such that $\ell(i_1, \dots, i_k) = \sum_{j \in [k]} \ell_j(i_j)$.

The corresponding tropical polynomial is

$$\begin{aligned} F(\mathbf{x}) &= \bigoplus_{\substack{(i_1, \dots, i_k) \\ \in [m_1] \times \dots \times [m_k]}} \ell(i_1, \dots, i_k) \odot \mathbf{x}^{\sum_{j \in [k]} \mathbf{a}_{j,i_j}} = \bigoplus_{\substack{(i_1, \dots, i_k) \\ \in [m_1] \times \dots \times [m_k]}} \bigodot_{j \in [k]} \ell_j(i_j) \odot \mathbf{x}^{\mathbf{a}_{j,i_j}} \\ &= \bigodot_{j \in [k]} \bigoplus_{i_j \in [m_j]} \ell_j(i_j) \odot \mathbf{x}^{\mathbf{a}_{j,i_j}} = \bigodot_{j \in [k]} F_j(\mathbf{x}), \end{aligned}$$

where F_j is the tropical polynomial associated to \mathbf{A}_j with lifting ℓ_j .

Lemma 101 ([Jos17, Lem. 6]). *Let F be a tropical polynomial obtained as a factorization $F = \bigodot_{j \in [k]} F_j$. Then, the vanishing locus $\mathcal{T}(F)$ is obtained by taking the union of the vanishing loci $\mathcal{T}(F_j)$ for $j \in [k]$ and the cells of $\mathcal{T}(F)$ are the intersections of the cells of all $\mathcal{T}(F_j)$ for $j \in [k]$. We say that these cells are *induced* by the arrangement of tropical hypersurfaces $\{\mathcal{T}(F_j) \mid j \in [k]\}$.*

We have the following statement as a consequence of the previous discussion on Minkowski sum and of Theorem 99.

Theorem 102. *The tropical dual of the mixed subdivision \mathcal{S} of a Minkowski sum of point configurations $\{\mathbf{A}_j \mid j \in [k]\}$ each with a lifting function ℓ_j is the polyhedral complex of cells induced by the arrangement of tropical hypersurfaces $\{\mathcal{T}(F_j) \mid j \in [k]\}$.*

6.2. Shard tropical hypersurfaces and polynomials.

Definition 103. Let $\alpha := (i, j, A, B, t)$ be an s -arc, and $\tilde{\alpha} := (i, j, A, B)$ the corresponding classical arc. For each $\tilde{\alpha}$ -alternate matching $\mu := \{i_1 < j_1 < \dots < i_q < j_q\}$ in $\mathcal{M}_{\tilde{\alpha}}$, we define the lifting $\ell_\alpha(\mu) := -(r-1)\mathbf{1}_{i_1=i} - \sum_{p \in [q]} \sum_{k \in B \cap [i_p, j_p[} \max(0, s_k - 1)$.

This lifting gives rise to the tropical polynomial

$$F_\alpha(\mathbf{x}) = \bigoplus_{\mu \in \mathcal{M}_{\tilde{\alpha}}} \ell_\alpha(\mu) \odot \mathbf{x}^{\mathbf{x}_\mu},$$

with associated tropical hypersurface $\mathcal{T}(F_\alpha)$.

Lemma 104. *The lifting ℓ_α induces the trivial subdivision of the shard polytope $\mathbb{SP}_{\tilde{\alpha}}$. Moreover, the unique minimal cell of $\mathcal{T}(F_\alpha)$ is the following subspace, of dimension $n - (j - i)$:*

$$\mathbb{C}_\alpha^{\min} := \left\{ \mathbf{x} \in \mathbb{R}^n \left| \begin{array}{l} x_i - x_j = r - 1 + \sum_{k \in B} \max(0, s_k - 1), \\ x_i - x_a = r - 1 + \sum_{k \in B \cap]i, a[} \max(0, s_k - 1) \text{ for all } a \in A, \\ x_i - x_b = r - 1 + \sum_{k \in B \cap]i, b[} \max(0, s_k - 1) \text{ for all } b \in B. \end{array} \right. \right\}$$

Proof. A minimal cell of $\mathcal{T}(F_\alpha)$ is the locus where the maximum of F_α is attained at a maximal subset S of \mathcal{M}_α . Let \mathbf{x} be a point in such a cell. We see that

- $\{\emptyset, \{i < j\}\} \subseteq S$ implies that $x_i - x_j = r - 1 + \sum_{k \in B} \max(0, s_k - 1)$,
- for all $a \in A$, $\{\emptyset, \{a < j\}\} \subseteq S$ implies that $x_a - x_j = \sum_{k \in B \cap]a, j[} \max(0, s_k - 1)$,
- for all $b \in B$, $\{\emptyset, \{i < b\}\} \subseteq S$ implies that $x_i - x_b = r - 1 + \sum_{k \in B \cap]i, b[} \max(0, s_k - 1)$,

and if all these equations are satisfied then $\{\emptyset, \mu\} \subseteq S$ for any $\mu \in \mathcal{M}_\alpha$. Hence there is a unique minimal cell of $\mathcal{T}(F_\alpha)$, where the maximum of F_α is attained for all $\mu \in \mathcal{M}_{\tilde{\alpha}}$, and it is equal to \mathbb{C}_α^{\min} . \square

Proposition 105. *For any \mathbf{s} -arc α , the tropical hypersurface $\mathcal{T}(F_\alpha)$*

- *contains the shard Σ_α ,*
- *is contained in the union of the shards Σ_β over all subarcs β of α .*

Proof. Note that this proposition is the analogue of [PPR23, Proposition 48], where the normal fan of the shard polytope \mathbb{SP}_α is replaced by the tropical hypersurface $\mathcal{T}(F_\alpha)$. The proof is very similar and relies on [PPR23, Lemma 49].

We consider an \mathbf{s} -shard $\alpha := (i, j, A, B, t)$. We recall that the \mathbf{s} -shard of α is the polyhedron

$$\begin{aligned} \Sigma_\alpha &= \left\{ \mathbf{x} \in \mathbb{R}^n \left| \begin{array}{l} x_i - x_j = r - 1 + \sum_{k \in B} \max(0, s_k - 1), \\ x_i - x_a \geq r - 1 + \sum_{k \in B \cap]i, a[} \max(0, s_k - 1) \text{ for all } a \in A, \\ x_i - x_b \leq r - 1 + \sum_{k \in B \cap]i, b[} \max(0, s_k - 1) \text{ for all } b \in B. \end{array} \right. \right\} \\ &= \left\{ \mathbf{x} \in \mathbb{R}^n \left| \begin{array}{l} -(r - 1) - \sum_{k \in B} \max(0, s_k - 1) + x_i - x_j = 0, \\ - \sum_{k \in B \cap]a, j[} \max(0, s_k - 1) + x_a - x_j \leq 0 \text{ for all } a \in A, \\ -(r - 1) - \sum_{k \in B \cap]i, b[} \max(0, s_k - 1) + x_i - x_b \leq 0 \text{ for all } b \in B. \end{array} \right. \right\} \end{aligned}$$

This corresponds to the locus where the maximum of F_α is attained for both $\mu = \{i < j\}$ and $\mu = \emptyset$, which shows that $\Sigma_\alpha \subseteq \mathcal{T}(F_\alpha)$. Indeed, for any $\mathbf{x} \in \Sigma_\alpha$ and $\mu := \{i_1 < \dots < j_q\} \in \mathcal{M}_{\tilde{\alpha}} \setminus \{\{i < j\}, \emptyset\}$,

we have

$$\begin{aligned}
\ell_\alpha(\mu) + \langle \chi_\mu, \mathbf{x} \rangle &= -(r-1)\mathbf{1}_{i_1=i} + \sum_{p \in [q]} \left(- \sum_{k \in B \cap]i_p, j_p[} \max(0, s_k - 1) + x_{i_p} - x_{j_p} \right) \\
&= -(r-1)\mathbf{1}_{i_1=i} + \sum_{p \in [q]} \left(- \sum_{k \in B \cap]i_p, j_p[} \max(0, s_k - 1) + x_{i_p} - x_{j_p} \right. \\
&\quad \left. - (r-1) - \sum_{k \in B} \max(0, s_k - 1) + x_i - x_j \right) \\
&= -(r-1)\mathbf{1}_{i_1=i} + \sum_{p \in [q]} \left(- (r-1) - \sum_{k \in B \cap]i, j_p[} \max(0, s_k - 1) + x_i - x_{j_p} \right. \\
&\quad \left. - \sum_{k \in B \cap]i_p, j[} \max(0, s_k - 1) + x_{i_p} - x_j \right) \\
&\leq 0.
\end{aligned}$$

Now we want to show that any codimension 1 cell of $\mathcal{T}(F_\alpha)$ is contained in a shard Σ_β for a certain subarc β of α . It follows from Lemma 104 that these cells are in correspondence with the edges of the shard polytope $\mathbb{SP}_{\tilde{\alpha}}$.

Let $\mathbf{x} \in \mathcal{T}(F_\alpha)$, which attains the maximum of F_α at exactly two $\tilde{\alpha}$ -alternate matchings μ_1 and μ_2 . This implies that there is an edge between the vertices χ_{μ_1} and χ_{μ_2} in the shard polytope $\mathbb{SP}_{\tilde{\alpha}}$ and we are in one of the four cases of [PPR23, Lemma 49]. We give the details for the first one and for the others we only specify β , the computations are similar:

- (1) If $\mu_1 = H < i' < j' < K$ and $\mu_2 = H < K$, we define $\beta := (i', j', A', B', r')$ with $A' := A \cap]i', j'[$, $B' := B \cap]i', j'[$ and $r' := r$ if $i' = i$ or $r' := 1$ otherwise. Then we have:

- $0 = \ell_\alpha(\mu_1) + \langle \chi_{\mu_1}, \mathbf{x} \rangle - \ell_\alpha(\mu_2) + \langle \chi_{\mu_2}, \mathbf{x} \rangle = -(r-1)\mathbf{1}_{i'=i} - \sum_{k \in B \cap]i', j'[} \max(0, s_k - 1) + x_{i'} - x_{j'}$.
- for any $a \in A'$,

$$\begin{aligned}
0 &< \ell_\alpha(\mu_1) + \langle \chi_{\mu_1}, \mathbf{x} \rangle - \ell_\alpha(\mu_3) + \langle \chi_{\mu_3}, \mathbf{x} \rangle \\
&= -(r-1)\mathbf{1}_{i'=i} - \sum_{k \in B \cap]i', a[} \max(0, s_k - 1) + x_{i'} - x_a,
\end{aligned}$$

where μ_3 denotes the $\tilde{\alpha}$ -alternate matching $\mu_3 := H < a < j' < K$.

- for any $b \in B'$,

$$\begin{aligned}
0 &< \ell_\alpha(\mu_1) + \langle \chi_{\mu_1}, \mathbf{x} \rangle - \ell_\alpha(\mu_3) + \langle \chi_{\mu_3}, \mathbf{x} \rangle \\
&= - \sum_{k \in B \cap]b, j'[} \max(0, s_k - 1) + x_b - x_{j'} \\
&= (r-1)\mathbf{1}_{i'=i} + \sum_{k \in B \cap]i', b[} \max(0, s_k - 1) + x_b - x_{i'},
\end{aligned}$$

where μ_3 denotes the $\tilde{\alpha}$ -alternate matching $\mu_3 := H < i' < b < K$.

- (2) If $\mu_1 = H < i' < j_1 < K$ and $\mu_2 = H < i' < j_2 < K$ with $j_1 < j_2$, we define $\beta := (j_1, j_2, A', B', s_{j_1})$ with $A' := A \cap]j_1, j_2[$, $B' := B \cap]j_1, j_2[$.
- (3) If $\mu_1 = H < i_1 < j' < K$ and $\mu_2 = H < i_2 < j' < K$, we define $\beta := (i_1, i_2, A', B', r')$ with $A' := A \cap]i_1, i_2[$, $B' := B \cap]i_1, i_2[$ and $r' := r$ if $i_1 = i$ or $r' := 1$ otherwise.
- (4) If $\mu_1 = H < i_1 < j_1 < i_2 < j_2 < K$ and $\mu_2 = H < i_1 < j_2 < K$, we define $\beta := (j_1, i_2, A', B', s_{j_1})$ with $A' := A \cap]i_1, j_2[$, $B' := B \cap]i_1, j_2[$.

We see that in all cases β is a subarc of α and $\mathbf{x} \in \Sigma_\beta$. \square

As a corollary of Proposition 105, Lemma 101 and Theorem 102 we obtain directly the following statement.

Theorem 106. *For any congruence \equiv of the \mathbf{s} -weak order, the quotient foam \mathcal{F}_\equiv is the polyhedral complex induced by the arrangement of tropical hypersurfaces $\{\mathcal{T}(F_\alpha) \mid \alpha \in \mathcal{A}_\equiv\}$. In particular,*

it is the tropical dual of the regular subdivision of the Minkowski sum of the point configurations $\{\chi_\mu \mid \mu \in \mathcal{M}_{\tilde{\alpha}}\}$ with lifting function ℓ_α , over all $\alpha \in \mathcal{A}_{\equiv}$.

Theorem 107. For any congruence \equiv of the s -weak order, for any $\lambda := (\lambda_\alpha)_{\alpha \in \mathcal{A}_{\equiv}}$ with $\lambda_\alpha > 0$, the cells of the quotientoplex $\mathcal{Q}_{\equiv}(\lambda)$ are the cells of the regular subdivision of the Minkowski sum of the point configurations $\{\lambda_\alpha \chi_\mu \mid \mu \in \mathcal{M}_{\tilde{\alpha}}\}$ with lifting function $\lambda_\alpha \ell_\alpha$, over all $\alpha \in \mathcal{A}_{\equiv}$.

Proof. Let $\alpha := (i, j, A, B, r) \in \mathcal{A}$. Lemma 104 implies that the cells of $\mathcal{T}(F_\alpha)$ are exactly the translation of the cones of the normal fan of the shard polytope $\lambda_\alpha \mathbb{SP}_{\tilde{\alpha}}$ by any vector $\mathbf{x} \in \mathbb{C}_{\alpha}^{\min}$. This means that the minimal cell of $\mathcal{T}(F_\alpha)$ that contains a point \mathbf{y} is the tropical dual of the face of $\lambda_\alpha \mathbb{SP}_{\tilde{\alpha}}$ with lifting function $\lambda_\alpha \ell_\alpha$, maximized in the direction $\mathbf{y} - \mathbf{x}$ for any $\mathbf{x} \in \mathbb{C}_{\alpha}^{\min}$.

Let $\mathbf{q} \in \mathbf{\Lambda}_s$. The tropical dual of the local shard polytope $\lambda_\alpha \mathbb{S}_{\alpha}^{\mathbf{q}}$ with lifting function $\lambda_\alpha \ell_\alpha$ is the minimal cell of $\mathcal{T}(F_\alpha)$ that contains the insertion fiber $\mathbb{F}_{\mathbf{T}_{\mathbf{q}}}$ (described in Example 16). Indeed, the point $\mathbf{y} := -\mathbf{q}$ is in $\mathbb{F}_{\mathbf{T}_{\mathbf{q}}}$, the point $\mathbf{x} := -\sum_{\ell \in [i, j]} (q_i + r - 1 + \sum_{k \in B \cap [i, \ell]} \max(0, s_k - 1)) \mathbf{e}_\ell - \sum_{\ell \in [i] \cup [j, n]} q_\ell \mathbf{e}_\ell$ is in $\mathbb{C}_{\alpha}^{\min}$, and $\mathbf{y} - \mathbf{x} = \sum_{\ell \in [i, j]} (q_i - q_\ell + r - 1 + \sum_{k \in B \cap [i, \ell]} \max(0, s_k - 1)) \mathbf{e}_\ell$ is a direction along which the face $\mathbb{S}_{\alpha}^{\mathbf{q}}$ is maximized in the polytope $\mathbb{SP}_{\tilde{\alpha}}$ (Definition 87).

This implies that the tropical dual of the sum $\sum_{\alpha \in \mathcal{A}} \lambda_\alpha \mathbb{S}_{\alpha}^{\mathbf{q}}$ with lifting function $\lambda_\alpha \ell_\alpha$ for each summand is the minimal cell of the arrangement $\{\mathcal{T}(F_\alpha) \mid \alpha \in \mathcal{A}_{\equiv}\}$ that contains $\mathbb{F}_{\mathbf{T}_{\mathbf{q}}}$.

Reciprocally, we only need to check that each minimal cell \mathbb{C} of the arrangement $\{\mathcal{T}(F_\alpha) \mid \alpha \in \mathcal{A}_{\equiv}\}$ is the tropical dual of a sum $\sum_{\alpha \in \mathcal{A}} \lambda_\alpha \mathbb{S}_{\alpha}^{\mathbf{q}}$ for a certain $\mathbf{q} \in \mathbf{\Lambda}_s$. It follows from Theorem 106 that such a \mathbb{C} is a minimal cell of \mathcal{F}_{\equiv} , thus it is also a minimal cell of the s -foam \mathcal{F}_s , that is of the form $\mathbb{F}_{\mathbf{T}_{\mathbf{q}}}$ for a $\mathbf{q} \in \mathbf{\Lambda}_s$. It follows from the previous discussion that \mathbb{C} is the tropical dual of the sum $\lambda_\alpha \sum_{\alpha \in \mathcal{A}} \mathbb{S}_{\alpha}^{\mathbf{q}}$. \square

Remark 108. Proposition 92 is a consequence of Theorem 107, Theorem 106 and Remark 100.

ACKNOWLEDGEMENTS

We are grateful to Daniel Tamayo Jiménez for his collaboration in the early stages of this work, to Arnau Padrol for many suggestions and comments during this project, to Cesar Ceballos and Viviane Pons for various discussions on the s -weak order that clarified the intersection of this paper with their ongoing work, and to Spencer Backman for suggesting Remark 98.

REFERENCES

- [ACFF25] Andrei Asinowski, Jean Cardinal, Stefan Felsner, and Éric Fusy. Combinatorics of rectangulations: Old and new bijections. *Comb. Theory*, 5(1):Paper No. 14, 57, 2025.
- [AP23] Doriann Albertin and Vincent Pilaud. The canonical complex of the weak order. *Order*, 40(2):349–370, 2023.
- [Bar19] Emily Barnard. The canonical join complex. *Electron. J. Combin.*, 26(1):Paper No. 1.24, 25, 2019.
- [BHKN01] François Boulier, Florent Hivert, Daniel Krob, and Jean-Christophe Novelli. Pseudo-permutations. II. Geometry and representation theory. In *Discrete models: combinatorics, computation, and geometry (Paris, 2001)*, Discrete Math. Theor. Comput. Sci. Proc., AA, pages 123–132 (electronic). Maison Inform. Math. Discrèt. (MIMD), Paris, 2001.
- [BNP25] Emily Barnard, Jean-Christophe Novelli, and Vincent Pilaud. On simple congruences of the weak order. [arXiv:2503.15053](https://arxiv.org/abs/2503.15053), 2025.
- [CLCdPBM04] Nathalie Caspard, Claude Le Conte de Poly-Barbut, and Michel Morvan. Cayley lattices of finite Coxeter groups are bounded. *Adv. in Appl. Math.*, 33(1):71–94, 2004.
- [CP17] Grégory Chatel and Vincent Pilaud. Cambrian Hopf Algebras. *Adv. Math.*, 311:598–633, 2017.
- [CP24a] Cesar Ceballos and Viviane Pons. The s -Weak Order and s -Permutahedra I: Combinatorics and Lattice Structure. *SIAM J. Discrete Math.*, 38(4):2855–2895, 2024.
- [CP24b] Cesar Ceballos and Viviane Pons. The s -weak order and s -permutahedra II: the combinatorial complex of pure intervals. *Electron. J. Combin.*, 31(3):Paper No. 3.12, 59, 2024.
- [CP25] Jean Cardinal and Vincent Pilaud. Rectangulotopes. *European J. Combin.*, 125:Paper No. 104090, 25, 2025.
- [CPS19] Cesar Ceballos, Arnau Padrol, and Camilo Sarmiento. Geometry of ν -Tamari lattices in types A and B. *Trans. Amer. Math. Soc.*, 371(4):2575–2622, 2019.
- [Day94] Alan Day. Congruence normality: the characterization of the doubling class of convex sets. *Algebra Universalis*, 31(3):397–406, 1994.
- [DC94] Vincent Duquenne and Ameziane Cherfouh. On permutation lattices. *Math. Social Sci.*, 27(1):73–89, 1994.

- [DHMP22] Aram Dermenjian, Christophe Hohlweg, Thomas McConville, and Vincent Pilaud. The facial weak order on hyperplane arrangements. *Discrete Comput. Geom.*, 67(1):166–202, 2022.
- [DHP18] Aram Dermenjian, Christophe Hohlweg, and Vincent Pilaud. The facial weak order and its lattice quotients. *Trans. Amer. Math. Soc.*, 370(2):1469–1507, 2018.
- [DIR⁺23] Laurent Demonet, Osamu Iyama, Nathan Reading, Idun Reiten, and Hugh Thomas. Lattice theory of torsion classes: Beyond τ -tilting theory. *Trans. Amer. Math. Soc. Ser. B*, 10:542–612, 2023.
- [DMP⁺23] Rafael S. González D’León, Alejandro H. Morales, Eva Philippe, Daniel Tamayo Jiménez, and Martha Yip. Realizing the s -permutahedron via flow polytopes. To appear in *Trans. Amer. Math. Soc.*, [arXiv:2307.03474](https://arxiv.org/abs/2307.03474), 2023.
- [Edm70] Jack Edmonds. Submodular functions, matroids, and certain polyhedra. In *Combinatorial Structures and their Applications (Proc. Calgary Internat. Conf., Calgary, Alta., 1969)*, pages 69–87. Gordon and Breach, New York, 1970.
- [Gir12] Samuele Giraudo. Algebraic and combinatorial structures on pairs of twin binary trees. *J. Algebra*, 360:115–157, 2012.
- [GR63] Georges Th. Guilbaud and Pierre Rosenstiehl. Analyse algébrique d’un scrutin. *Math. Inform. Sci. Humaines*, (4):9–33, 1963.
- [Han24] Eric Hanson. A facial order for torsion classes. *Int. Math. Res. Not. IMRN*, (12):9849–9874, 2024.
- [HM21] Hung P. Hoang and Torsten Mütze. Combinatorial generation via permutation languages. II. Lattice congruences. *Israel J. Math.*, 244(1):359–417, 2021.
- [HNT05] Florent Hivert, Jean-Christophe Novelli, and Jean-Yves Thibon. The algebra of binary search trees. *Theoret. Comput. Sci.*, 339(1):129–165, 2005.
- [Jos17] Michael Joswig. The Cayley trick for tropical hypersurfaces with a view toward Ricardian economics. In *Homological and computational methods in commutative algebra*, volume 20 of *Springer INdAM Ser.*, pages 107–128. Springer, Cham, 2017.
- [Jos21] Michael Joswig. *Essentials of tropical combinatorics*, volume 219 of *Graduate Studies in Mathematics*. American Mathematical Society, Providence, RI, [2021] ©2021.
- [KLN⁺01] Daniel Krob, Matthieu Latapy, Jean-Christophe Novelli, Ha-Duong Phan, and Sylviane Schwer. Pseudo-Permutations I: First Combinatorial and Lattice Properties. 13th International Conference on Formal Power Series and Algebraic Combinatorics (FPSAC 2001), 2001.
- [Lac22] Stephen Lacina. Poset topology of s -weak order via SB-labelings. *J. Comb.*, 13(3):357–395, 2022.
- [LCdPB94] Claude Le Conte de Poly-Barbut. Sur les treillis de Coxeter finis. *Math. Inform. Sci. Humaines*, (125):41–57, 1994.
- [LP18] Carsten Lange and Vincent Pilaud. Associahedra via spines. *Combinatorica*, 38(2):443–486, 2018.
- [LR98] Jean-Louis Loday and María O. Ronco. Hopf algebra of the planar binary trees. *Adv. Math.*, 139(2):293–309, 1998.
- [LR12] Shirley Law and Nathan Reading. The Hopf algebra of diagonal rectangulations. *J. Combin. Theory Ser. A*, 119(3):788–824, 2012.
- [McM03] Peter McMullen. Fibre tilings. *Mathematika*, 50(1-2):1–33 (2005), 2003.
- [Pil18] Vincent Pilaud. Brick polytopes, lattice quotients, and Hopf algebras. *J. Combin. Theory Ser. A*, 155:418–457, 2018.
- [Pil24] Vincent Pilaud. Acyclic reorientation lattices and their lattice quotients. *Ann. Comb.*, 28(4):1035–1092, 2024.
- [Pon22] Viviane Pons. Sagemath code and demo for s -weak order and s -permutahedra, 2022. [doi:10.5281/zenodo.8380308](https://doi.org/10.5281/zenodo.8380308).
- [Pon24] Viviane Pons. Personnel communications, 2024.
- [Pos09] Alexander Postnikov. Permutohedra, associahedra, and beyond. *Int. Math. Res. Not. IMRN*, (6):1026–1106, 2009.
- [PP18] Vincent Pilaud and Viviane Pons. Permutrees. *Algebraic Combinatorics*, 1(2):173–224, 2018.
- [PPR23] Arnau Padrol, Vincent Pilaud, and Julian Ritter. Shard polytopes. *Int. Math. Res. Not. IMRN*, (9):7686–7796, 2023.
- [PR06] Patricia Palacios and María O. Ronco. Weak Bruhat order on the set of faces of the permutohedron and the associahedron. *J. Algebra*, 299(2):648–678, 2006.
- [PRV17] Louis-François Préville-Ratelle and Xavier Viennot. The enumeration of generalized Tamari intervals. *Trans. Amer. Math. Soc.*, 369(7):5219–5239, 2017.
- [PRW08] Alexander Postnikov, Victor Reiner, and Lauren K. Williams. Faces of generalized permutohedra. *Doc. Math.*, 13:207–273, 2008.
- [PS19] Vincent Pilaud and Francisco Santos. Quotientopes. *Bull. Lond. Math. Soc.*, 51(3):406–420, 2019.
- [PSZ23] Vincent Pilaud, Francisco Santos, and Günter M. Ziegler. Celebrating Loday’s associahedron. *Arch. Math. (Basel)*, 121(5-6):559–601, 2023.
- [Rea03] Nathan Reading. Lattice and order properties of the poset of regions in a hyperplane arrangement. *Algebra Universalis*, 50(2):179–205, 2003.
- [Rea04] Nathan Reading. Lattice congruences of the weak order. *Order*, 21(4):315–344, 2004.
- [Rea05] Nathan Reading. Lattice congruences, fans and Hopf algebras. *J. Combin. Theory Ser. A*, 110(2):237–273, 2005.

- [Rea06] Nathan Reading. Cambrian lattices. *Adv. Math.*, 205(2):313–353, 2006.
- [Rea12] Nathan Reading. Generic rectangulations. *European J. Combin.*, 33(4):610–623, 2012.
- [Rea15] Nathan Reading. Noncrossing arc diagrams and canonical join representations. *SIAM J. Discrete Math.*, 29(2):736–750, 2015.
- [Rea16] Nathan Reading. Lattice theory of the poset of regions. In *Lattice theory: special topics and applications. Vol. 2*, pages 399–487. Birkhäuser/Springer, Cham, 2016.
- [Tam51] Dov Tamari. *Monoides préordonnés et chaînes de Malcev*. PhD thesis, Université Paris Sorbonne, 1951.
- [Ton97] Andy Tonks. Relating the associahedron and the permutohedron. In *Operads: Proceedings of Renaissance Conferences (Hartford, CT/Luminy, 1995)*, volume 202 of *Contemp. Math.*, pages 33–36. Amer. Math. Soc., Providence, RI, 1997.

(Eva Philippe) SORBONNE UNIVERSITÉ AND UNIVERSITAT DE BARCELONA.

Email address: `eva.philippe@imj-prg.fr`

URL: <https://perso.imj-prg.fr/eva-philippe/>

(Vincent Pilaud) UNIVERSITAT DE BARCELONA & CENTRE DE RECERCA MATEMÀTICA, BARCELONA

Email address: `vincent.pilaud@ub.edu`

URL: <https://www.ub.edu/comb/vincentpilaud/>